



**UNIVERSITÀ DEGLI STUDI DI
NAPOLI FEDERICO II**

Facoltà di Ingegneria

Tesi di Dottorato di Ricerca in Ingegneria dei Sistemi Meccanici

XXVII Ciclo

**THERMO-ECONOMIC ANALYSIS OF SOLAR
HEATING AND COOLING SYSTEMS**

Coordinatore del Corso

Ch.mo Prof. FABIO BOZZA

Relatore

Ch.mo Prof. CARLO ROSELLI

Candidato

FRANCESCO TARIELLO

Index

List of personal publications.....	5
Introduction.....	7
Chapter 1 Desiccant Cooling: The Experimental Plant	13
1.1 Overview	14
1.1.1 General considerations about conventional and innovative HVAC systems 14	
1.1.2 Literature review	18
1.2 Experimental plant.....	26
1.2.1 Desiccant-based AHU.....	27
1.2.2 Microcogenerator.....	29
1.2.3 Boiler	30
1.2.4 Electric chiller.....	30
1.2.5 Thermal storage	31
1.3 From the test facility to the simulated plant	31
Chapter 2 Solar-assisted Desiccant-based Air Handling Unit: Assessments for Different Italian Climatic Conditions.....	33
2.1 Introduction	34
2.2 Loads characterization.....	34
2.3 Innovative Plant Configurations.....	37
2.3.1 Cooling mode operation.....	37
2.3.2 Heating mode operation.....	40
2.4 Conventional system	43
2.5 Simulation software and performance assessment methodology.....	44
2.5.1 TRNSYS	44
2.5.2 Mathematical Models	45
2.5.2.1 Solar thermal collector	45
2.5.2.2 Desiccant wheel.....	47

2.5.2.3	Tank Storage.....	49
2.5.2.4	Other components.....	52
2.5.3	Assessment of energy, environmental and economic performance.....	53
2.6	Simulation and results	56
Chapter 3	Desiccant-based AHU interacting with a CPVT collector: Simulation of energy and environmental performance	65
3.1	Introduction	66
3.2	Loads characterization.....	66
3.3	Plant configuration and operation	67
3.3.1	Concentrating Photovoltaic/Thermal Solar Collector [76].....	69
3.4	Mathematical models.....	70
3.4.1	CPVT collectors [76].....	70
3.5	Simulation and results	75
Chapter 4	Solar-assisted Desiccant-based Air Handling Unit: Alternative Scenarios	84
4.1	Introduction	85
4.2	Loads characterization.....	86
4.3	Alternative layouts for the innovative system	86
4.3.1	Desiccant-based AHU with heat recovery from chiller condenser (Scenario B).....	87
4.3.2	Desiccant-based AHU with cross-flow heat recovery unit (Scenario C) .	88
4.3.3	Desiccant-based AHU with pre-cooling of process air (Scenario D).....	90
4.4	Models and performance assessment methodology	91
4.5	Simulation and results	91
Chapter 5	Micro-trigeneration system with a desiccant-based air handling unit in Southern Italy climatic conditions.....	104
5.1	Introduction	105
5.2	Loads characterization.....	105
5.3	Plant configuration and operation	106

5.4	Mathematical models.....	110
5.4.1	Loads and external factors	110
5.4.2	Reciprocating internal combustion engine cogeneration model.....	111
5.4.3	Assessment of economic performance	112
5.5	Simulation and Results	114
	Conclusions.....	121
	Nomenclature.....	127
	References.....	133
	List of tables.....	143
	List of figures.....	144

List of personal publications

1. G. Angrisani, C. Roselli, M. Sasso, F. Tariello, *Simulazione di sistemi di solar cooling basati su ruota deumidificatrice*, Proceeding of 67° Congresso Nazionale ATI, 11-14 Settembre 2012 Trieste, Italia.
2. F. S. Marra, G. Angrisani, K. Bizon, R. Chirone, G. Continillo, G. Fusco, S. Lombardi, F. Miccio, C. Roselli, M. Sasso, R. Solimene, F. Tariello, M. Urciuolo, *Development of a new concept solar-biomass cogeneration system*, Energy Conversion and Management, 75 (2013) 552–560.
3. F. Calise, M. Dentice d'Accadia, C. Roselli, F. Tariello, *Simulation of energy and environmental performance of a desiccant-based AHU interacting with CPVT collector*, Proceeding of 3rd edition of the International Conference on Microgeneration and Related Technologies, Naples, 15-17 April 2013.
4. G. Angrisani, K. Bizon, R. Chirone, G. Continillo, G. Fusco, S. Lombardi, E. Mancusi, F. S. Marra, F. Miccio, C. Roselli, M. Sasso, F. Tariello, R. Solimene, M. Urciuolo, *MEGARIS: a new concept of hybrid solar-biomass-stirling chp system*, Proceeding of 3rd edition of the International Conference on Microgeneration and Related Technologies, Naples, 15-17 April 2013.
5. G. Angrisani, C. Roselli, M. Sasso, F. Tariello, *Simulazioni delle prestazioni energetiche, economiche e d'impatto ambientale di un sistema di solar desiccant cooling*, La Termotecnica, Anno LXVII – N. 5, 2013.
6. F. Calise, M. Dentice d'Accadia, C. Roselli, M. Sasso, F. Tariello, *Desiccant-based AHU interacting with a CPVT collector: Simulation of energy and environmental performance*, Solar Energy 103 (2014) 574–594.
7. G. Angrisani, C. Roselli, M. Sasso, F. Tariello, *Dynamic performance assessment of a micro-trigeneration system with a desiccant-based air handling unit in Southern Italy climatic conditions*, Energy Conversion and Management 80 (2014) 188–201.
8. G. Angrisani, C. Roselli, M. Sasso, F. Tariello, *Simulation of a micro-trigeneration system based on a desiccant-based cooling system in Southern Italy climatic conditions*, A Report of Subtask B of Integration of Micro-Generation and Related Energy Technologies in Buildings Annex 54 of the International Energy Agency Energy Conservation in Buildings and Community Systems Programme.
9. G. Angrisani, C. Roselli, M. Sasso, F. Tariello, *Thermo-Economic analysis of a solar heating and cooling system with desiccant-based air handling unit by means*

- of dynamic simulations*, Proceeding of ASME 2014 12th Biennial Conference on Engineering Systems Design and Analysis (ESDA2014).
10. G. Angrisani, C. Roselli, M. Sasso, F. Tariello, *Selection of Solar Collectors Technology and Surface for a Desiccant Cooling System based on Energy, Environmental and Economic Analysis*, Proceeding of 1st International e-conference on Energies 14–31 March 2014.
 11. G. Angrisani, C. Roselli, M. Sasso, F. Tariello, *Assessment of Energy, Environmental and Economic Performance of a Solar Desiccant Cooling System with Different Collector Types*, Energies 7(10) (2014) 6741-6764.
 12. G. Angrisani, C. Roselli, M. Sasso, F. Tariello, *Dynamic performance assessment of a solar-assisted desiccant-based air handling unit. Part I: influence of outdoor air conditions*, sottomesso alla rivista internazionale Renewable Energy.
 13. G. Angrisani, C. Roselli, M. Sasso, F. Tariello, *Dynamic performance assessment of a solar-assisted desiccant-based air handling unit. Part II: alternative scenarios*, sottomesso alla rivista internazionale Renewable Energy.

Introduction

During last years, air conditioning demand has spread, both in the commercial and the residential sector. This caused a sensible increase in primary energy consumption, especially in industrialized Countries, where people spend the major part of the day in confined environments, requiring high indoor air quality and suitable thermal comfort.

The operation of a heating, ventilation and air-conditioning (HVAC) system is usually performed to achieve comfortable indoor conditions. But HVAC systems consume large amounts of energy. Therefore, it is very important to investigate the possibility of efficiently achieving, for the specific application and building type, the desired indoor environmental conditions, reducing energy consumption and greenhouse gas emissions.

The demand for summer cooling in domestic and commercial sectors is usually satisfied by electrically driven units; this involves high electric demands. This trend is determining increasing interest in those technologies able to shift energy demand in summer from electricity to other sources that are widely available, exploitable efficiently and environmentally friendly.

From a more general point of view, it is observed that the energy requirements in the World are mainly met by using fossil fuels, among which oil is the most widely used. The combustion of these fuels causes greenhouse gas emissions, and so environmental issues that are becoming very important in recent years. On the basis of these considerations it follows easily that the prospect of:

- reducing the energy demands,
- employing more efficient systems,
- exploiting renewable energy sources,

has become a matter of interest not only of the most fervent environmentalists or of the research but also of the governments.

In this regard, several international agreements have been ratified and then national and regional measures were derived from these. Without going into the details of individual documents, here one just says that they have had as objective to make obligatory innovative solutions but also have favored their diffusion by providing instruments of financial support. As a consequence it is observed in the last years a growing increase in the use of renewable sources for the “production” of electrical and thermal energy, the construction of buildings that have low or almost zero energy demands and the installation of more efficient plants.

The three levers mentioned above: actions to reduce the energy demands, use of more efficient plants and the possibility to exploit renewable energy sources, are all extremely interesting and do not exclude each other, they are often interrelated and can lead to important results if followed simultaneously.

More than 30% of energy for the users in industrialized Countries is required in buildings. A share between 40÷80% of this energy is employed for heating or cooling purposes. In the European Union energy used in the residential and tertiary sector accounts for over 40% of final energy consumption. Italy is one of the European Countries with the highest energy consumption, on average, in the existing residential buildings more than 100 kWh/m² per year of energy are required. Also in Italy increased demands of electricity, especially in summer, took place in the last decade. National electrical data shows:

- a progressive increase of the electrical demands that stops only in the last years due to the economic recession;
- an electricity peak demand in the summer period, for the first time in 2006 and then always since 2008, occurs in June or July.

These demands of electricity are connected to the massive spread of summer conditioning devices.

On the other hand it is well known that the solar radiation is the largest source of energy of our Planet and the global energy demands are equal to only a small fraction of the solar energy reaching Earth. Italy and Mediterranean Countries have temperate and/or warm climates and a high level of radiation; therefore they are well suited to exploit solar energy for air conditioning.

The use of solar energy for summer air conditioning, *solar cooling* or *solar air conditioning*, appears to be a very attractive scenario especially for those areas of the World where there are no conventional sources of energy, problems of energy supply and management of the energy system itself.

Considering that the cooling load is usually high when solar radiation is high and that, currently, there are proven technologies that enable the conversion of solar energy into electricity (photovoltaic systems) and thermal energy (solar thermal systems), it is interesting to analyze the so-called solar-driven air conditioning systems, i.e. those that "produce cooling energy" from solar radiation.

Typically an air conditioning system ensures space cooling and heating of a building. Solar energy can be usefully employed not only for cooling but also for heating aims. Therefore a solar cooling system is usually a solar heating and cooling system.

There are different types of solar cooling plant, these systems are based on different thermally-driven refrigeration devices: absorption and adsorption heat pumps, ejector refrigeration systems, desiccant and evaporative cooling systems, etc.

In this thesis a particular solar heating and cooling system is analyzed. The following chapters describe in detail the analyzed technologies.

At the Università degli Studi del Sannio (Benevento, Italy) an experimental plant, whose main component is a hybrid desiccant wheel-based air handling unit is installed. This device uses the thermal energy of a microcogenerator to regenerate the hygroscopic material in summer mode operation.

The temperature levels required to operate the system are low and so the air handling unit can be advantageously coupled to the solar collectors, realizing a hybrid desiccant and evaporative cooling system. Moreover, the system can be simply modified and operate even during the winter period.

Since there is not a complete solar desiccant cooling system at Università degli Studi del Sannio, the assessments proposed below are carried out through dynamic simulations performed with the dynamic simulation software TRNSYS 17.

The methodology followed in the analyses (Figure I) is divided into the following phases:

- Step 0 → characterization of the configuration of the innovative and traditional system;
- Step 1 → modeling of the plants by the simulation software, characterizing the components with experimental and literature data;
- Step 2 → dynamic simulations and collection of results;
- Step 3 → on the base of simulated data, comparison of the proposed alternative system (innovative system) and the conventional one (traditional system), developing energy, environmental and economic analyses.

The conventional system consists of the most widespread solutions for summer and winter air conditioning in the geographic area of interest.

In summer period an air handling unit that realizes the dehumidification by cooling, and then the post-heating of the air is considered. It is connected to a natural gas fired boiler and an electric chiller.

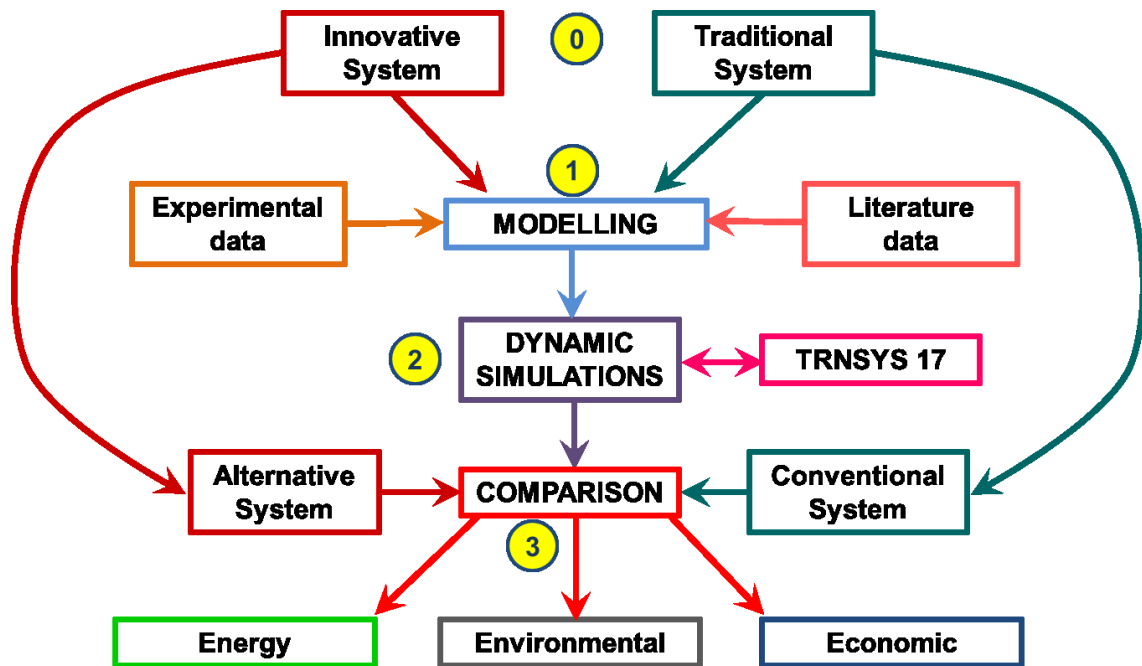


Figure I: Analysis methodology

In winter period the system is similar to the innovative one, with the difference that the thermal energy for the pre and post-heating is totally supplied by the boiler.

Hereinafter it is initially illustrated the operation of a desiccant cooling system, in general, and that of the experimental plant, in detail. Also the characteristics of the main components are listed (Chapter 1).

In the other chapters, the operation of the system, considering the coupling of the innovative air handling unit with different solar collectors types (flat plate, evacuated tube, concentrated photovoltaic and thermal collectors), is analyzed; the influence of climatic conditions on the performance of the system is assessed, and also modifications to the air handling unit layout are considered. Finally, for completeness, the system constituted by the desiccant-based air handling unit and the microgenerator is studied. In detail, Chapter 2 is dedicated to the description of the simulated alternative and conventional systems considering the coupling of the desiccant-based air handling unit with flat plate and evacuated tube collectors and assuming the system located in two Italian cities: Benevento and Milano. Furthermore the simulated heating mode operation of the system and the performance assessment methodology are shown.

A parametric analysis involving the collectors types (flat-plate and evacuated tube) the surface (20, 27 and 34 m²), the tilt angle (in the range 20-55°) and the installation site (Benevento and Milano) is performed comparing the innovative system with a conventional HVAC unit. The two cities taken into consideration are representative of

two climate zones of the Italian territory. The results show that from an energy and environmental point of view innovative systems should always be preferred to conventional ones, even when the solar thermal energy surplus is fully dissipated. A maximum primary energy saving of about 10% with flat plate collectors and over 20% with evacuated tube collectors, compared to the conventional air conditioning system, occurs in Benevento. In Milano, the same indices are over 11% and about 19% respectively. These savings increase up to about 58 and 72% in the simulations done for Benevento and to about 43 and 58% in those carried out for Milano when the solar heat excess is completely used for further energy demands.

In the considered application, the innovative solar heating and cooling plants do not get an economic advantage in terms of simple payback period if they are exclusively used for the air conditioning of the building, but they become interesting also from this point of view if it is possible to exploit the solar thermal energy surplus. Systems with evacuated tube collectors are preferable where there is little space available for the solar field (20 m²), while with larger surfaces (27 and 34 m²) flat plate collectors are advantaged. The shortest simple pay back periods are 4 and 6 years respectively for Benevento and Milano.

In Chapter 3 the coupling of the innovative air handling unit with a new hybrid photovoltaic/thermal collector is investigated. In this case the solar device consists of a parabolic mirror and a triangular receiver that simultaneously produces thermal and electric energy. Electricity produced by the hybrid collector is used to power the auxiliaries of the Air Handling Unit, the chiller and also further electric loads of users, while thermal energy is employed to heat the regeneration air flow during the summer period and the process air in the winter. Electricity in excess is sold to the grid, whereas the thermal energy surplus is exploited for production of domestic hot water. Eventual integrations of electricity and thermal energy are provided by the electric grid and by a gas-fired boiler, respectively.

In this configuration the heat provided by the concentrated photovoltaic/thermal collectors covers about 60% of thermal energy required by regeneration air and 30% of process air in winter operating mode. On an annual basis, the analyzed system obtains a primary energy saving between 81% and 89%, depending on the domestic hot water required.

In Chapter 4 three alternative scenarios to improve the performance of the innovative solar-assisted hybrid desiccant-based air handling unit are investigated. For each

scenario, different collector types (flat plate, evacuated tube), surface (20, 27 and 34 m²) and tilt angle (in the range 20-55°) are considered in order to identify the optimal set-up. The first scenario consists in the recovery of the heat rejected by the condenser of the chiller, to pre-heat the regeneration air flow. The second scenario consists in the pre-heating of regeneration air with the warm regeneration air exiting the desiccant wheel. Finally the last scenario provides pre-cooling of the process air before entering the desiccant wheel.

Results state that evacuated solar collectors can ensure primary energy savings (15-24% with optimal tilt angle) and avoided equivalent CO₂ emissions (14-22% with optimal tilt angle), about 10 percentage points more than flat plate collectors (5-19% and 4-17% respectively, with optimal tilt angle), if solar thermal energy surplus is completely dissipated. The further analysis shows that if 50% of the thermal energy surplus is used, a huge performance improvement is obtained (30-60% of primary energy saving with respect to reference system). As regards economic analysis, the shortest simple payback period is 7 years, obtained with maximum flat plate solar collectors surface and 50% surplus thermal energy recovery. When the whole use of solar thermal energy is considered, the best results, with optimal tilt angle and 34 m² of evacuated tube collectors, are approximately 73% of primary energy saving and 71% of avoided equivalent CO₂ emissions, a simple payback period of 3 years.

In Chapter 5, a small scale trigeneration device, based on a heat-led microcogenerator interacting with a silica-gel desiccant-based cooling system is analyzed.

A sensitivity analysis is performed, to assess the effect of the cogenerated electricity consumed on-site. The analysis shows encouraging results, given the Italian energy context for the small scale trigeneration system, in terms of primary energy consumption and equivalent carbon dioxide emissions reductions, with maximum values of 7.70% and 15.3%, respectively; on the other hand, it is difficult to achieve a reasonably short pay-back period for the system, even if it accesses all the support mechanisms introduced by Italian legislation for small scale gas fuelled trigeneration systems and a very high amount of cogenerated electricity is used on-site.

The analyses and the results reported in the following pages are a part of the research activities carried out during the PhD period and published in international and national journals and conferences, as indicated in the list of personal publications (see page 5).

Chapter 1 Desiccant Cooling: The Experimental Plant

1.1 Overview

Summer air conditioning of buildings is a spreading need in both industrialized and emerging Countries. The challenge to make it sustainable from an energy, environmental and economic point of view involves the identification of clever, efficient and environmentally friendly technical solutions and cannot neglect the use of renewable energy sources.

In traditional Heating, Ventilation and Air Conditioning systems (HVAC) the most energy-intensive process consists of the air cooling and dehumidification. The so-called “*mechanical dehumidification*” or “*cooling dehumidification*” is commonly used to reduce the moisture content of the air flow.

In the last few years the Desiccant and Evaporative Cooling (DEC) devices have been widely studied as a suitable alternative to conventional electrical-driven HVAC systems. Unconventional Air Handling Unit (AHU), like those that employ Desiccant Wheels (DW), remove moisture from the air through a desiccant material and reduce its temperature through an evaporative cooler.

Thanks to its benefits this technology is also spreading in residential and tertiary sectors and office buildings; however, in Europe desiccant-based solutions are still rarely implemented, neither in Countries with significant cooling requirements of building, such as Italy, due to several obstacles, such as high investment costs and lack of knowledge about performances and cost/benefit ratio.

1.1.1 General considerations about conventional and innovative HVAC systems

Air conditioning systems designed for civil purposes have the objectives of:

- controlling three indoor air thermophysical properties (temperature, humidity and speed);
- ensuring a good air quality in the conditioned space (air changes),

in order to maintain comfort conditions for the occupants [1].

In summer operation, on the basis of the typical outdoor conditions, plants have to reduce the moisture content and the temperature of the air taken from the outside to meet the latent and sensible loads of the buildings.

The simplest way to realize the first process is to reduce the air temperature to low values, lower than the dew point temperature. However the latter temperature results too low, and the dehumidified air must be heated before being introduced into the

conditioned space to avoid create discomfort. Hereinafter this air flow, handled by the air handling units, will be referred to as *process air*.

The basic configuration of the AHU that operates in cooling mode is outlined in the Figure 1.1. Moreover the real transformations, cooling with dehumidification (1-A) and heating (A-4) are reported in the psychrometric chart of Figure 1.2.

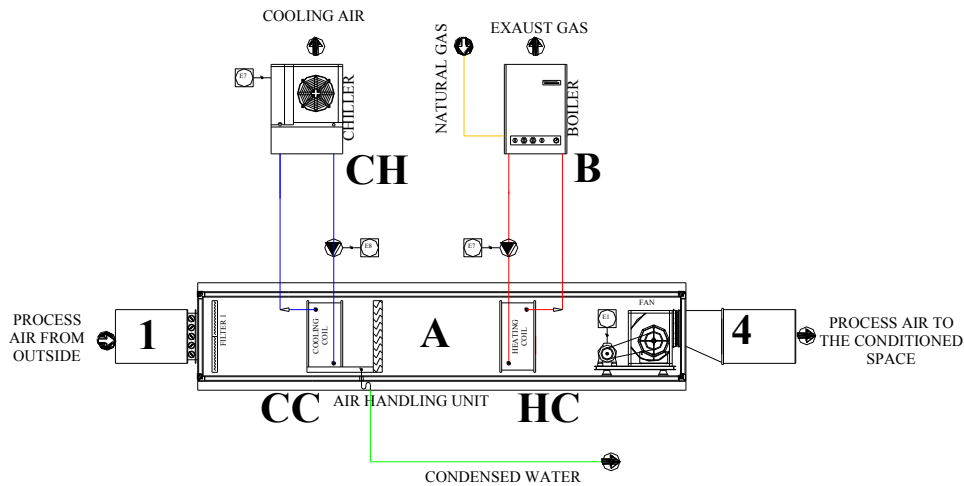


Figure 1.1: Layout of the AHU in the CS for summer operation.

A vapor compression chiller (CH) is conventionally installed to feed the cooling coil (CC), whereas a natural gas boiler, B, feeds the heating coil (HC).

The plant described above is considered as the reference or conventional system (CS) for the subsequent performance assessments of the innovative plants when operate in cooling mode.

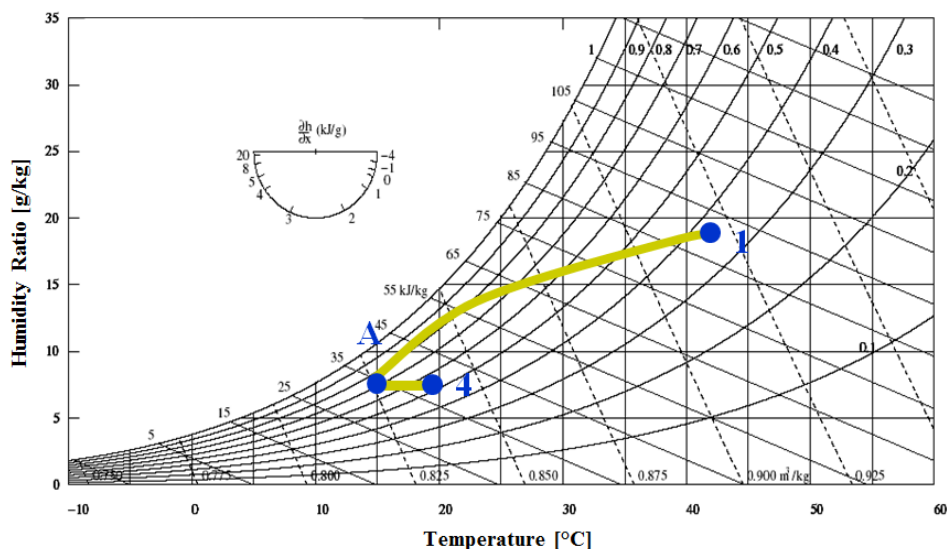


Figure 1.2: Psychrometric diagram with standard AHU transformations.

As an alternative to mechanical dehumidification, liquid or solid *desiccant materials*, can be employed in the AHUs. Desiccant dehumidification is an exothermic process. When the process air flow passes through the component made of hygroscopic material its vapour content is removed (adsorption), and simultaneously it heats up. Hence, the process air flow has to be cooled before it is introduced into the room. This cooling can be realized with a direct or indirect evaporative cooler, and/or with a cooling coil fed by a refrigeration machine (air-to-air heat pump, air-to-water chiller). Furthermore to have a continuous operation the desiccant materials need to be regenerated, this is commonly obtained by means of a hot air flow. A rotor, filled with a solid desiccant material, called *Desiccant Wheel* (DW) is the most common innovative dehumidifier configuration. It slowly rotates between two air flows: the process air and the regeneration air.

Desiccant-based plants exploiting evaporative cooling are called DEC (Desiccant and Evaporative Cooling) systems, while those with electric-driven cooling machine are defined *hybrid* systems.

As an example in Figure 1.3 the scheme of a hybrid DEC AHU with a rotary heat exchanger (R-HX) is shown. This device allows the indirect evaporative pre-cooling of the process air that can be further cooled in the cooling coil.

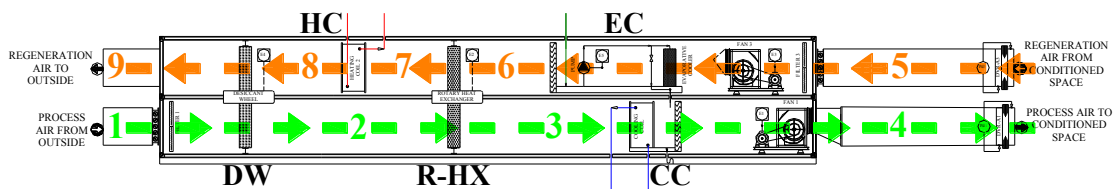


Figure 1.3: Example of hybrid DEC AHU layout.

The hybrid DEC AHU handles two air streams (Figure 1.4):

- *regeneration air*: it is outdoor air evaporatively cooled (5-6), pre-heated (to indirectly cool the process air) in the R-HX (6-7) and definitively heated (1-5) through the heating coil (HC) in order to regenerate the desiccant wheel (DW) (5-6);
- *process air*: it is outdoor air dehumidified at almost constant enthalpy in the DW (1-2) and then cooled in the rotary heat exchanger, R-HX, (2-3) and in the cooling coil (CC) (3-4);

The most interesting advantages achievable with DW-based systems compared to conventional AHUs are as follows [2,3]:

- latent and sensible load are controlled separately;

- better indoor air quality;
- in hybrid systems the chiller has a lower cooling capacity and operates at a small temperature lift with a greater COP;
- lower electric energy demands;
- primary energy savings;
- reduced environmental impact.

Regeneration energy in desiccant-based AHU can be provided by solar collectors, in fact the regeneration phase takes place at low temperatures (50–70 °C), values that are compatible with the temperatures achievable with solar collectors. In this case there is a further reduction in the use of fossil fuels and a differentiation of the energy sources in addition to the advantages listed above.

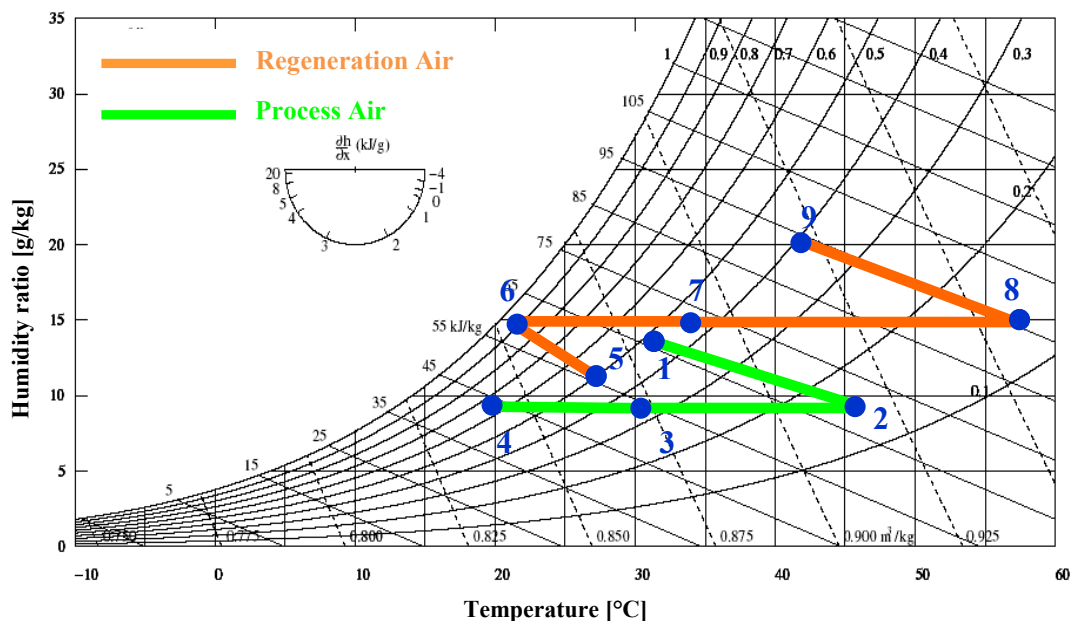


Figure 1.4: Psychrometric diagram with hybrid DEC AHU transformations.

Solar energy is the largest source of energy on our planet. The current global energy demands are only a very small share of solar energy reaching the Earth.

Despite the huge availability there are the following limitations in the exploitation of solar energy:

- low energy density;
- discontinuity:
 - day / night;
 - seasons;
 - weather conditions;

- low conversion efficiency;
- huge gap between potential and use.

Therefore solar-driven desiccant and evaporative cooling systems are composed of two main parts: a solar field and an air handling unit. The solar energy collected by the solar collectors is used to regenerate the hygroscopic material that ensures the dehumidification of process air. Storage and back-up systems are often used in these innovative plants to compensate for the temporary lack or reduction of the solar source.

1.1.2 Literature review

Desiccant cooling systems are an interesting alternative to conventional cooling-based air conditioning systems with electrically-driven vapor compression cooling units, as they exploit the hygroscopic properties of some materials, such as silica gel, which need to be periodically regenerated with low temperature heat, to allow the dehumidification of the process air. Waste heat [4], from cogeneration devices [2,5,6], from industrial processes [7,8] or solar thermal energy [9,10] is typically used as thermal energy for regeneration.

The first example of a system with DW is credited to Pennington and dates back to 1955 [11]. This device operates in an open cycle known as the ventilation cycle or Pennington cycle. An early alternative to the Pennington cycle is the recirculation cycle, that employs 100% recirculation air as process air, while fresh air is used only to regenerate the DW [12].

Other modifications to ventilation and recirculation cycles have been thought. Dunkle cycle (1965) [12,13], SENS cycle [12,14], REVERS cycle [12,14], the DINC cycle [12,14] are some examples. Many other studies investigate alternative configurations to the basic DW system and these deal with staged regeneration, isothermal dehumidification and hybrid plant.

In hybrid solutions, electric heat pumps help the thermally driven system to reach the desired supply temperature in the process air and the heat rejected from the condenser can be used to heat the regeneration air flow [15,16].

To improve performance of unconventional AHU, the regeneration can be divided in two stages; a pre-regeneration and a regeneration flow obtained by dividing the regeneration flow after that it is passing in the rotary heat exchanger is considered in [17]. Higher thermal coefficient of performance (COP_{th}) with low regeneration temperature are obtained with multi-stage dehumidification. Ideally an infinite number

of stages could allow an isothermal dehumidification, but most of the systems investigated in the literature consider only two stages which can take place in one DW [18,19] or in two [16,20]. In the last few years several other studies based on experimental tests and numerical simulations have been carried out to evaluate different configurations of the innovative air handling units (as for example in [8,21-28].

In order to improve the performance of the Solar Desiccant and Evaporative Cooling (SDEC) plants, researchers have evaluated alternative solutions for both the solar subsystem and, the AHU configurations, as already mentioned before.

Solar technologies typically considered in the literature are solar air collectors, flat plate and evacuated tube collectors, but in few cases also hybrid devices (Photovoltaic-Thermal collectors), or concentrated thermal collectors and concentrated hybrid devices (Concentrated Photovoltaic Thermal collectors) are adopted.

Enteria et al. [23,24] considered a SDEC system whose main components were a silica-gel desiccant wheel, two cross-flow heat exchangers and a flat plate solar sub-system with an electric auxiliary heater. The first measured experimental data showed that about three-quarters of the thermal energy of the system was derived from the solar field and the total coefficient of performance of the AHU (considering electrical and thermal requests) is 0.25. A more detailed analysis that considers different regeneration temperatures (in the range 60-75 °C) showed an improvement of dehumidification performance with the regeneration temperature and a decreases of thermal COP.

Bourdoukan et al. [29] developed and experimentally validated the simulation model of a solar heat pipe vacuum collectors and a stratified storage tank under various operation conditions. These components were simulated in combination with a desiccant based AHU in three different locations characterized by different climates. They demonstrated to be more efficient than conventional flat plate collectors.

Two kinds of evacuated glass tube solar air collectors, aluminum pipe and stainless steel pipe, coupled with a two rotor two stage DEC system operating in cooling and heating mode, were experimentally investigated by Li et al. [22]. Solar air collectors with a total area of 120 m² were chosen because they allow the direct use of hot air for space heating in winter and because they permitted to thermally drive desiccant cooling in summer, even if they required higher electricity consumption to drive fans. The efficiency of the two types of collectors was quite similar due to the nearly same thermal resistance on the air side, it could reach 50% in summer. The system could

convert more than 40% of the received solar radiation for cooling/heating purposes in sunny days.

Li et al. [30] arranged a Matlab/Simulink model of a solar heating and cooling desiccant system coupled with solar air collectors. The simulated results showed good agreement with experimental data and so the simulator was used to optimize collector parameters: area, air leakage and insulation.

In [31] the authors experimentally validated the TRNSYS model of a gas fired pre-cooled hybrid desiccant cooling plant and then simulated this system in four modes (configurations) coupled with solar air collectors considering the installation in two Pakistan cities. An economic assessment of the solar collector was undertaken and the payback period was calculated to be equal to 14 years. Energy and environmental payback periods of the solar collector were found to be 1.5 years and 1 year, respectively.

Hatami et al. [32] performed the optimization of a collector surface in a typical configuration of a solar desiccant wheel cycle. Design parameters, such as air velocity, rotor speed, thickness and hydraulic diameter of the desiccant wheel and also operating conditions, such as outside temperature and relative humidity, regeneration air temperature and total solar irradiance, were taken into account. Optimum design parameters and minimum solar collector surface was calculated.

In the literature there are many papers where the coupling of solar thermal collectors and desiccant-based AHUs are analyzed, but there are fewer works in which these collectors are Photovoltaic/Thermal collectors (PVT) and even fewer are the papers where concentrating PVT collectors (CPVT) are considered.

Fong et al. [33] evaluated with TRNSYS simulations the year-round performance of six hybrid desiccant cooling systems used for air-conditioning of an office in the subtropical Hong Kong. The different design alternatives considered electric-driven chillers and a solar-driven absorption chiller as refrigeration devices, evacuated tube solar collectors and photovoltaic/thermal panels as thermal and/or electric source. These systems had a primary energy consumption ranging from 10 to more than 61% less than a SDEC standard plant and an energy saving potential compared to the conventional air-conditioning up to 35.2%. Among the solar-driven systems, those with PVT collectors seemed to be the most efficient solutions from the energy point of view, even if they still have higher initial costs.

Single glaze standard air and hybrid photovoltaic/thermal collectors were simulated in [34] as the source of heat and electricity/heat for three different SDEC systems. A standard DEC plant, a DEC system with integrated heat pump and a DEC AHU with an enthalpy wheel were compared by means of energy and economic analysis. The best result occurred with photovoltaic/thermal collector because of further contribution of electricity. As concern the AHU arrangements, the heat pump integrated solution seemed to operate better than the others.

In [35] a building integrated ventilated photovoltaic façade, a photovoltaic shed and solar air collectors supplied the regeneration energy for the silica-gel desiccant wheel. The TRNSYS simulation system demonstrated that the solar fraction could reach 75% and the average COP 0.518.

The simulation model of Sukamongkol et al. [36] predicted with good agreement the results obtained in the experimental tests under the prevailing meteorological and operating conditions in tropical climate. In the facility setup the heat recovery from a hybrid PV/T air heating collector integrated the thermal energy rejected at the condenser of the heat pump to regenerate a desiccant wheel. The use of PV/T collector could save about 18% of the total energy request.

Concentrating photovoltaic/thermal collectors were the solar technology considered by Al-Alili et al. [37,38]. In the first paper the authors investigated by means of dynamic simulation the influence of key parameters on a hybrid SDEC plant in which the thermal output regenerated the desiccant wheel and the electric output fed the vapor compression chiller. The second work dealt with the experimental investigation of a hybrid desiccant based air-conditioning system in which a zeolite desiccant wheel was installed. The innovative device kept the indoor conditions within the comfort zone reaching COP higher than unity. These predicted results were obtained considering three different concentrating photovoltaic/thermal collector efficiencies.

As regards the desiccant system, a great number of possible layout arrangements and alternative components exist and were analyzed in literature. They deal with staged regeneration/dehumidification, isothermal dehumidification and hybrid plant, innovative hygroscopic material, batch systems, recovery systems, etc.

The solution most widely adopted to improve the performance of the dehumidification process in DEC plants considers the division of dehumidification in two stages separated by a refrigeration. This is the easiest way to approximate an isothermal

dehumidification (infinite stage). From a technical point of view in the literature there are systems that employ one or two desiccant wheels.

Ghali [39] analyzed a desiccant-based hybrid air-conditioning system in which an electric heat pump (EHP) was integrated in the air handling unit (AHU); the evaporator of the EHP was used to cool the process air while its condenser was used to partially heat the regeneration air. The plant was dimensioned to serve a 150 m² office as replacement of a conventional HVAC system with a 23 kW EHP. In the very humid climatic condition of Beirut (Lebanon) even if the latent load was high, the performance improves. In fact, a lower size EHP was employed (15 kW), and during 20 years, considered as useful life, economic benefits were obtained

In the study of Sheng et al. [40] the performance of a DW used in an AHU operating with an integrated high temperature heat pump was evaluated by means of experimental investigation and regression analysis. The combined influences of multiple variables on the performance of desiccant wheel, the most influential being regeneration temperature and outdoor air humidity ratio rather than outdoor air temperature and ratio between regeneration and process air flow rates, were investigated based on evaluating the indices of moisture removal capacity, dehumidification effectiveness, dehumidification coefficient of performance and sensible energy ratio.

In Uçkan et al. 2014 [41] the major inefficiencies of the components of a DEC system with a new configuration were evaluated by exergetic analysis. The system consisted of two direct evaporative coolers, a DW, three heat exchangers and an electric heater, arranged on the three channels that compose the system, fed with outdoor air. The study showed that the major irreversibility results from the electric heater, therefore this device could be advantageously replaced by a solar system, by waste heat recovery or by a gas heater.

La et al. [18] analyzed two plants in which the desiccant wheel was divided into four sections, two for the dehumidification and two for regeneration. The process air passed successively in the adsorbent sections while two outdoor air streams were heated for the two stages of regeneration. The second of the two proposed systems showed a regenerative evaporative cooling that allowed to overcome the obstacle of low possibility of reducing the temperature in very humid climatic conditions.

La et al. [16] proved that a two-rotor two-stage hybrid desiccant cooling unit was a suitable solution for very humid climates. The cooling capacity of the innovative subsection of the plant was relatively small, 30-40% of the total one but it balanced

about 60% of the latent load. The demand for electricity was reduced in a range from 22 to 34% in relation to the city of installation (Shanghai, Beijing, Hong Kong).

La et al. [20] pointed out that the low exergy efficiency of the basic desiccant cooling could be improved by using a AHU. The regeneration temperature was reduced in the new layout from 80 °C to 60 °C.

In [19] the effect of the thickness and the speed of rotation in a plant with one rotor and two-stage DEC unit was evaluated to determine the maximum removal of steam and thermal COP, that was approximately equal to 1. The optimal speed increased with temperature and decreased with the thickness.

In a subsequent paper of Ge et al. [21] a solar-driven two-stage two-rotor desiccant cooling system and a conventional vapor compression AHU were evaluated and compared in order to quantify the energy saving and the economic profit, considering an office building of Shanghai and Berlin as thermal loads. Higher regeneration temperature availed in Shanghai (85 °C) than in Berlin where instead a shorter payback period was observed.

A mathematical model was introduced and experimentally validated by Elzahzby et al. [42]. It was realized to preventively evaluate the performance of a solar-driven hybrid air-conditioning system. It was a one-rotor six-stage unit. A two-stage dehumidification, two-stage precooling and two-stage regeneration process was realized in only one silica-gel desiccant wheel (DW).

In Zhu and Chen 2014 [43] a novel marine desiccant-based air conditioning system was developed and studied; experimental tests were performed on a test rig in order to assess the most significant influencing factors on the system efficiency and to find optimal sets of parameters that maximize utilization of the ship residual heat. It was a one-rotor two-stage system with compact size and good performance. The regeneration process was guaranteed by the thermal energy not converted by the diesel engine and by that not employed for the daily use. The cooling process was achieved by direct or indirect contribution with the abundant seawater source.

A two-stage two-rotor system that supplies cool air to produce chilled water was designed, constructed and tested by La et al. [44]. Experimental results obtained under different conditions revealed that the novel device can supply chilled water at 15-20 °C with a thermal coefficient of performance of 0.3-0.6 using a low-grade heat source (solar air collectors). The specific thermal coefficient of performance of the novel rotary

desiccant cooling system was around 0.8–0.9 considering the production of both chilled water and dry air.

DW-based dehumidifiers are not the only solution for desiccant-based AHU.

Myat et al. [8] proposed a second law analysis of a multi-bed desiccant dehumidifier operating in batch manner in order to obtain the entropy minimization and the highest COP. The theoretical analysis was confirmed by experimental data. The system comprised two beds with V-shaped arrangement of silica gel packed heat exchanger, alternatively one of this is the adsorber bed while the other one is the desorber. Rang et al. [45] proposed a new multistage dehumidification process integrated with a heat pump. Plates coated with desiccant material were arranged in the channel of dehumidification and regeneration alternating respectively with heating and cooling coils that constituted the evaporator and the condenser of the refrigeration unit. Couples of plates superimposed moved periodically and alternately between the two channels. The regeneration of the hygroscopic material was carried out at temperature below 50 °C. A mathematical model validated with experimental results was adopted to locate the optimal switch time (3-5 min) and evaluate the influence of the number of stages.

Bongs et al. [46] studied experimentally and through simulations the main and innovative component of an air-conditioning system eventually powered by solar energy. It was an evaporatively cooled sorptive-coated cross-flow heat exchanger, an air-to-air plate heat exchanger. The side of a plate in contact with the process air was coated with desiccant material while at the opposite side took place an evaporative cooling process with the aim of removing the heat released by adsorption. This solution, from a technical point of view, required the duplication of the component to have the continuous operation of the plant. It allowed to increase by 46% the mass of water absorbed and an enhancement of the cooling capacity by a factor of 4.1 compared to the system without evaporative cooling.

Internal cooling is simple to implement with packed bed systems but involves a batch operation.

A new concept of desiccant wheel was introduced by Goldsworthy and White [47]. This device could operate continuously and aimed to realize an isothermal dehumidification. It was a desiccant wheel with a liquid internal cooling system realized as a shell and tube heat exchanger. An alternative solution with air-cooled desiccant wheel was analyzed by Narayanan et al. [48]. With respect to an adiabatic desiccant wheel

dehumidification level grew by about 43-53% depending on supply and regeneration air conditions.

Beccali et al. [27] considered a hybrid SDEC AHU in which two cooling coils were utilized, one to control the air supply temperature (as often happens in DEC systems) and the other to pre-dehumidify the process air; moreover the rejected heat of the electric chiller pre-heated the regeneration air. Monitoring data of summer and winter operation were elaborated to calculate instantaneous, daily and monthly performance indicators; all in all a summer electric COP of 2.4, a Primary Energy Saving of 49.2% in comparison to the reference conventional AHU, a thermal COP of 1.0 and a possible reduction of the solar collector area in the design phase by about 30% were obtained. Solar Fraction and primary energy saving in heating operation were respectively 44% and 27% respectively.

In order to overcome some issues related to the combined use of indirect evaporative cooling and rotary heat exchanger and to increase the efficiency of the system Finocchiaro et al., [49] brought technical innovations to the AHU investigated in [27]. The introduction of a wet plate heat exchanger allowed a better exploitation of evaporative cooling, reducing the cooling energy demand to the chiller and then the electrical requirements. The electrical COP calculated in the new configuration appeared to be about twice than the previous.

Wrobel et al. [50] introduced a pilot installation of a solar and geothermal assisted desiccant-based air conditioning system. The behavior of the system, compared to conventional one, was estimated by a simulation model referring to peak and year-long conditions in different geographical locations. The maximum cooling and heat demand reduced respectively of 28-32% and 30-51%. The energy benefits that occur on an annual basis were higher where there was a greater demand for dehumidification, instead the innovative system was always not cost-competitive.

Eicker et al. [28] evaluated through experimental test how operative parameters affect the performance of DW made of different materials (silica-gel, lithium-chloride or mix of silica-gel and lithium-chloride).

TRNSYS simulations were performed by Enteria et al. [25] to compare the operation of a SDEC plant equipped with two desiccant wheel coating hygroscopic materials (silica-gel, titanium dioxide) in three different locations of East Asia. Titanium dioxide revealed higher performance than silica-gel; it guaranteed lower indoor temperature and humidity ratio.

The main activities that scientific research is following with regard to desiccant-based cooling systems have been reported above. On the basis of examined literature the layouts of the simulated plants have been identified. The choices considered and presented below are based on their techno-economic feasibility on the experimental facility taken as reference.

1.2 Experimental plant

In order to analyze the performance of an air conditioning system equipped with DW over the past few years, the University of Sannio designed and built an experimental plant (Figure 1.5) whose main components include:

- an air handling unit (AHU) equipped with a desiccant wheel (DW),
- a microcogenerator ([51]) fuelled by natural gas (MCHP),
- an electric air-cooled water chiller (CH),
- a natural gas boiler (B),
- a thermal energy storage tank (TS).

This experimental plant was designed to handle outdoor air in summer conditions and bring it in supply conditions, established in each time step on the basis of simulated sensible and latent loads. All the components of the system have been designed considering an outdoor air temperature of 30 °C and absolute humidity of 15 g/kg, with a flow rate of 800 m³/h and the possibility of supplying air to the conditioned space at a temperature variable between 13 °C and 19 °C and humidity of 7–11 g/kg. The thermal and cooling powers exchanged in the heat exchangers can be adjusted in order to achieve such design parameters. The desiccant wheel, in rated conditions, reduces the air humidity by 7 g/kg. For the conditions described before, the regeneration process requires 12 kW of thermal power that could be delivered by natural gas boiler and MCHP. In the design conditions, the recovery heat exchanger should exchange 5.7 kW, and the cooling coil, a power of 7.5 kW (approximately equal to the one of the chiller), with the supply water temperature of 10 °C and the return equal to 15 °C.

The experimental air handling unit is a hybrid system that operates in summer configuration with thermal energy for regeneration purposes provided by the MCHP and/or by the boiler and cooling energy subtracted by the electric chiller. A certain amount of electricity serves for the chiller and for the other auxiliary devices (pumps and fans). This energy is supplied by the cogenerator and/or by the electric grid.

Thermal energy from the MCHP can be either transferred directly to the heating coil 1 of the AHU or in the TS. The thermal recovery circuit of the MCHP is connected to the internal heat exchanger (IHE) placed at the bottom of the TS (IHE1 in Figure 1.5). Several experimental tests have been carried out with this test facility configuration ([2,5,52,53]).

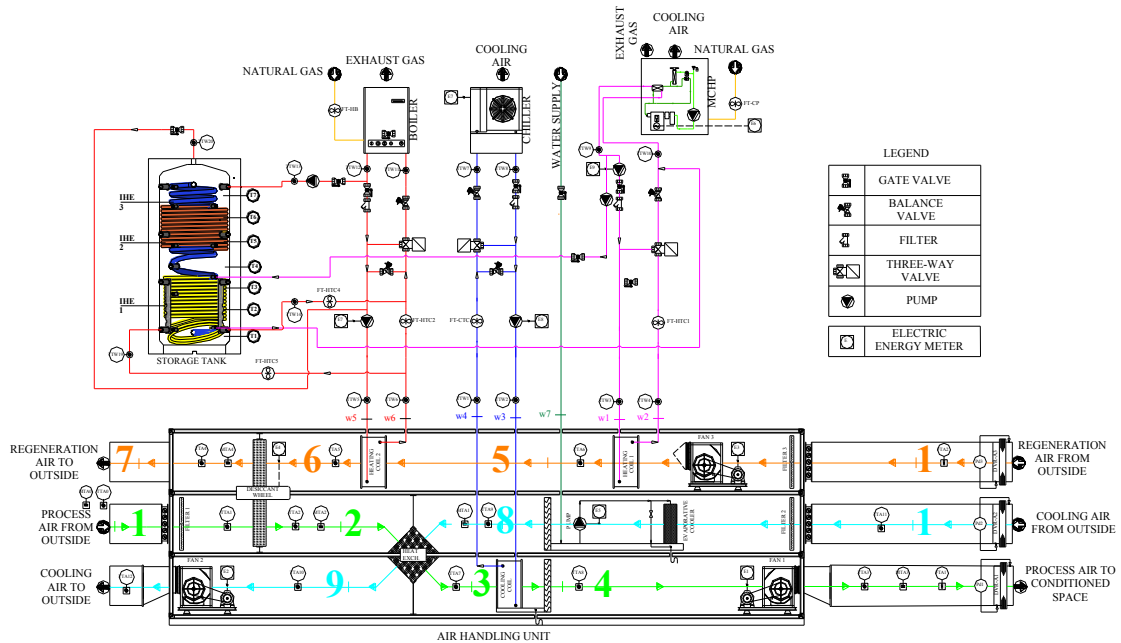


Figure 1.5: Layout of the experimental plant.

In the following sections the main components included in the experimental AHU and the related processes that take place in them are discussed.

1.2.1 Desiccant-based AHU

Specifically the AHU (Figure 1.6) handles three air flows, each one having a nominal flowrate of 800 m³/h:

- *regeneration air* which is heated through the heating coil 1 and 2 (1–5–6) fed by the MCHP and by the boiler, in order to regenerate the DW (6–7);
- *cooling air* which is cooled by a direct evaporative cooler (1–8), and subsequently passes through the cross-flow recovery heat exchanger the (8–9) to precool the process air;
- *process air*, i.e. the one sent to the room. As a first component it meets the DW, which reduces its specific humidity and raises its temperature (1–2). In order to ensure the correct thermo-hygroscopic conditions, the flow is then cooled in the

recovery heat exchanger (2–3) and in the heat exchanger fed by the chiller (3–4) in both components at constant specific humidity.



Figure 1.6: The desiccant-based AHU.

These processes are also reported in the psychrometric chart of Figure 1.7.

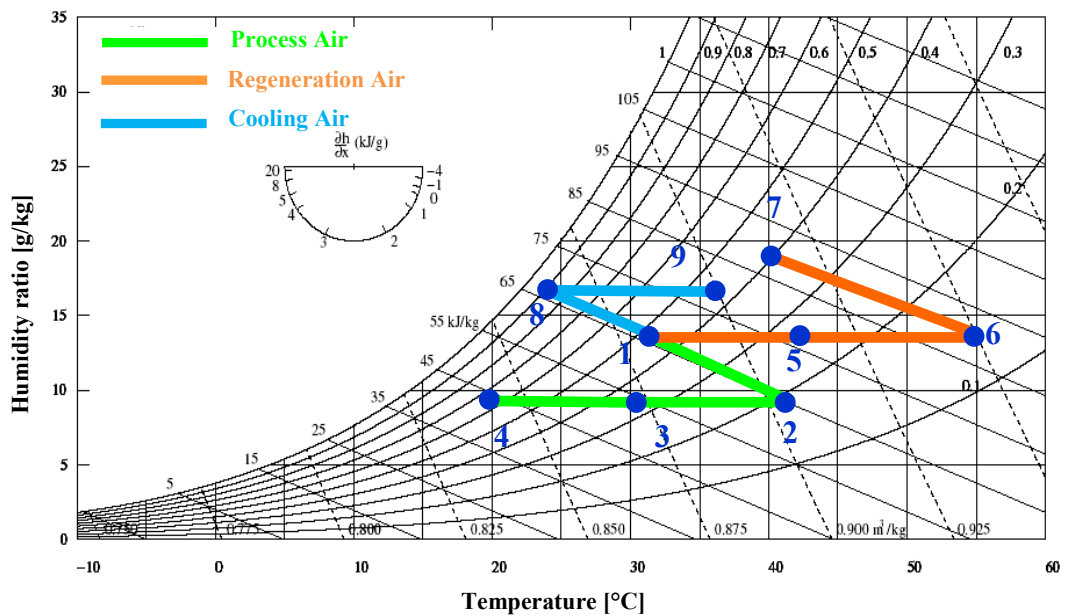


Figure 1.7: Psychrometric diagram with experimental desiccant-based AHU transformations.

The DW installed in the air handling unit of the experimental plant is equipped with a matrix composed of alternating layers of smooth and corrugated silica gel and metal silicates sheets, chemically incorporated into a support of inorganic fibers. The so

realized honeycomb structure maximizes the contact surface with air, reduces the pressure drop and weight, and increases the structural strength. The wheel has a weight of 50 kg and its dimensions are 700–200 mm (diameter to thickness). The frontal area of the wheel exposed to process and regeneration air flows is characterized by a diameter of about 600 mm (even if the nominal diameter is 700 mm), because a circular crown of the total area is obstructed by the metallic frame of the wheel cassette. The rated rotation speed is 12 revolutions per hour. Also 60% of the cross section of the DW is crossed by process air while the remaining 40% by regeneration air.

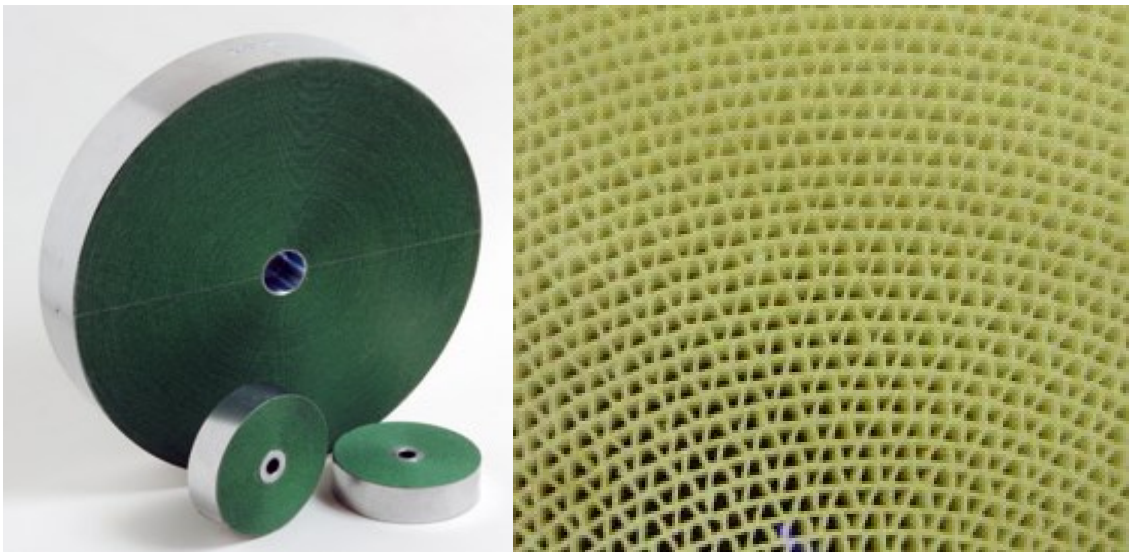


Figure 1.8: The desiccant wheel and the rotor matrix.

1.2.2 Microcogenerator

The installed MCHP (Figure 1.9) is equipped with a 6.0 kW permanent magnet type, 16 pole synchronous generator coupled with a water cooled, 952 dm³, natural gas-fuelled internal combustion engine. Furthermore the system can supply a thermal power of 11.7 kW with a water flow rate of 33.5 l/min and an output temperature of 60-65 °C. This heat is recovered by flowing the engine coolant (45% glycol-ethylene mixture) through a pipe heat exchanger, where the exhaust gas is cooled down, and through the engine walls. In the above condition the electric, thermal and overall efficiency are 28.8, 56.2 and 85 % respectively [54].



Figure 1.9: The microcogenerator.

1.2.3 Boiler

It is a natural gas boiler (Figure 1.10) with a rated heating capacity of 24.1 kW and a rated thermal efficiency of 90.2%. The boiler provides eventual additional heat to the fluid, pumped from the tank, up to the temperature required for regeneration. The boiler is activated only when the tank temperature is lower than the fixed set-point required to drive the heating process.



Figure 1.10: The boiler.

1.2.4 Electric chiller

This is a vapor compression chiller that operates only in summer conditions. The rated cooling capacity is 8.5 kW and the nominal COP is 3.0, with nominal supply/return water temperature of 7 °C and 12 °C respectively. The refrigerant used is R407C.



Figure 1.11: The chiller.

1.2.5 Thermal storage

The tank volume is 1000 dm³ (net volume 855 dm³), it is made of stainless steel, insulated with a layer of flexible polyurethane having a thickness of 100 mm and thermal conductivity of 0.038 W/(mK). It is equipped with three internal heat exchangers, two of which are connected to the heat sources and the third one, which extends along the whole height of the tank, is used for DHW preparation.



Figure 1.12: The storage tank.

1.3 From the test facility to the simulated plant

As stated in the previous sections the hybrid HVAC system in the test facility of Università degli Studi del Sannio interacts with a natural gas fuelled microcogenerator,

an electric air-cooled water chiller and a natural gas boiler. Moreover a storage tank was introduced to better manage heat flows.

The system in the current configuration is designed to operate only in cooling mode but it can be exploited all year round, even in heating mode operation, introducing some simple modifications to the plant.

In the performed simulation activity heating mode operation was also simulated. In addition to the MCHP, different types of solar collectors were evaluated. Furthermore three alternative layouts for the standard desiccant based AHU were analyzed.

As concern solar field, standard type collectors, flat plate and evacuated tube, and a hybrid innovative one (a Concentrated Photovoltaic/Thermal collector, CPVT) were considered.

Regarding the AHU the introduced modifications concern:

- the pre-heating of the regeneration air with heat recovery from chiller condenser;
- the pre-heating of the regeneration air with heat recovery from the exhaust regeneration air in a cross-flow heat exchanger;
- the pre-cooling/dehumidification of the process air.

Finally, to complete the analysis the results of simulations, carried out on an annual basis for the plant that provides the coupling air handling unit with CHP, was performed.

All the different simulated plant configurations and the obtained results are described in the following chapters.

Chapter 2

Solar-assisted Desiccant-based Air Handling

Unit: Assessments for Different Italian Climatic Conditions

2.1 Introduction

A rarely studied subject is the influence of climatic conditions on desiccant-based systems for Italian territory, nor a similar analysis is carried out using a parametric study. In this chapter the hybrid desiccant-based air handling unit coupled with standard solar thermal collectors is analyzed and results obtained in two Italian locations are shown. The system components are modelled by means of experimental tests carried out at the test facility of Università degli Studi del Sannio (Italy), whereas energy, environmental and economic performance are assessed through the dynamic simulation software, TRNSYS. A parametric analysis involving the collectors types (flat-plate and evacuated tube) the surface (about 20, 27 and 34 m²), the tilt angle (in the range 20-55°) and the installation site (Benevento and Milano) is performed comparing it with conventional HVAC units. The two cities taken into consideration are representative of two climate zones of the Italian territory.

The results show that from an energy and environmental point of view innovative systems should always be preferred to conventional ones, even when the solar thermal energy surplus is fully dissipated.

2.2 Loads characterization

The thermal loads have been evaluated by modeling a university classroom of 63.5 m² located in Benevento and in Milano with 30 seats and an occupancy schedule, expressed as a percentage of the maximum capacity, with the daily trend shown in Figure 2.1. Table 2.1 lists the dimensions and thermal insulation characteristics of the opaque and transparent components of the building envelope [9].

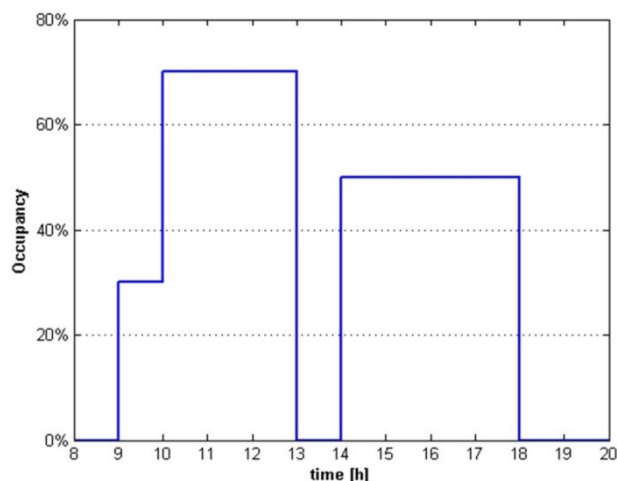


Figure 2.1: Classroom attendance.

The air conditioning system is switched on at 08:30 in the morning, half an hour before the opening of the classroom, and it is turned off at 18:00 in the afternoon, when the classroom is closed. The indoor air set-point temperatures in winter and summer operation are 20 °C and 26 °C, respectively, while the relative humidity is constantly maintained at 50%.

Table 2.1: Building characteristics [9].

	Opaque Components			Transparent Components			
	Roof	External walls (N/S)	External walls (E/W)	On the ground floor	North	South	East/West
U [W/m ² K]	2.30	1.11	1.11	0.297	2.83	2.83	2.83
Area [m ²]	63.5	36	15.87	63.5	8.53	9.40	0.976
g [-]	-	-	-	-	0.755	0.755	0.755

The endogenous loads are determined by considering the internal gains (occupants, “seated – very light writing” degree of activity and lighting). Heating and cooling loads for the building are evaluated using weather data of Benevento (Southern Italy, 41°07’ N, 14°46’ E, 1316 HDD – Heating Degree Days [55]) and Milano (Northern Italy, 45°27’ N, 9°11’ E, 2404 HDD [55]). The sensible, latent and electrical loads are reported in Table 2.2.

Table 2.2: Building Gains and Loads for Benevento (BN) and Milano (MI).

Gains per occupants		Sensible [W]		65		
(seated – very light writing, ISO 7730)		Latent [W]		55		
Gain from artificial lighting		[W/m ²]		10		
(9:00-18:00)						
Load	Cooling Period		Heating Period		Intermediate Period	
	BN	MI	BN	MI	BN	MI
Sensible [MWh]	1.54	1.31	2.90	4.94	-	-
Latent [MWh]	0.69	0.61	0.56	0.66	-	-
Electric [MWh]	0.44	0.44	0.56	0.75	0.50	0.31

In Table 2.3 the three main climatic variables (solar radiation, outdoor temperature and humidity ratio) that affect the operation of the innovative air conditioning plant are compared. The mentioned quantities, differentiated on a monthly basis, were derived from the climate data used in the simulations. The city of Benevento shows a higher level of radiation than Milano all year round. The outdoor air temperature is significantly lower in Milano than in Benevento in the winter months while the two values are very close in the summer period. Finally Benevento has a higher average relative humidity than Milano.

Table 2.3: Main climatic variables of Benevento (BN) and Milano (MI).

City	Monthly average daily solar radiation on horizontal surface [MJ/m ²]		Monthly average Temperature [°C]		Humidity Ratio [g/kg]	
	BN	MI	BN	MI	BN	MI
January	6.19	3.79	6.05	1.63	4.94	3.56
February	9.20	6.47	6.34	3.17	4.82	3.67
March	13.72	11.14	8.48	7.22	5.40	4.50
April	18.64	15.52	11.43	10.49	6.62	6.04
May	22.10	18.81	16.02	15.61	8.87	8.09
June	24.89	21.50	19.65	19.16	11.12	10.14
July	25.00	21.82	22.78	22.32	13.03	12.01
August	22.10	18.98	22.76	21.73	13.22	11.75
September	17.08	13.98	19.46	18.08	11.16	9.72
October	12.47	8.46	15.10	12.29	8.58	7.13
November	7.31	4.30	9.65	5.98	6.33	4.89
December	5.85	3.20	7.38	2.16	5.36	3.75

In addition, during some periods of the year (especially in the intermediate season and in the weekend days) excesses of solar thermal energy can take place; in order to optimize the operation of the system a certain production of domestic hot water (DHW) or thermal energy for other purposes can be obtained from the plant and transferred to a user with a great demand of it (for example a gym, a swimming pool, a hotel or a university campus).

2.3 Innovative Plant Configurations

On the base of the experimental AHU of Università degli Studi del Sannio (Benevento, Southern Italy) the innovative HVAC system considered in this chapter is arranged. The experimental AHU in the current configuration can operate only in summer mode, instead the simulated plants can operate also during the winter season to meet the sensible and latent loads of the conditioned spaces, described before. Some modifications have been implemented to the system and some new components have been introduced in the simulations for the winter operation.

The hybrid HVAC system in the test facility interacts with a natural gas fuelled microgenerator, an electric air-cooled water chiller and a natural gas boiler. Moreover a storage tank was introduced to better manage heat flows. In the following analyses, the MCHP which is previously considered as a heat and an electric source, is replaced by solar thermal collectors, whereas all the electricity is drawn from the grid.

The details of the design condition and the characteristics of the main elements of the air-conditioning system are described in Angrisani et al. 2010 [56] and Calise et al. 2014 [9]. In its current configuration, the plant was tested and studied to calibrate and validate a model for its main components [52], as well as to evaluate the influence of several parameter on the performance [53].

2.3.1 Cooling mode operation

The solar subsystem (behind the red dashed line in Figure 2.2) is constituted by the solar thermal collectors (SC), the storage tank (TS), the heat exchanger that produces hot water for sanitary use or for other low temperature heating purposes (HW-HX) and the circulation pumps. The solar field is arranged in rows of collectors connected in series as described in Table 2.4. In particular the surface used in the following analyses is the product of the number of collectors and the aperture area as indicated by the manufacturers (2.25 m^2 for flat plate collectors, 3.43 m^2 for evacuated ones). In all the analyzed configurations, the maximum number of collectors in series, as established by the manufacturer, is considered. Solar radiation is collected by the solar field all year round, it heats the mixture of water and glycol that circulates in the solar loop. The circulation pump is switched on when solar collectors outlet temperature exceeds that measured by the temperature sensor placed in correspondence of the heat exchanger in the tank. In order to avoid solar thermal energy dissipation, the heat dissipation system conventionally installed in solar cooling systems, a dry cooler, is here replaced with a

heat exchanger to produce DHW or, in general, to heat water for low temperature applications. This thermal energy is assumed to be used on-site (university campus) or exploited by a nearby user with large demands for DHW and heating such as a gym or a hotel. So the heat exchanger (HW-HX in Figure 2.2) avoids that the fluid temperature in the solar loop becomes too high but does not perform a classical dissipative action, making available domestic hot water or heat at 45 °C.

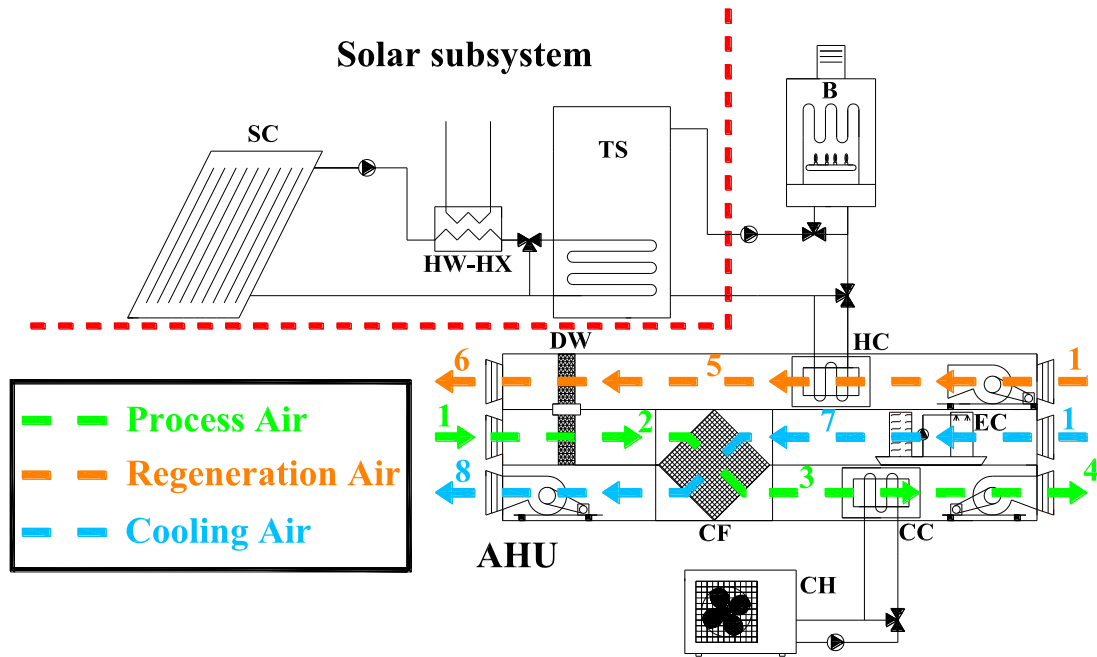


Figure 2.2: Scheme of the simulated innovative plant (cooling mode).

Table 2.4: Solar collectors configurations.

Collector Types	Aperture Area [m ²]	Arrangements	Solar Loop Pump Power [W]
Flat-Plate	9x2.25=20.3	1 row of 4 collectors + 1 row of 5 collectors	200
	12x2.25=27.0	3 rows of 4 collectors	300
	15x2.25=33.8	3 rows of 5 collectors	375
Evacuated Tube	6x3.43=20.6	2 rows of 3 collectors	200
	8x3.43=27.4	4 rows of 2 collectors	300
	10x3.43=34.3	2 rows of 3 collectors +1 row of 4 collectors	330

The control strategy of the temperature in the solar loop, carried out through the heat exchanger, changes between the days when the air-conditioning system is switched on (weekdays of the activation period of heating or cooling modes) and those in which it is switched off (the weekends and the intermediate season). When the AHU is turned on the HW-HX is set to maximize the storage of the thermal energy in the tank, intervening only to maintain the temperature in the solar loop below 100 °C. An appropriate amount of water is circulated in the secondary circuit of the heat exchanger to have hot water at 45 °C and to maintain the solar loop temperature below the maximum value.

During weekend days and the intermediate season, when the air conditioning system is turned off, the three-way valve excludes the tank from the solar loop and only domestic hot water or heat for other users is produced through the HW-HX. Some water passes continuously in the secondary circuit as long as it can be heated up to 45 °C, in this case the temperature in the solar loop is slightly higher than that of the heated water. In this way all solar thermal energy excesses, which are usually dispelled, are exploited from the user (for example, a gym, a hotel, or a university campus), ensuring optimized operation of the system all year round.

Thermal energy stored in the tank is used to heat the regeneration air in the cooling period and the process air in the heating one. The control system, according to the required temperature level of the regeneration air, reduces by means of a three-way valve the flow rate of the secondary fluid (water) to the heating coil, HC, when its temperature is higher than necessary. On the contrary, the control system turns on the back-up boiler, B, to provide an extra amount of thermal energy when its temperature is lower than necessary.

As regards the AHU (beyond the red dashed line in Figure 2.2) it handles three air streams, each one with 800 m³/h nominal volumetric flow rate (Figure 2.3):

- *regeneration air*; it is outdoor air heated (1-5) through the heating coil (HC) in order to regenerate the desiccant wheel (DW) (5-6);
- *process air*; it is outdoor air dehumidified at almost constant enthalpy in the DW (1-2) and then cooled in the cross-flow heat exchanger (CF) (2-3) and in the cooling coil (CC) (3-4) fed by the chiller (CH); then it is supplied to the university classroom for air-conditioning purposes;
- *cooling air*; it is outdoor air cooled by evaporating water in the evaporative cooler (EC) (1-7) before passing into the cross-flow heat exchanger (7-8) to pre-cool the process air.

The boiler and chiller pumps have an electric consumption of 150 W each. The process, regeneration and cooling air fans require 300 W each, with a total electric requirements of auxiliaries equal to 1200 W.

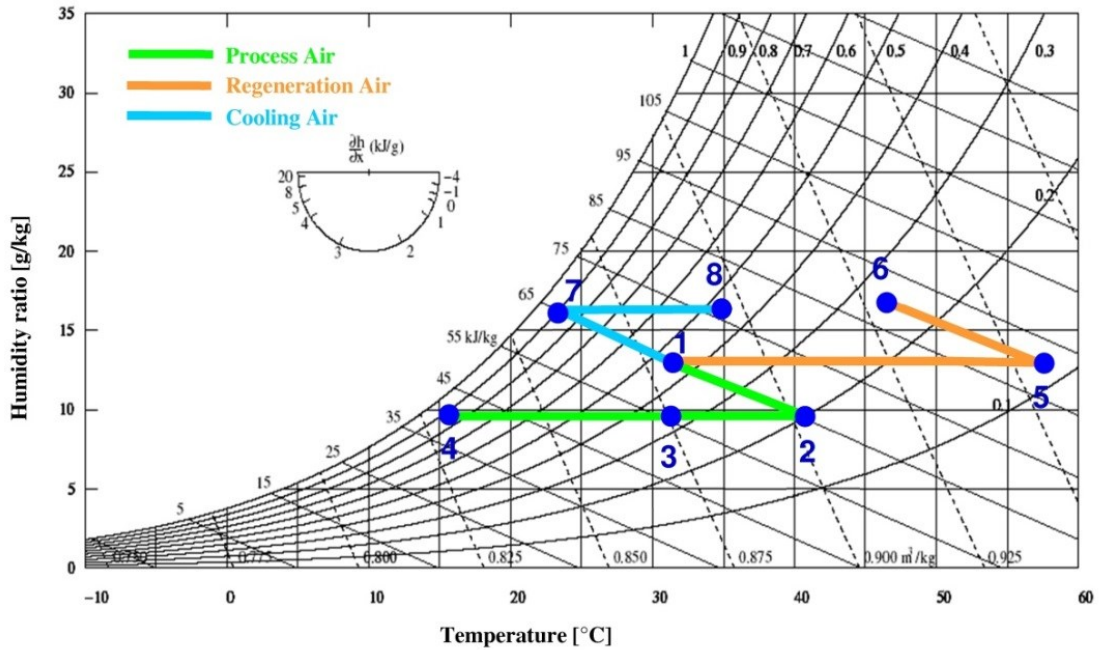


Figure 2.3: Psychrometric diagram with standard AHU transformation in cooling mode.

2.3.2 Heating mode operation

In order to utilize solar energy all year round and to increase the number of operation hours per year, winter operation is also simulated considering some modifications to the existing plant. Such modifications consist in (Figure 2.4, only dark components and devices are active) [9]:

- the use of only two ducts of the AHU, respectively for the *process air* and the *recovery* one, the latter coming from the heated space and also using the duct of the cooling air during summer;
- by-passing the DW (in winter the process air has to be humidified, not dehumidified); supplying the first coil in the process air duct (HC1 in Figure 2.4, that was a CC during summer period), with water from the tank and/or the boiler and not from the chiller as occurred during summer;
- adding a wet pack humidifier (EC1) and an additional air-to-water heat exchanger (HC2) in the process air duct which is fed with hot water from the tank and/or the boiler;

- switching off the regeneration air fan, the chiller (CH), the direct evaporative cooler, EC, (that was active on the cooling air flow during summer period) and the DW.

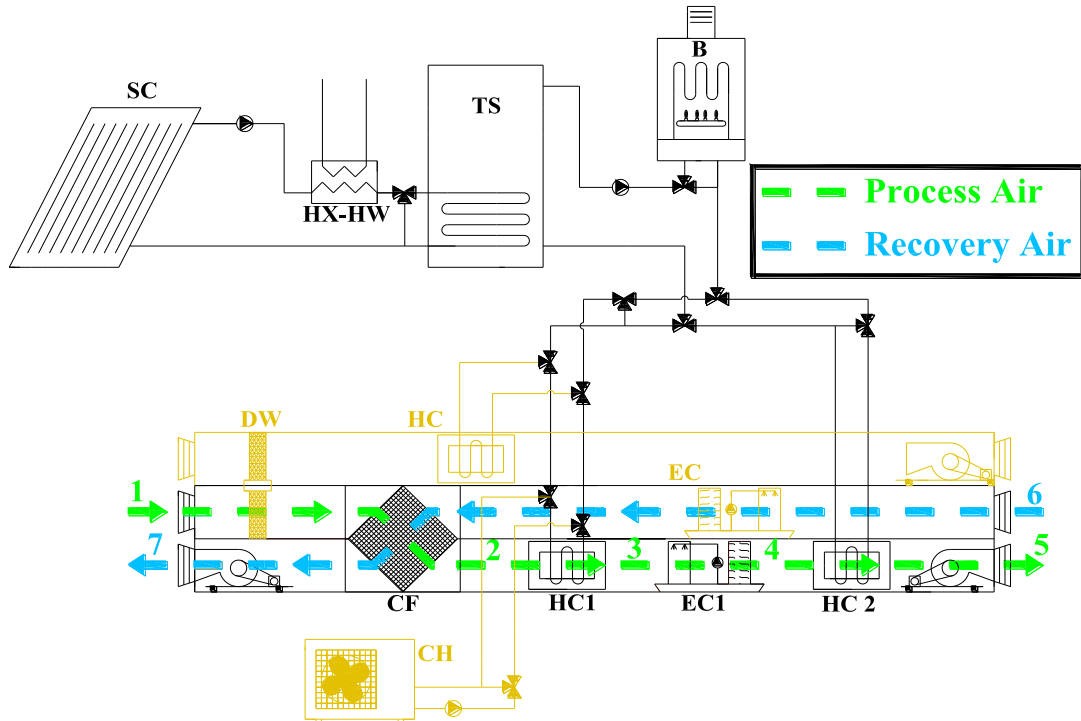


Figure 2.4: Scheme of the simulated innovative plant (heating mode).

Specifically the AHU, when operating in heating mode, handles two air flows in heating mode, each one having a nominal flowrate of $800 \text{ m}^3/\text{h}$:

- *process air*; it is the flow of outdoor air which is pre-heated (1-2-3), humidified (3-4) and then post-heated (4-5) as would happen in a conventional AHU [1], with the difference that in this case thermal energy is derived from the solar subsystem;
- *recovery air*; it is air expelled from the building that is used to pre-heat the process air in the cross-flow heat exchanger (6-7).

These processes are shown on the psychrometric chart of Figure 2.5.

In heating operation, the control system evaluates the temperature of the water coming out from the tank such that when it is lower than the one required for the preheating and post-heating, the system turns on the auxiliary boiler (B) to heat the fluid.

By analyzing climatic data, the sensible and latent load, it is clear that it is not always possible to ensure the desired temperatures and humidity to the process air.

The control system assesses at each step of the simulation the air states A, B and C (Figure 2.5), that represent respectively the thermohygrometric conditions that the process air has to reach after pre-heating, humidification and post-heating processes to ensure the comfort of the occupants of the classroom. It is observed that the most common condition is certainly the previous one where the humidity ratio required in the process air is higher than that of the outside ($\omega_C > \omega_1$) and also the process air temperature coming out from the pre-heating coil is lower than the required one ($T_2 < T_A$), (see Figure 2.5).

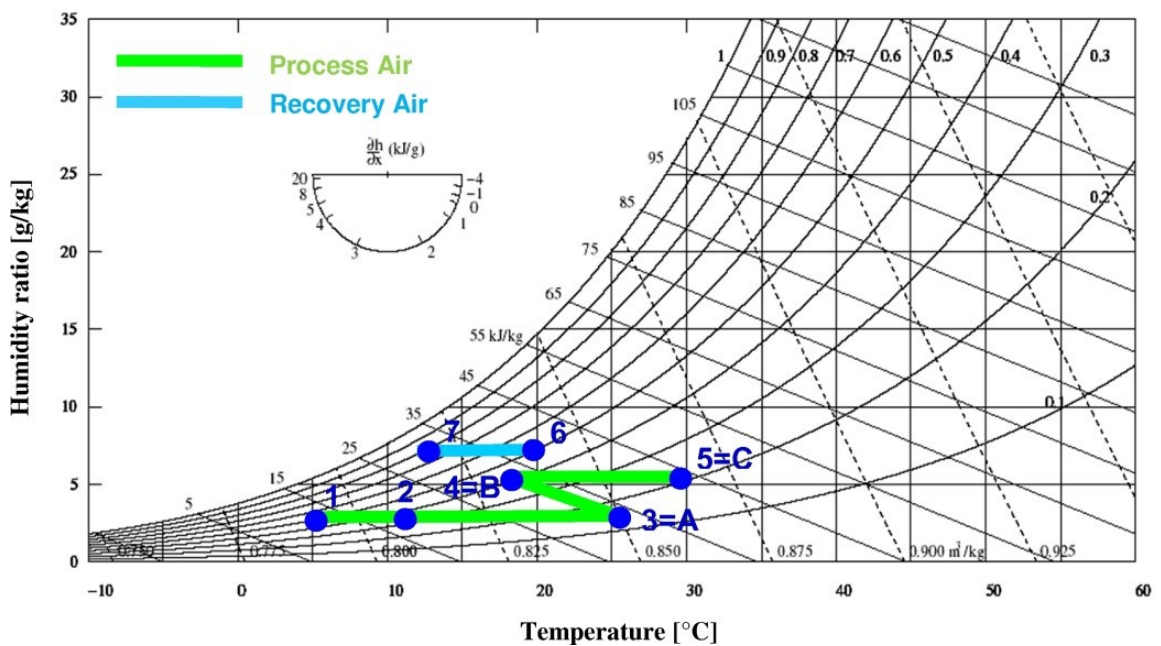


Figure 2.5: Psychrometric diagram with AHU transformation in winter operation.

The simulation system of the AHU considers also other two conditions:

- $\omega_C > \omega_1$ and pre-heating process provides the desired condition before humidification by the total or even partial use of the recovery air. In this case the conditions “2” and “3” coincide with “A” (HC1 is unused), and conditions “4” and “5” coincide with respectively “B” and “C” (see Figure 2.6).
- $\omega_C < \omega_1$: in order to balance the latent load it would be necessary to dehumidify the process air, however in this simple configuration, the simulated system proceeds to balance the sensible load only ($T_C = T_5$ and $\omega_C < \omega_1$), while excluding the dehumidification process (see Figure 2.7). However, it can be seen that changing the supply state from “C” to “5”, a relative humidity in the range 30–70% is maintained, a condition in which people are still comfortable.

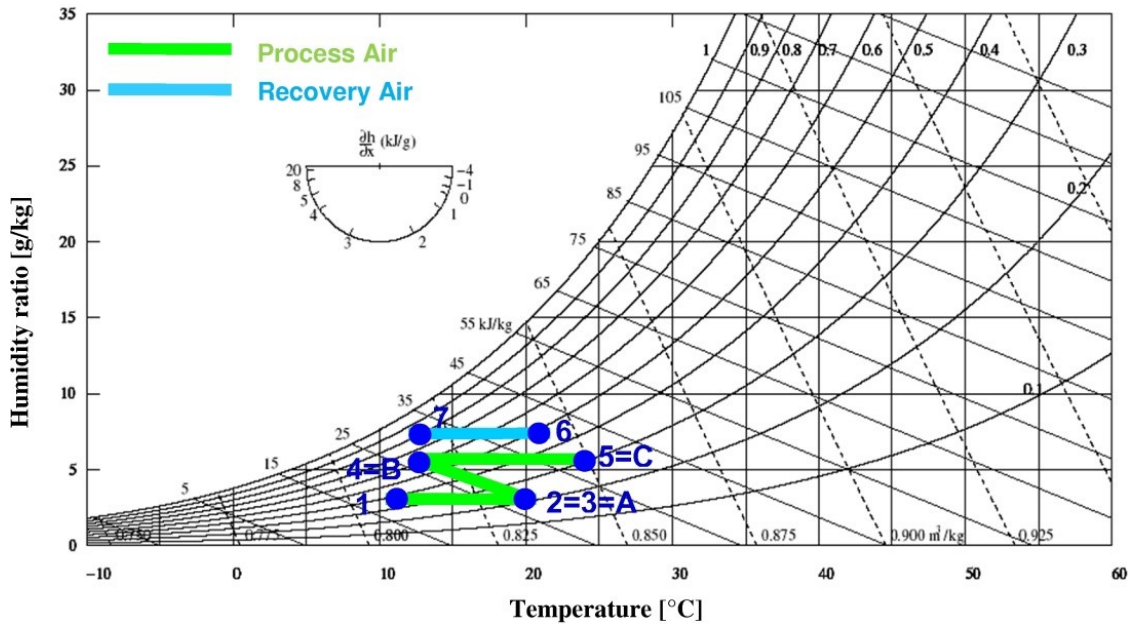


Figure 2.6: Psychrometric diagram with AHU transformation in winter operation control 1.

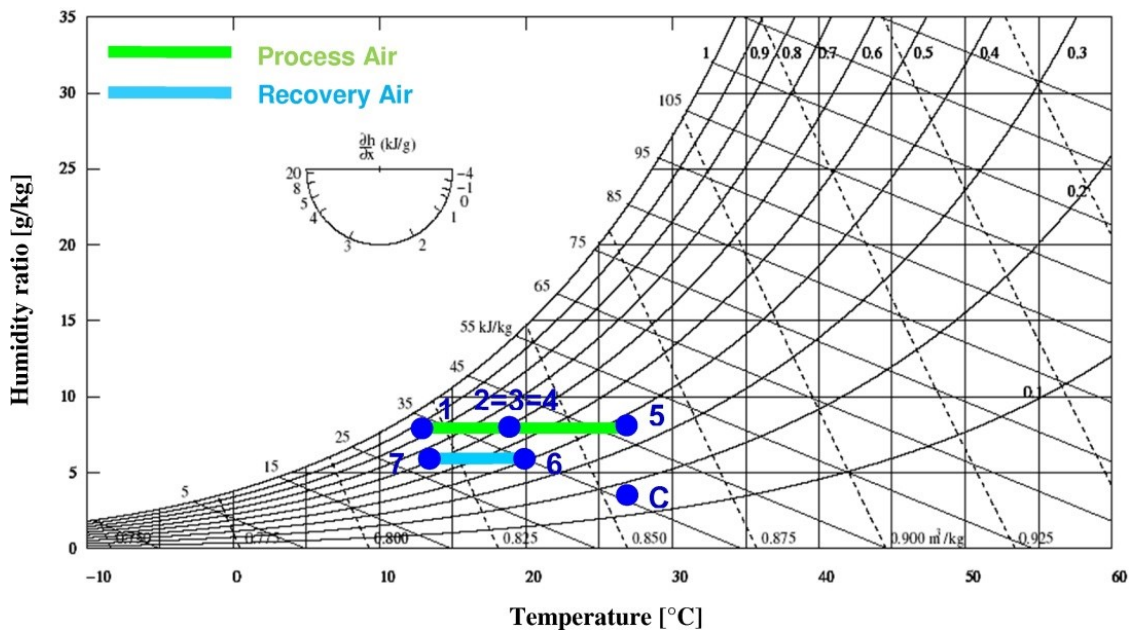


Figure 2.7: Psychrometric diagram with AHU transformation in winter operation control 2.

2.4 Conventional system

As regards the Conventional System (CS) in the summer period, a standard AHU (Figure 1.1) in which the process air is mechanically dehumidified (1-A, Figure 1.2) and then post-heated (A-4, Figure 1.2), has been simulated. A vapor compression chiller with a cooling capacity of 16 kW fed the cooling coil (CC), whereas a 24 kW boiler, B, ($\eta_B = 90.2\%$) fed the post-heating coil (HC) [57] Figure 1.1. This boiler has the same characteristics of that in the AS. In winter the AHU is the same for CS and AS, except

for the source of heat that consists solely of the boiler in the CS (Figure 2.8). All electricity is taken from the grid and hot water (HW) is produced with the boiler.

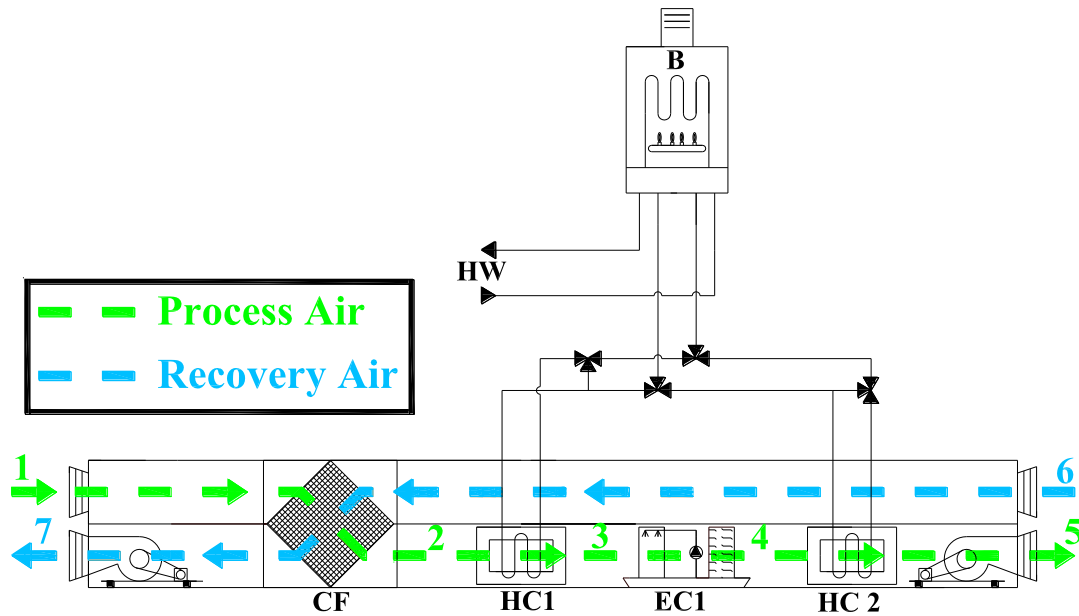


Figure 2.8: Scheme of the simulated conventional plant (heating mode).

2.5 Simulation software and performance assessment methodology

The dynamic simulation software “TRNSYS 17” [58] integrated with the “TESS” libraries [59] has been used to perform the simulations. The time-step was chosen equal to 1.5 min. According to a methodology widely used by several researchers in literature [60], [61], [62], [16], [63], the validation of the whole plant has not been carried out because the test facility does not include the collectors. However, considering that all the other components were previously and successfully validated against experimental data, it can be assumed that the simulated results are highly reliable. TRNSYS models of the main components and their most important parameters are described in the subsequent sections.

2.5.1 TRNSYS

TRNSYS (Transient System Simulation Program) is a dynamic simulation software developed by the Solar Energy Laboratory (SEL, Solar Energy Laboratory) of the University of Wisconsin and the Laboratory for Applications of Solar Energy at the University of Colorado in 1970 [58].

It is a complete and robust platform for the dynamic simulation of various systems, including multi-zone buildings. It is used to simulate the behavior of the building-plant system, enabling the user to implement control strategies, comfort conditions of the occupants, as well to allow the modeling of various alternative energies-based systems. It has an internal library of standard components for various applications, it also allows links to various external programs (eg, Matlab and Excel), and the use of climate data in standard or user-defined formats.

In addition to the default library, the distributor Thermal Energy System Specialists (TESS, [59]) and others (STEC, HYDROGEMS) provide a wide range of additional components that allow the modeling of hybrid integrated energy systems able to exploit both renewable and conventional energy sources. Its modular structure makes the software very flexible, easy to use and allows the addition of mathematical models that are not included in the pre-existing libraries or modifying the existing ones.

Each component is represented by a "*Type*", that is configurable through a graphical interface. Each "*Type*" is described by a mathematical model and presents a series of parameters, inputs and outputs required for its configuration.

A project in TRNSYS consists of a series of components, connected together in a suitable manner according to the physical and logical connections that are intended to simulate. TRNSYS contains in it a series of subroutines that contain models of system components. The types are characterized by a number or by a number and a letter that identifies them univocally.

For every step of the simulation (the time step is set by the user) the software (TRNSYS) simultaneously solves the system of equations associated with mathematical models of the different components that compose the model (building-system), and returns the results.

2.5.2 Mathematical Models

Therefore the basic elements of modelling in TRNSYS are the types. Each type implements a mathematical model representative of the real device simulated.

2.5.2.1 Solar thermal collector

Flat plate and evacuated tube solar collectors models in TRNSYS (type 1b and 71 respectively) are based on a quadratic equation for the efficiency, which is essentially a generalization of the Hottel-Willier equation [64]:

$$\eta_{col} = \eta_0 + a_1 \frac{\Delta T}{G} + a_2 \frac{\Delta T^2}{G} \quad (2-1)$$

Normally, the temperature difference is the difference between the temperature of the working fluid and the ambient air. The temperature of the fluid is the average temperature between collector inlet and outlet.

The model calculates the performance of a solar field constituted by rows of collector. Each row can be in turn formed by a certain number of collectors in series. The efficiency of the solar field is determined by the number of modules in series and by the characteristics of the basic module, that are evaluated in certain test conditions. In addition, it takes into account the Incidence Angle Modifier (IAM) factor, which is the parameter that represents the effects on the intercept efficiency (η_0) of the collector due to a non-zero angle of incidence of solar radiation.

Therefore, it is necessary to consider three corrections in the model to take into account:

- different values of flow rate of the working fluid compared to the test conditions;
- number of identical collectors connected in series;
- non-zero angle of incidence of solar radiation.

The evacuated tube collectors are not symmetrical from an optical point of view, thus a double IAM factor (Transversal and Longitudinal IAM) is required (see Table 2.5).

Table 2.5: Evacuated tube collectors IAM factors

Direction	Transversal IAM	Longitudinal IAM
[°]	[-]	[-]
0	1.00	1.00
10	1.00	1.00
20	1.00	1.00
30	1.00	1.00
40	1.03	0.98
50	1.08	0.96
60	1.15	0.87
70	1.11	0.72
80	0.72	0.50
90	0.00	0.00

Table 2.6 and Table 2.7 show the parameters used for the simulations of flat plate and evacuated tube collectors respectively. They have been obtained from solar collectors data sheets [65,66].

Table 2.6: Flat plate collectors parameters.

Parameters	Value	Units
Fluid specific heat	3.84	kJ/(kg K)
Efficiency mode	1	-
Tested flow rate	40.36	kg/(h m ²)
Intercept efficiency η_0	0.673	-
Efficiency slope a_1	2.98	W/(m ² K)
Efficiency curvature a_2	0.0078	W/(m ² K ²)
Optical mode 2	2	-
1st-order IAM	0.072	-
2nd-order IAM	0	-

Table 2.7: Evacuated tube collectors parameters.

Parameters	Value	Units
Fluid specific heat	3.84	kJ/(kg K)
Efficiency mode	1	-
Tested flow rate	30.36	kg/(h m ²)
Intercept efficiency η_0	0.676	-
Efficiency slope a_1	1.15	W/(m ² K)
Efficiency curvature a_2	0.004	W/(m ² K ²)
Logical unit of file containing biaxial IAM data	222	-
Number of longitudinal angles for which IAMs are provided	7	-
Number of transverse angles for which IAMs are provided	7	-

2.5.2.2 Desiccant wheel

The DW with silica gel adsorbent material is modeled with the type 1716 of TESS library. From a mathematical point of view, the performance of the component is

determined using the simplified Maclaine-Cross and Banks approach [67] that models the dehumidification process, which is a combination of mass and heat transfer, in analogy to a simple process of thermal energy transfer in a heat exchanger.

The coupled equations that describe the two processes are reduced to two uncoupled differential equations with two independent variables, called characteristic potentials F_1 and F_2 , [68,69]. The isopotential lines F_1 approximate constant specific enthalpy lines while the constant potential F_2 lines approximate constant relative humidity curves in the psychrometric chart. The potential functions depend on the thermohygroscopic properties of the air and on the thermophysical properties of the adsorbent material, [70]. These relations have been expressed for the pair silica gel-air by Jurinak [69], and they are:

$$F_{1,j} = \frac{-2865}{(t_j + 273.15)^{1.49}} + 4.344(\omega_j / 1000)^{0.8624} \quad (2-2)$$

$$F_{2,j} = \frac{(t_j + 273.15)^{1.49}}{6360} - 1.127(\omega_j / 1000)^{0.07969} \quad (2-3)$$

where the subscript “ j ” refers to the generic thermohygroscopic state of the air at which the two potential are evaluated, whereas t and ω are the air temperature ($^{\circ}\text{C}$) and the humidity ratio (g/kg) respectively.

The intersection of isopotential lines provides the output conditions of the process air in the ideal case, in which both the adsorption and the desorption process are isoenthalpic. The Jurinak’s model assesses that the conditions of real output are estimated using two indices of efficiency of the wheel, η_{F1} and η_{F2} , calculated in analogy with the efficiency of a heat exchanger as:

$$\eta_{F1} = (F_{1,2} - F_{1,1}) / (F_{1,5} - F_{1,1}) \quad (2-4)$$

$$\eta_{F2} = (F_{2,2} - F_{2,1}) / (F_{2,5} - F_{2,1}) \quad (2-5)$$

where potentials F_1 and F_2 must be evaluated in the states 1, 2 and 5 of Figure 2.3.

Specifically, η_{F1} represents the degree to which the process approximates the adiabatic one, while η_{F2} represents the degree of dehumidification. In addition the model returns the temperature of the process air exiting the component. This model has been calibrated and validated in [52], the indices of efficiency obtained are listed in Table 2.8.

Table 2.8: Desiccant Wheel parameters.

Parameters	Value	Units
Effectiveness η_{F1}	0.207	-
Effectiveness η_{F2}	0.717	-

2.5.2.3 Tank Storage

The tank is modeled by means of the type 60 of the TRNSYS standard library, which is the most detailed model available in the software, used to simulate a stratified thermal storage.

The model allows one to consider up to a maximum of three internal heat exchangers (the first of them is connected to the solar loop). In addition, the water stored in the tank can be fed by two generic points of its lateral surface (return connections) and taken from two other points (supply connections). In order to simulate the thermal stratification, the tank is divided into a certain number of fully-mixed equal dimension cylindrical sections (nodes) in which uniform temperature is assumed.

The tank model allows the insertion of different levels of insulation in its different sections. Therefore an increased coefficient of loss is assigned to the node corresponding to the base of the tank, which is not isolated from the ground.

The energy balance for the generic node, Figure 2.9, neglecting the terms related to the auxiliary electrical and gas heaters, options for the model, is as follows:

$$\begin{aligned}
(m_i c_p) \frac{dT_i}{d\tau} = & \frac{(k + \Delta k) A_{c,i}}{\Delta x_{i+1 \rightarrow i}} (T_{i+1} - T_i) + \frac{(k + \Delta k) A_{c,i}}{\Delta x_{i-1 \rightarrow i}} (T_{i-1} - T_i) + (U_{tank} + \Delta U_i) A_{s,i} (T_a - T_i) \\
& + \dot{m}_{down} c_p T_{i-1} - \dot{m}_{up} c_p T_i - \dot{m}_{down} c_p T_i - \dot{m}_{up} c_p T_{i+1} + UA_{hx1} \Delta T_{ln1} + UA_{hx2} \Delta T_{ln2} + UA_{hx3} \Delta T_{ln3} \quad (2-6) \\
& + \dot{m}_{lin} c_p T_{lin} - \dot{m}_{lout} c_p T_i + \dot{m}_{2in} c_p T_{2in} - \dot{m}_{2out} c_p T_i
\end{aligned}$$

where the term on the left side represents the time variation of energy in the node, the first two terms on the right side represent the conductive interactions of the considered node with the upper and lower one; the third term evaluates the heat losses towards the surrounding ambient; the terms related to \dot{m}_{up} , \dot{m}_{down} , \dot{m}_{in} and \dot{m}_{out} are the convective terms, and the remaining terms, marked with the subscript “hx”, represent the contributions of the exchangers.

This model has been validated and calibrated with experimental data in [71], the parameters used in the TRNSYS type are shown in Table 2.9.

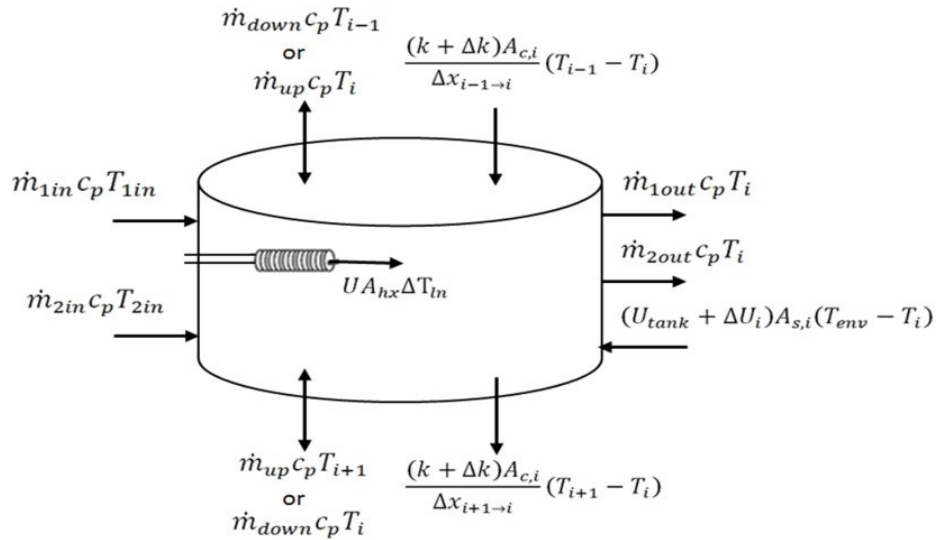


Figure 2.9: Generic node of a detailed stratified tank storage.

Table 2.9: Tank parameters

N°	Parameters	Value	Unit
1	Inlet position mode	2	-
2	Tank volume	986	L
3	Tank height	2.04	m
4	Tank perimeter	-1	m
5	Height of flow inlet 1	1.37	m
6	Height of flow outlet 1	2.04	m
7	Height of flow inlet 2	1.76	m
8	Height of flow outlet 2	0.36	m
9	Fluid specific heat	4187	J/(kg K)
10	Fluid density	985	kg/m ³
11	Tank loss coefficient	1.37	W/(m ² K)
12	Fluid thermal conductivity (water)	0.580	W/(m K)
13	Destratification conductivity	0.285	W/(m K)
14	Boiling temperature	127	°C
15	Auxiliary heater mode	-	-
16	Height of 1st auxiliary heater	-	m
17	Height of 1st thermostat	-	m
18	Set point temperature for element 1	-	°C
19	Dead band for heating element 1	-	°C

20	Maximum heating rate of element 1	-	kW
21	Height of heating element 2	-	m
22	Height of thermostat 2	-	m
23	Set point temperature for element 2	-	°C
24	Dead band for heating element 2	-	°C
25	Maximum heating rate of element 2	-	kW
26	Overall loss coefficient for gas flue	-	kW/K
27	Flue temperature	-	°C
28	Fraction of critical time-step	6	-
29	Gas heater	-	-
30	Number of internal heat exchangers	3	-
31	Node heights supplied	1	-
32	Additional loss coefficients supplied	1	-
33	Heat exchanger fluid indicator-1	1	-
34	Fraction of glycol-1	0	-
35	Heat exchanger inside diameter-1	0.029	m
36	Heat exchanger outside diameter-1	0.032	m
37	Heat exchanger fin diameter-1	0.032	m
38	Total surface area of heat exchanger-1	3.1	m ²
39	Fins per meter for heat exchanger-1	0	-
40	Heat exchanger length-1	30.85	m
41	Heat exchanger wall conductivity-1	45	W/(m K)
42	Heat exchanger material conductivity-1	45	W/(m K)
43	Height of heat exchanger inlet-1	0.85	m
44	Height of heat exchanger outlet-1	0.25	m
45	Heat exchanger fluid indicator-2	1	-
46	Fraction of glycol-2	0	-
47	Heat exchanger inside diameter-2	0.029	m
48	Heat exchanger outside diameter-2	0.032	m
49	Heat exchanger fin diameter-2	0.032	m
50	Total surface area of heat exchanger-2	2.5	m ²
51	Fins per meter for heat exchanger-2	0	-
52	Heat exchanger length-2	24.88	m
53	Heat exchanger wall conductivity-2	45	W/(m K)

54	Heat exchanger material conductivity-2	45	W/(m K)
55	Height of heat exchanger inlet-2	1.54	m
56	Height of heat exchanger outlet-2	1.08	m
57	Heat exchanger fluid indicator-3	1	-
58	Fraction of glycol-3	0	-
59	Heat exchanger inside diameter-3	0.0254	m
60	Heat exchanger outside diameter-3	0.0381	m
61	Heat exchanger fin diameter-3	0.0381	m
62	Total surface area of heat exchanger-3	7.8	m ²
63	Fins per meter for heat exchanger-3	0	-
64	Heat exchanger length-3	61	m
65	Heat exchanger wall conductivity-3	16.0	W/(m K)
66	Heat exchanger material conductivity-3	16.0	W/(m K)
67	Height of heat exchanger inlet-2	0.15	m
68	Height of heat exchanger outlet-3	1.6	m
69	Height of node -1	0.0408	m
70	Additional loss coefficient for node -1	0	W/(m ² K)
71-167	Node parameters		
168	Additional loss coefficient for node -50	17.55	W/(m ² K)

2.5.2.4 Other components

The main components used for the simulations, that have not been described before, the related TRNSYS type, as well as the value of the main parameters and related references are listed in the are reported in Table 2.10. The library (standard or TESS) in which each type can be found is also specified.

Table 2.10: Main models used for the simulation and their main parameters.

Component (Reference)	Type	Library	Main parameters	Value	Units
Cross flow heat exchanger [52]	91	Standard	Effectiveness	0.446	-
Humidifier [52]	506c	TESS	Saturation efficiency	0.551	-

Natural gas boiler [52]	6	Standard	Nominal thermal power	24.1	kW
			Efficiency	0.902	-
Air-cooled chiller [52]	655	TESS	Rated capacity	8.50	kW
			Rated COP	2.98	-
Heating coil [52]	670	TESS	Liquid specific heat	4.190	kJ/(kg K)
			Effectiveness	0.864	-
Cooling coil [52]	508	TESS	Liquid specific heat	4.190	kJ/(kg K)
			Bypass fraction	0.177	-

2.5.3 Assessment of energy, environmental and economic performance

The thermo-economic analysis is based on the comparison, typically performed on an annual basis and considering equal users' demands, between an innovative system (or Alternative System, AS) and a reference one, also called conventional system (CS), since it is the most widely used technology in the installation region. The CS is typically based on the separate "production" of electricity, heat and cooling energy, whereas the AS is characterized by a higher efficiency and/or by the exploitation of renewable energy sources, but also by a higher initial cost.

From the energy point of view the comparison is carried out between the primary energy requirements, by calculating the Primary Energy Saving:

$$PES = \left(1 - E_p^{AS} / E_p^{CS} \right) \quad (2-7)$$

where the primary energy of the alternative and conventional system ($E_p^{AS/CS}$) is evaluated taking into account that the energy efficiency of the Italian national electric system (η_{EG}), including transmission and distribution losses, is 42% [72], [73], [74] and using the boiler efficiency reported in Table 2.10, 90.2%. In addition it is assumed that there is no primary energy associated to solar energy because it is a renewable energy source, so CS and AS use the grid and a natural gas boiler for electricity and thermal energy requirement respectively (in AS the boiler is a back-up system). Therefore a similar equation, but with different electricity and thermal requirements, can be written for the AS and the CS:

$$E_p^{AS/CS} = \left(E_{el,chil}^{AS/CS} + E_{el,aux}^{AS/CS} \right) / \eta_{EG} + E_{th,B}^{AS/CS} / \eta_B \quad (2-8)$$

To assess the positive effects on the environment of the AS installation, equivalent CO₂ emissions of the two systems are calculated and the equivalent CO₂ avoided emissions are derived:

$$\Delta CO_2 = \left(1 - CO_2^{AS} / CO_2^{CS} \right) \quad (2-9)$$

where CO_2^{AS} and CO_2^{CS} are evaluated with a similar equation, but with different electricity and thermal requirements, according to the above considerations regarding the primary energy:

$$CO_2^{AS/CS} = \left(E_{el,chil}^{AS/CS} + E_{el,aux}^{AS/CS} \right) \gamma + E_{th,B}^{AS/CS} \cdot \beta / \eta_B \quad (2-10)$$

where β is the specific emission factor of primary energy related to natural gas combustion, equal to 0.207 kgCO₂/kWh_{Ep}, ([74]) and γ is the specific emission factor of electricity drawn from the grid, equal to 0.573 kgCO₂/kWh_{el} [56].

As regards the economic analysis, the feasibility of the AS can be assessed by means of the Simple Pay Back (SPB) method, that evaluates the payback period of an investment and is defined as:

$$SPB = EC / \sum_{k=1}^N F_k \quad (2-11)$$

where N is the number of years to payback the investment, i.e. the number of years for which the equation is verified, EC is the extra cost of the AS (desiccant-based AHU, storage tank and collectors) with respect to the reference system, F_k is the cash flow for the generic year k :

$$F_k = OC_k^{CS} - OC_k^{AS} \quad (2-12)$$

where OC_k^{AS} and OC_k^{CS} are the operating costs of the AS and CS; the former is given by:

$$OC_k^{AS} = \sum_r V_{NG,r} c_{NG,r} + \left(E_{el,chil}^{AS} + E_{el,aux}^{AS} \right) \cdot c_{el} - I_{a,tot} \quad (2-13)$$

where the following assumptions, according to Italian conditions, were considered:

- Lower Heating Value (*LHV*) of natural gas equal to 9.52 kWh/Nm³;
- the total volume of natural gas $V_{NG,tot} = \sum_r V_{NG,r} = E_{th,B} / (\eta_B \cdot LHV)$ should be divided according to the brackets of Table 2.11, to which different unitary costs ($c_{NG,r}$) are associated;
- unitary cost of electricity (c_{el}) equal to 0.211 €/kWh;
- extra cost of desiccant-based AHU with respect to the conventional one equal to 10,000 €;
- investment cost of storage tank equal to 3,000 €;
- specific cost of collectors: 360 €/m² for flat-plate collectors; 600 €/m² for evacuated collectors.

Table 2.11: Unitary costs.

r	Volume brackets [Nm³]	$c_{NG,r}$ [€/Nm³]
1	1 – 120	0.561
2	121 – 480	0.884
3	481 – 1560	0.912
4	1561 – 5000	0.943
5	5001 - 80000	0.896

The Italian legislation recently introduced a mechanism to incentivize the use of renewable energy-based technologies to “produce” thermal energy [75]. In the case of solar collectors, the annual incentive is provided for only two years ($k=1, 2$) if the installed surface is lower than 50 m² and it can be evaluated as:

$$I_{a,tot} = C \cdot S \quad (2-14)$$

where $I_{a,tot}$ is the annual economic incentive, C is a valorization coefficient depending on the type of plant (equal to 255 €/m² for solar cooling systems) and S is the gross solar collectors area. To access the support mechanism, solar collectors must have a thermal efficiency higher than a minimum value, depending on the type of collectors, the average fluid temperature, the outdoor temperature and the total radiation.

OC^{CS} can be evaluated with an equation very similar to eq. 2-13, obviously no incentives are included.

2.6 Simulation and results

The operation of the Alternative and Conventional systems has been simulated considering three periods:

- Summer (June 1st – September 15th): Air-conditioning (space cooling) and hot water production for further thermal energy demands (solar thermal energy surplus);
- Winter (November 15th – March 31st for Benevento and October 15th – April 15th for Milano): Air-conditioning (space heating) and hot water production for further thermal energy demands (solar thermal energy surplus);
- Intermediate period: hot water production for further thermal energy demands only.

The Italian legislation constrains only the heating period based on HDD while does not provided restrictions for the cooling season. In this article it is chosen to consider the heating period defined by law and to use the same cooling period for the two cities since their summer weather conditions are very similar.

The electrical load of the classroom is switched on according to its opening hours.

The simulation parameters of the components have been set according to the values obtained from the experimental tests, when available. In all the other cases they were set on the basis of the rated values.

The results were obtained considering three sub-scenarios differentiated by the amount of thermal energy surplus used.

When the solar thermal energy surplus for DHW or for other heating purposes is not taken into account, the effect of the climate of the installation place on the annual performance is more evident. When, instead, it is considered, two further sub-scenarios, 50% and 100% of the solar thermal energy surplus is exploited, respectively, are assumed.

Regarding the energy analysis the PES index is plotted as a function of the solar collector slope and area, in Figures 2.10, 2.12 and 2.14 for the hybrid AHU with flat plate collectors and in Figures 2.11, 2.13 and 2.14 for the same AHU with evacuated tube collectors.

As a general comment, in Figures 2.10-2.15 it is observed that for all configurations, with and without further thermal energy demands, innovative systems require less primary energy than conventional ones (PES>0%) and, as expected, the primary energy saving increases with the collecting surface and with the percentage of solar thermal

energy surplus used. SDEC plants with evacuated solar thermal collectors show performance, in term of PES, better than those equipped with flat plate collectors. The optimal tilt angle is shifted toward greater values for the systems installed in Milano in comparison to those located in Benevento.

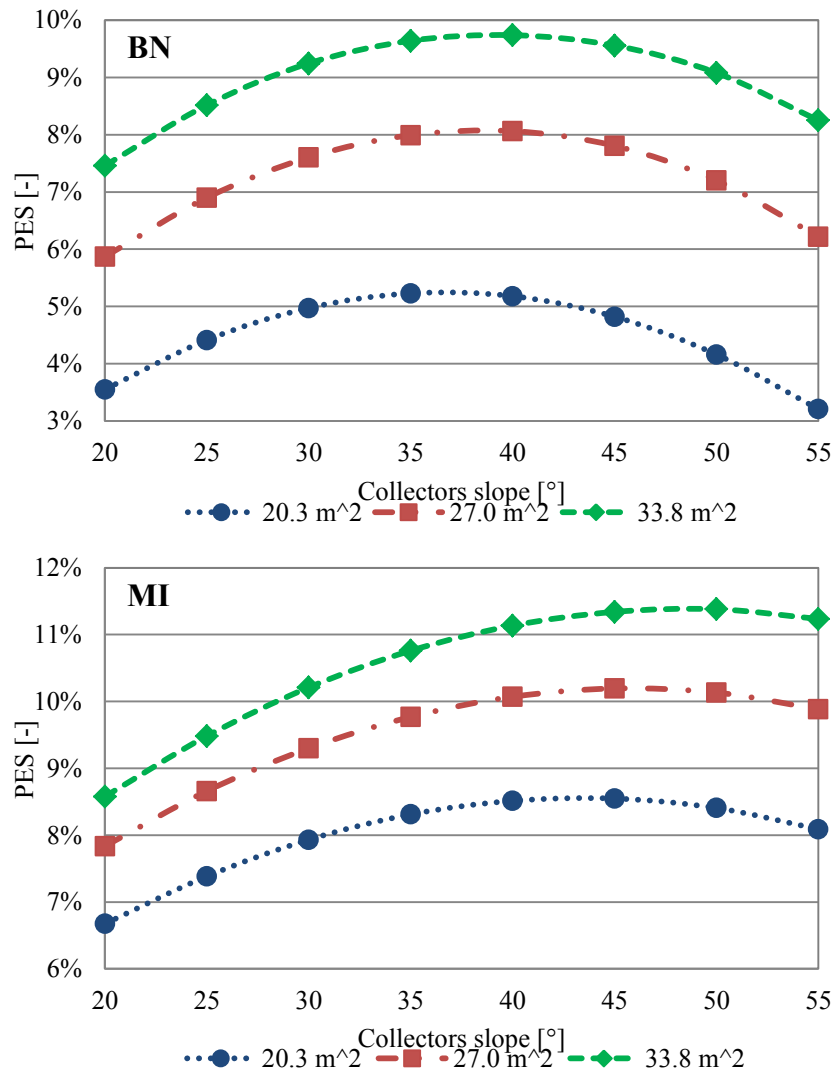


Figure 2.10: Primary Energy Saving of the Alternative Systems without further energy thermal demands and with flat plate collectors in Benevento (BN) and Milano (MI).

As regards the operation for air-conditioning only, the primary energy saving is greater for Milano installations than for Benevento ones, when employing flat plate collectors (Figure 2.10). This evidently derives from a longer activation period, during the heating season, so that the maximum PES in Milano is obtained with collectors inclination of the between 45° and 50°. In Benevento the operation is more biased towards the summer cooling mode, with lower optimal tilt angles.

The trends of the PES curves are similar for systems with evacuated tube collectors when solar thermal energy surplus is not taken into account (Figure 2.11). About a doubling of performance is observed for Benevento while the increase is less marked for Milano. The minor increase of the PES values that occurs in Milano, even if strange, because evacuated collectors are better suited for installation in colder locations, becomes clearer by analyzing the energy demands and availability. In Milano there are higher user demands, and so greater primary energy requirements of the CS than in Benevento (18.53 MWh instead of 14.50 MWh), and solar energy lower availability.

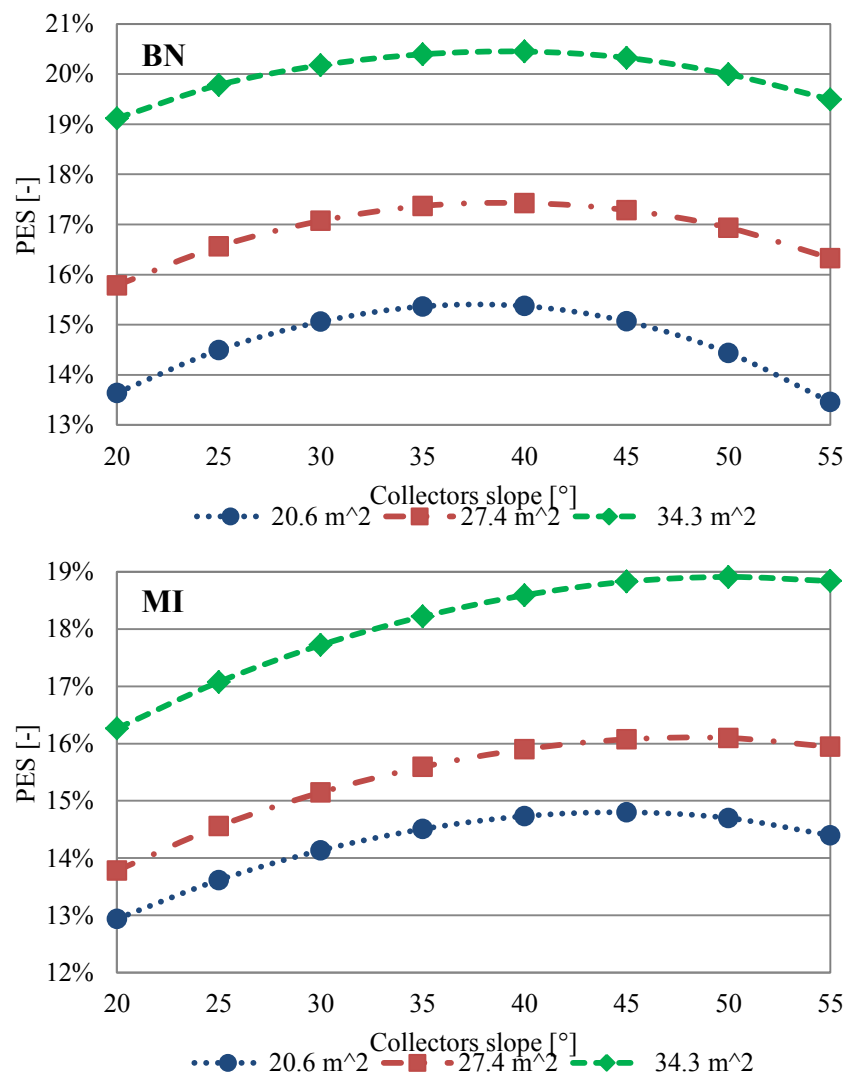


Figure 2.11: Primary Energy Saving of the Alternative Systems without further thermal energy demands and with evacuated tube collectors in Benevento (BN) and Milano (MI).

It follows that the benefits are compensated by these cons. In fact, if the solar subsystem is analyzed in greater detail, for the sake of brevity considering only the solutions with 34 m² of collectors and a tilt angle of 40°, it is observed that the percentage increase

(Improvement in Table 2.12) of net solar thermal energy (it takes into account the tank losses) in comparison with flat plate collectors is greater for Milano than for Benevento. Scenarios with further thermal energy demands highlight a marked improvement of the energy performance (Figures 2.12-2.15).

Table 2.12: Net solar thermal energy in the plants with 34 m² of solar collectors 40° tilt angle.

	BN	MI
Flat Plate [MWh]	7.14	5.89
Evacuated Tube[MWh]	8.67	7.42
Improvement [%]	21.05	25.67

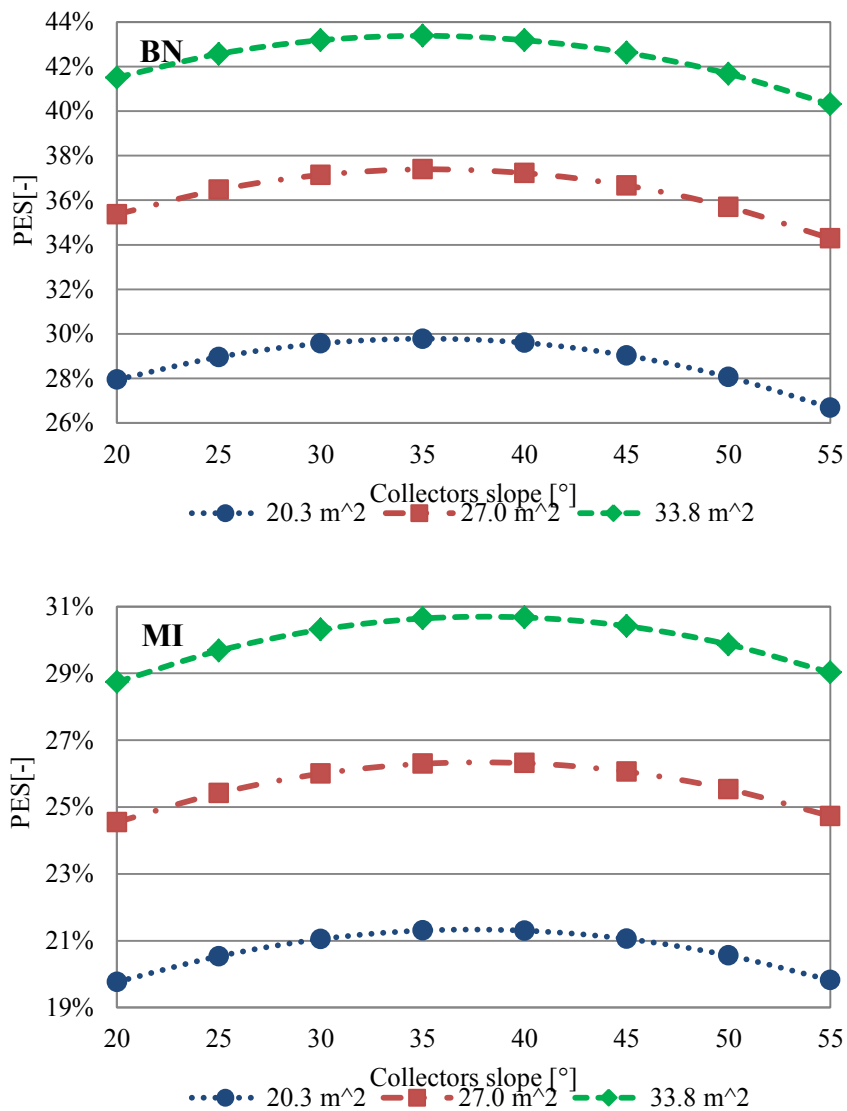


Figure 2.12: Primary Energy Saving of the Alternative Systems with 50% of solar thermal energy surplus exploited and with flat plate collectors in Benevento (BN) and Milano (MI).

The greater availability of solar energy and less severe outdoor conditions during winter imply that locations in Southern Italy are favored compared to Northern ones on an annual basis. This also determines that in Milano the optimum tilt angle is reduced (35-40°) and is a bit higher than in Benevento (35°) due to the different latitude. Plants with flat plate collectors ensure in Benevento a PES, which varies between 27 and 43% (Figure 2.12), depending on the collecting surface and the collectors inclination; when 50% of solar thermal energy surplus is used for DHW or other heating purposes, a PES between 40 and 58% occurs when evacuated tube collectors are considered (Figure 2.13). Energy performance remain in the range 20-31%, 30-45% for Milano (Figure 2.12 and Figure 2.13) when considering flat plate and evacuated tube collectors, respectively, as well as 50% of solar thermal energy surplus used for further energy demands.

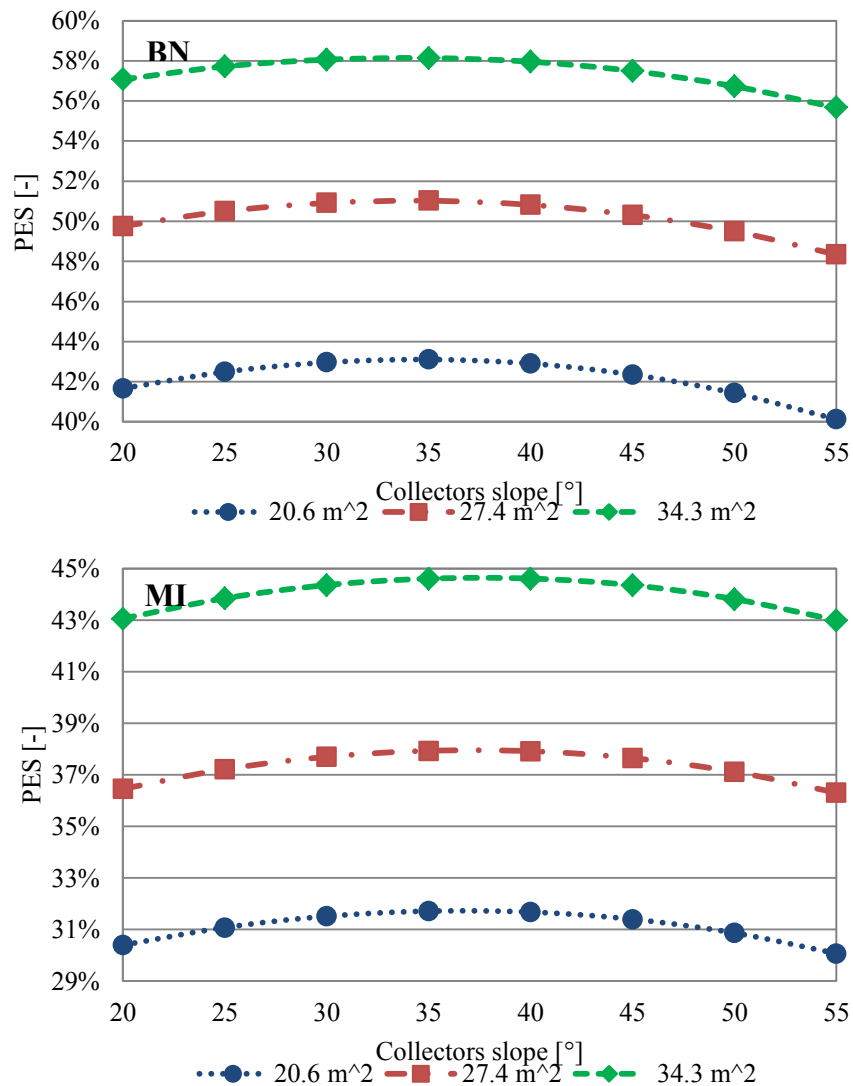


Figure 2.13: Primary Energy Saving of the Alternative Systems with 50% of solar thermal energy surplus exploited and with evacuated tube collectors in Benevento (BN) and Milano (MI).

The total use of thermal energy surplus further enhances energetic analysis (Figure 2.14 and Figure 2.15) for Benevento, a PES equal to over 71% is reached with evacuated tube collectors and it does not drop below 40% with flat plate ones. In Milano, instead, the variation is between 29% (minimum PES value with 20 m² flat plate collectors) and 58% (maximum PES value with 34 m² evacuated tube collectors).

Regarding the environmental analysis, the trends of equivalent CO₂ emissions curves are very similar to those of the PES ones. It was found that these curves are simply reduced by about 2 percentage points for plants with flat plate collectors, and by about 3 percentage points for systems with evacuated tube collectors. Therefore these graphs are not reported for brevity.

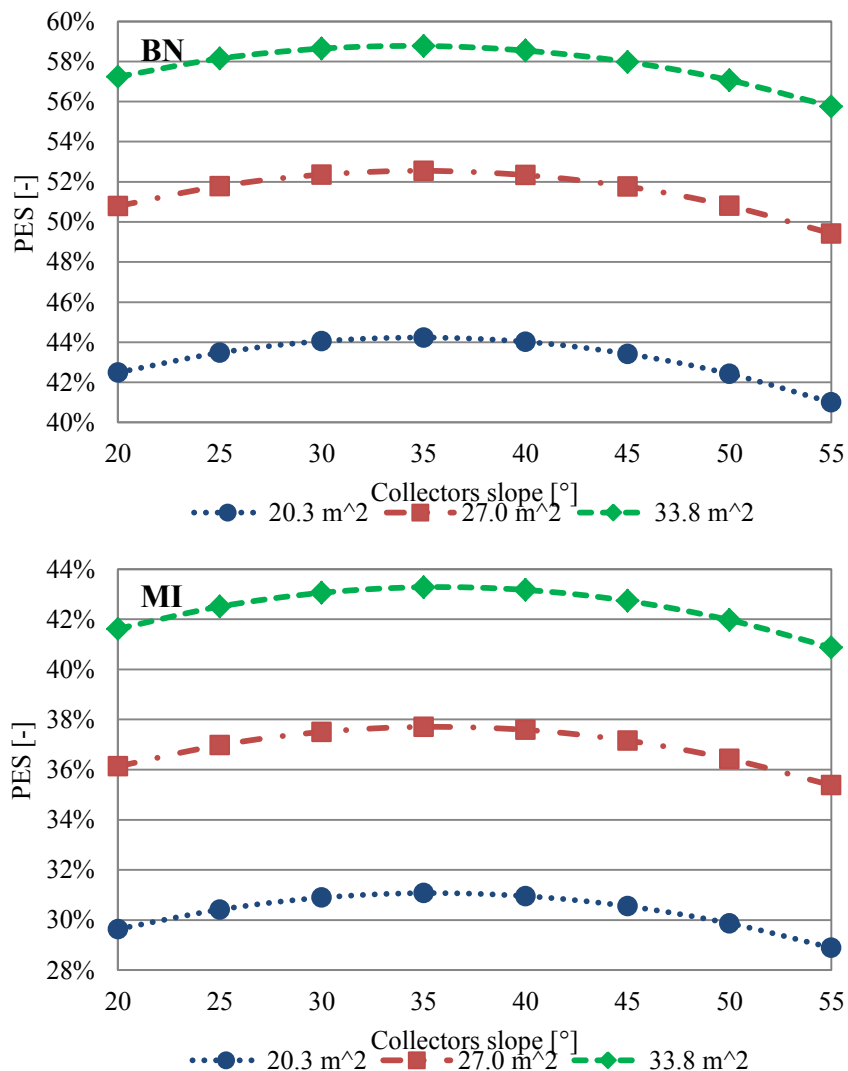


Figure 2.14: Primary Energy Saving of the Alternative Systems with 100% of solar thermal energy surplus exploited and with flat plate collectors in Benevento (BN) and Milano (MI).

As regards economic analysis, initial costs of alternative systems are still too high compared to those of conventional ones. The AHUs with DW are not very common devices and represent an important cost contribution to the total investment. Also the cost of the thermal storage tank is not negligible. Finally, the solar field has a cost that increases with the surface and the efficiency of the chosen collectors.

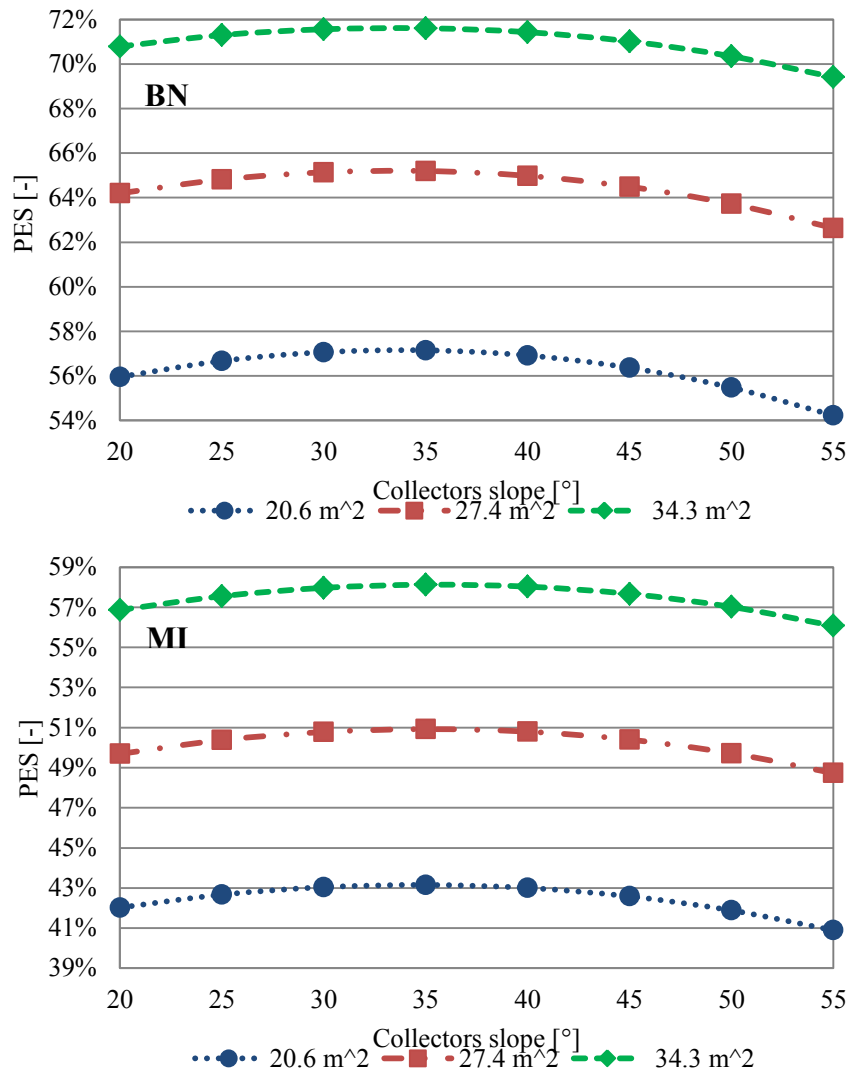


Figure 2.15: Primary Energy Saving of the Alternative Systems with 100% of solar thermal energy surplus exploited and with evacuated tube collectors in Benevento (BN) and Milano (MI).

The mechanism of financial support to the production of thermal energy from renewable sources, currently in force in Italy, establishes an incentive which is a function of the collectors area and type (with or without concentration). Considering the results of the simulations with flat plate and evacuated tube collectors, in Benevento and in Milano the innovative air-conditioning systems do not allow to obtain SPB compatible with the useful life of the plant components if the solar thermal energy surplus exploitation, at

least partial, is not taken into account. However, for Milano the SPB periods are shorter than those for Benevento thanks to the greater number of operation hours.

When considering the surplus of solar thermal energy, used for half or completely, SPB periods become interesting. Histograms of Figures 2.16 and 2.17 represent the SPB periods with optimal tilt angle for systems with flat plate and evacuated tube collectors, respectively, as a function of the solar thermal energy surplus used and of the collecting surfaces. The effect of the tilt angle on the SPB is not shown, however it can imply a maximum increase of 3 years.

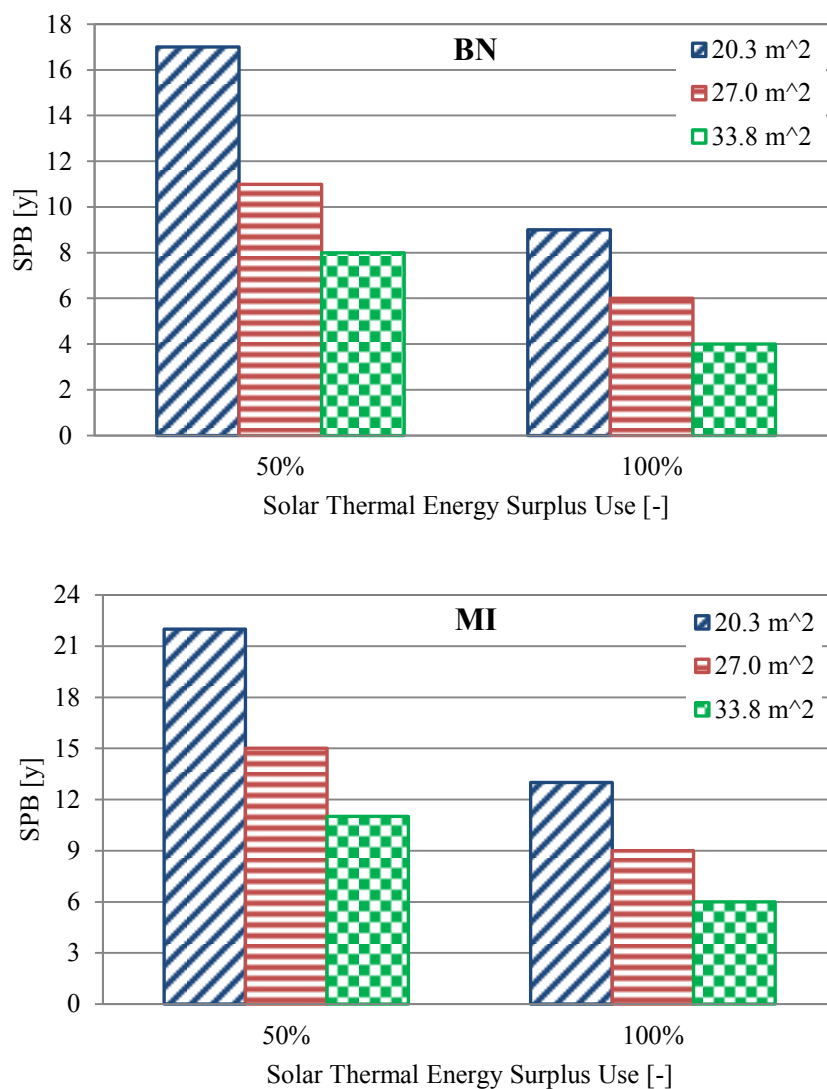


Figure 2.16: The best Simple Pay Back periods of the Alternative System with flat plate collectors in Benevento (BN) and Milano (MI).

The results are better for Benevento than for Milano because of the more favorable climatic conditions during winter; in addition they improve when both the collecting

surface and the percentage of solar thermal energy surplus exploited increase. Systems with flat plate collectors with the smallest solar field surface show SPB periods longer than those with evacuated tube collectors. Vice versa with a surface of 27 and 34 m², plants with flat plate collectors are equivalent or better from an economic point of view than those with evacuated tube collectors. Exploiting 50% of the solar thermal energy that is not used for conditioning of the building a minimum SPB period of 8 years is obtained in Benevento and 12 years in Milano. It decreases to a minimum of 6 years when the full use of solar thermal energy is assumed.

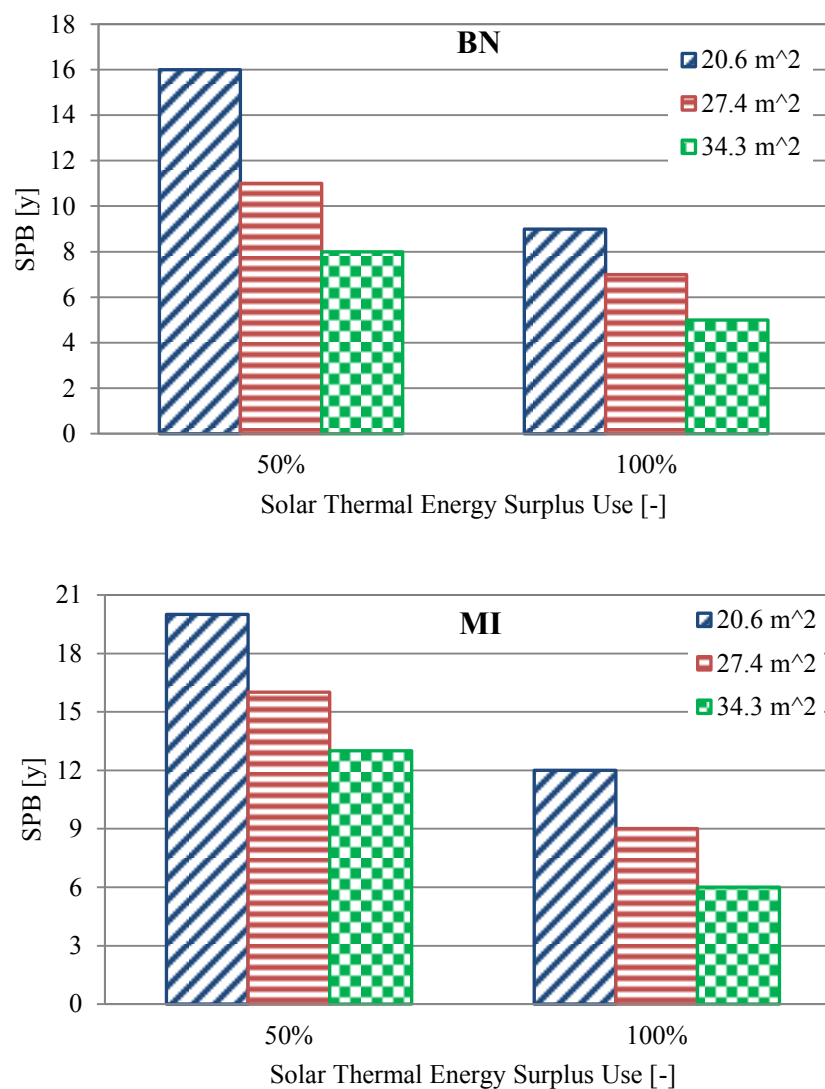


Figure 2.17: The best Simple Pay Back periods of the Alternative System with evacuated tube collectors in Benevento (BN) and Milano (MI).

**Chapter 3 Desiccant-based AHU interacting with a
CPVT collector: Simulation of energy and
environmental performance**

3.1 Introduction

Desiccant-based Air Handling Units (AHU) provide significant technical and energy/environmental advantages with respect to conventional systems, especially when the regeneration of the desiccant material is obtained by means of a renewable energy source, such as solar energy. In this chapter one considers that thermal energy for DW regeneration is provided by CPVT (Concentrating Photovoltaic/Thermal) collectors, simultaneously producing also electricity. These collectors are considered one of the most promising solar technologies. In fact, CPVT thermal energy can drive (integrated by a natural-gas fired boiler) a desiccant-based AHU, since the silica-gel wheel, used for the dehumidification and included in that system, must be continuously regenerated. The regeneration temperature of the wheel (40–70 °C, depending on the dehumidification required) is compatible with the CPVT outlet temperature (80–100 °C). Simultaneously, the electricity produced by CPVT collectors can feed the auxiliary devices of the plant and balance the electric load of the building. Furthermore, the heat supplied from the solar collector can be used for the pre and post heating of the process air during winter operation.

3.2 Loads characterization

The sensible and latent loads have been determined by simulating the same building described previously (Section 2.2) only in Benevento. The occupancy schedule, the activities done, the temperature and humidity set points are the same. The only difference from the simulations of Chapter 2 concerns the air-conditioning operation period that, in this case, starts with the opening of the classroom. The loads calculated on an annual basis are reported in Table 3.1.

Table 3.1: Building loads.

Load	Summer Period	Winter Period	Intermediate Period
Sensible [MWh]	1.50	2.65	-
Latent [MWh]	0.68	0.57	-
Electric [MWh]	0.44	0.56	0.50

3.3 Plant configuration and operation

In this paper, the MCHP which is considered as a heat source in the test facility, is replaced by CPVT collectors equipped with triple junction cells (Figure 3.1). In order to supply the system with a high amount of thermal energy through the renewable energy source, two CPVT solar collectors are considered in the following set-up.

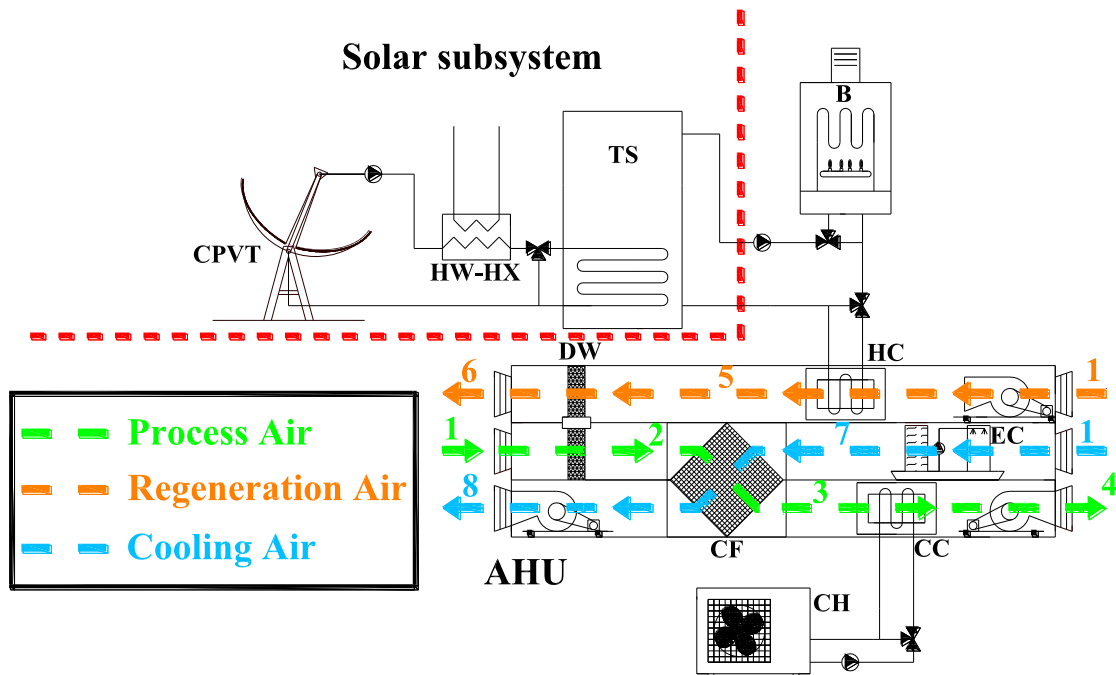


Figure 3.1: Scheme of the simulated plant in summer period.

For an easier understanding of the operation of the system, it can be divided into two subsystems: which are the solar subsystem, and the cooling/heating subsystem. The solar subsystem includes: solar collectors, pump, heat exchanger for the domestic hot water and thermal storage tank. The cooling/heating subsystem instead includes: the chiller (only in summer operation), the boiler and the air handling units. As regards the solar subsystem, CPVT collectors all year long collect solar radiation and convert it simultaneously in thermal and electrical energies. Thermal energy, available as hot water, is stored in the tank. The circulation pump of the solar loop is switched on only when the solar collectors outlet temperature is higher than the inlet one. In addition, the plant control system regulates the flow rate of the pump in the solar loop (from 10% to 100% of its rated power) in order to achieve the CPVT set-point outlet temperature (80 °C during the summer period and 60 °C during the winter). However, when solar radiation is particularly high and/or heat demand is scarce, CPVT outlet temperature

may exceed the fixed set point. In this case, the temperature of the fluid is reduced by a heat exchanger simultaneously producing domestic hot water. The heat exchanger is therefore a further tool for the control of the temperature of the heat transfer fluid which, unlike the classical dissipation systems used in solar cooling plants (dry coolers), allows one to convert exceeding solar energy into useful energy (domestic hot water). Moreover, in order to improve CPVT thermal production also when the air-conditioning system is switched off (intermediate season and weekend days), a three-way valve is set to bypass the tank, using only the heat exchanger to continuously produce domestic hot water instead of maintaining the collectors out of focus. In this period, the control system tries to maintain the heat transfer fluid at a temperature of 60°C. For example, considering the energy needs given in Italian Standards (UNI TS 11300) for sports centers, the system is estimated to be able to meet entirely the demand for DHW of a sports center equipped with 18 showers (100 l/(shower day)). As regards the cooling/heating subsystem, the AHU supplies air to the conditioned space in order to maintain comfort conditions. During the summer period the thermal energy, taken from the tank, is used to regenerate the hygroscopic material (silica-gel) of the desiccant wheel, this process is necessary for the dehumidification of the outdoor air. The temperature at which the regeneration process takes place depends on the amount of moisture to remove from the outdoor air. The control system compares the tank and the regeneration temperatures and if the former is lower it turns the boiler on. After this dehumidification process, the chiller provides cooling energy to the process air to also balance the sensible load. The processes taking place in the AHU have already been described in detail in Section 2.3.1. During the winter, the thermal energy stored into the tank is exploited to heat the outdoor air, however if storage temperature is too low when compared to that required for the processes that have been described in Section 2.3.2, then the natural gas boiler supplies the missing energy. The electricity produced by the CPVT collectors drive the pumps, the AHU auxiliaries, the electric chiller and satisfies as far as possible the electric load. When the electricity production is low compared to the amount required to operate the system, further electric power is taken from the electric grid; instead, when the production exceeds the demand, the exceeding part is fed into the grid. Hereinafter, the main component of the system, the CPVT solar collector, not previously described (Chapter 1 and Chapter 2), is briefly described.

3.3.1 Concentrating Photovoltaic/Thermal Solar Collector [76]

The idea of CPVT considered in this study is based on the work of Bernardo [77] and Bernardo et al. [78] and on a prototype that has been recently commercialized [77-79]. The CPVT (Figure 3.2) consists of a parabolic trough concentrator and a one-axis tracking system that uses the same operating principle of solar thermal Parabolic Trough Collectors (PTC) [80-82]. The collector is placed horizontally with its axis North–South oriented, whereas the tracking system follows the solar azimuth angle. In solar thermal PTC, an evacuated tube for heating the fluid is installed at the focus of the parabola while in the considered CPVT system the focus of the parabola is equipped with a triangular receiver (Figure 3.2). A metallic substrate is used between the circular fluid channel and the external surfaces (PV layer and top surface in Figure 3.2) in order to allow conductive heat transfer.

The two sides of the triangle facing the parabolic concentrator are equipped with triple-junction PV layers, whereas the top side of the receiver is equipped with a thermal absorber. The triangular receiver includes an inner channel through which the fluid to be heated flows.

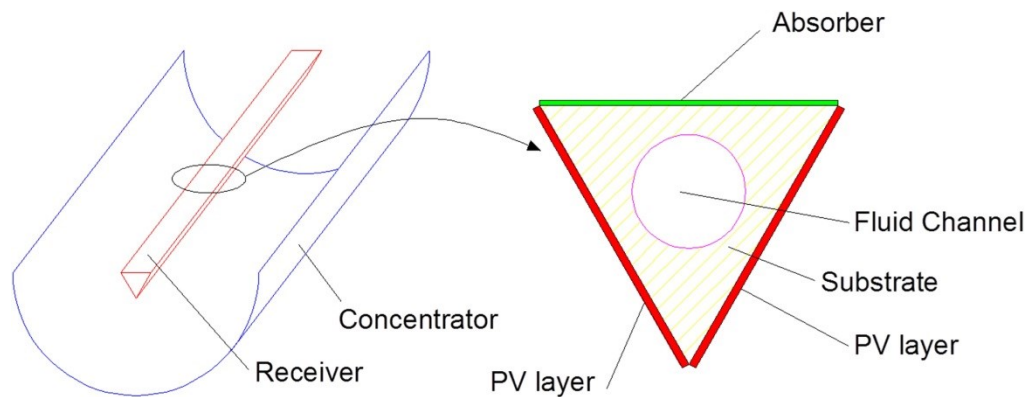


Figure 3.2: CPVT layout [76].

Therefore, the solar irradiation collected is converted simultaneously into electricity by the PV layer and into thermal energy by the heated fluid. In summary, the system considered in this work is basically the same as the one shown in the references [77-78], with only two main differences:

- a) there is no covering glass;
- b) the PV layer is based on InGaP/InGaAs/Ge triple-junction solar cells [83].

These two modifications increase significantly the electrical efficiency of the system with respect to the values reported in references [77-78]. In fact, the covering glass is used to increase the thermal efficiency of the system, as it reduces convection and

radiation losses. The glass also reduces the radiation incident on the PV layer, causing a possible decrease of the electrical efficiency of the system. However, the triple-junction cells are significantly more efficient than silicon ones and they are also less sensitive to the variation of the operating temperature.

3.4 Mathematical models

In this chapter, the presented simulations are also performed using the commercial software TRNSYS 17 [58] integrated with the TESS libraries [59]. The project has been developed, implementing some models taken from TRNSYS libraries. Additional models were developed by Calise et al. [76], during their research activities. Such models was implemented in Fortran and linked to the TRNSYS simulation environment. All the models included in TRNSYS library are considered highly reliable by the scientific community. The models of the used components were previously validated by experimental data, as shown in references.

The validation of the whole plant has not been carried out because the experimental set-up, unfortunately does not include the CPVT collectors. However, considering that all the components were previously and successfully validated against experimental data, it can be assumed that the simulated results are highly reliable. The model of the CPVT collector is described below. The other components are the same ones of the system described in the previous chapter, therefore, are not described again.

The performance assessment of the proposed system is carried out by calculating the energy and environmental indices introduced in Section 2.5.3, however, it should be noted that in this case there are bidirectional flows of electricity with the electric grid and so the primary energy (E_p) of the alternative system is evaluated taking into account that the energy efficiency of the Italian national electric system, including transmission and distribution losses is 42% (CO₂ equivalent emission is 0.573 kgCO₂/kWh_{el}) when the energy is taken from the grid, 43.5% (CO₂ equivalent emission is 0.550 kgCO₂/kWh_{el}) when the energy is fed into the grid (since transmission losses are avoided). The economic analysis cannot be performed because the solar collector is not yet commercialized.

3.4.1 CPVT collectors [76]

The general assumptions adopted for the model are: thermodynamic equilibrium, steady state, negligible kinetic and gravitational terms in the energy balances and radiation

uniformly concentrated along PV area. In addition, negligible temperature gradients in the PV film and in the substrate are assumed due to the small thickness of the PV layer and the high conductivity in the metal substrate. In other words, PV and substrate temperatures are assumed uniform. The system is assumed to operate below 100 °C, since it is safer for the reliability of PV cells, although the system can theoretically operate up to 240 °C [84]. In this case, the CPVT could drive a double effect Absorption Chiller, significantly increasing the overall efficiency of the system. However, this possibility must still be explored by experimental tests. Water was assumed as cooling fluid. Nevertheless, several types of cooling fluids can be considered in the model.

The thermodynamic and thermo-physical properties of the fluids, namely air and water, are calculated using the appropriate routine included in TRNSYS. The concentration ratio is defined as the ratio between the area, A_{PVT} , of the two PV triangular sides of the receiver, and the aperture area, A_{ap} , of the concentrator:

$$C_{PVT} = A_{ap} / A_{PVT} \quad (3-1)$$

The optical efficiency (η_{opt}) of the concentrator is assumed being constant [84]. Therefore, the radiation incident on the PV surface is:

$$G_{PVT} = A_{PVT} I_b C_{PVT} \eta_{opt} IAM_{th} \quad (3-2)$$

As it is commonly done in concentrating systems, only the beam incident radiation (I_b) is considered in the previous equation. Such radiation is corrected considering both the optical efficiency of the receiver and the Incidence Angle Modifier (IAM_{th}) [64], that takes into account that the radiation decreases when the angle of incidence increases. The IAM_{th} , related to the thermal production is evaluated on the basis of the data experimentally calculated by Bernardo et al. [77,78].

Simultaneously, additional thermal energy is absorbed by the surface, A_{top} , of the top thermal absorber whose absorptance is α_{top} .

$$\dot{Q}_{top} = A_{top} G \alpha_{top} \quad (3-3)$$

The radiative heat transfer between the top absorber and the sky can be calculated as follows [64]:

$$\dot{Q}_{top-sky} = A_{top} \varepsilon_{top} \sigma (T_{top}^4 - T_{sky}^4) \quad (3-4)$$

Here, the sky equivalent temperature (T_{sky}) is calculated using TRNSYS routine. T_{top} is the temperature of the top surface, ε_{top} is its emittance and σ is the Stefan-Boltzmann constant.

Similarly, the radiative heat transfer between the PVT and the concentrator [64]:

$$\dot{Q}_{PVT-conc} = A_{PVT} \varepsilon_{PVT} (T_{PVT}^4 - T_{conc}^4) \quad (3-5)$$

where T_{PVT} and T_{conc} are respectively PVT and concentrator surfaces temperatures.

The convective heat transfer between the PVT and the air is calculated as follows [85]:

$$\dot{Q}_{conv,PVT} = A_{PVT} h_{c,PVT} (T_{PVT} - T_a) \quad (3-6)$$

where $h_{c,PVT}$ is the convective heat transfer coefficient between lateral absorber and the air.

The convection heat transfer between the top absorber and the air is [85]:

$$\dot{Q}_{conv,top} = A_{top} h_{c,top} (T_{top} - T_a) \quad (3-7)$$

where $h_{c,top}$ is the convective heat transfer coefficient between top absorber and the air.

The gross electrical power produced by the PV layer is:

$$P_{PVT,gross} = C_{PVT} A_{PVT} I_b \eta_{opt} \eta_{PV} IAM_{el} \quad (3-8)$$

The electrical efficiency of the triple-junction PV (η_{PV}) is experimentally related to the concentration ratio and to the temperature [84]:

$$\eta_{PV} = 0.298 + 0.0142 \ln(C_{PVT}) + [-7.15 + 0.697 \ln(C_{PVT})] \cdot 10^{-4} (T_{PVT} - 298) \quad (3-9)$$

Note that this equation returns ultra-high values of electrical efficiency, also approaching 40%, as usual in III-V PV cells. The IAM_{el} is also evaluated on the basis of the experimental data provided by Bernardo et al. [77,78].

The net power produced by the system is reduced by the amount of electricity lost in the module connections and in the inverter, considering the corresponding efficiencies (η_{mod} and η_{inv}) [84]:

$$P_{PVT,net} = P_{PVT,gross} \eta_{mod} \eta_{inv} \quad (3-10)$$

Finally, the heat absorbed by the cooling fluid is:

$$\dot{Q}_f = \dot{m}_f (h_{f,out} - h_{f,in}) \quad (3-11)$$

Therefore, the overall energy balance on a control volume that included the entire triangular receiver is:

$$A_{PVT} I_b C_{PVT} \eta_{opt} IAM_{th} + A_{top} G \alpha_{top} = \dot{m}_f (h_{f,out} - h_{f,in}) + C_{PVT} A_{PVT} I_b \eta_{opt} \eta_{PV} IAM_{el} + A_{PVT} I_b \eta_{opt} IAM_{th} \rho_{PVT} + A_{top} \varepsilon_{top} \sigma (T_{top}^4 - T_{sky}^4) + A_{top} \varepsilon_{PVT} \sigma (T_{PVT}^4 - T_{conc}^4) + A_{PVT} h_{c,PVT} (T_{PVT} - T_a) + A_{top} h_{c,top} (T_{top} - T_a) \quad (3-12)$$

A second energy balance considers the control volume that includes the metallic substrate and the fluid channel. In this study, this control volume can be considered as a heat exchanger. In particular, it is assumed here that the temperature of the metallic substrate is homogeneous along both radial and circumferential directions. According to the 0-D approach implemented here, the performance of the heat exchanger can be calculated using the well-known ε -NTU technique [86]. For the case under consideration, the NTU number is:

$$NTU = \left(\frac{A_{HEX}}{\dot{m}_f c_{p,f}} \right) \bigg/ \left(\frac{1}{h_f} + r_{sub} \right) \quad (3-13)$$

where r_{sub} is the thermal resistance of the metallic substrate, \dot{m}_f is the fluid mass flow rate and $c_{p,f}$ its specific heat.

The energy balance for the considered heat exchanger is:

$$\dot{m}_f (h_{f,out} - h_{f,in}) = \varepsilon \dot{m}_f c_{p,f} (T_{sub} - T_{in}) \quad (3-14)$$

where T_{sub} is the temperature of the metallic substrate.

The third of the required five equations is derived from an energy balance on a control volume including the PVT layer, and the metallic substrate.

$$A_{PVT} \frac{T_{PVT} - T_{sub}}{r_{PVT-sub}} = \dot{m}_f (h_{f,out} - h_{f,in}) + A_{top} \frac{T_{sub} - T_{top}}{r_{top}} \quad (3-15)$$

A fourth energy balance can be considered with respect to the control volume that includes the top side of the substrate and the top surface of the triangular receiver:

$$A_{top} \frac{T_{sub} - T_{top}}{r_{top}} + A_{top} G \alpha_{top} = A_{top} G \alpha_{top} \rho_{top} + A_{top} \varepsilon_{top} \sigma (T_{top}^4 - T_{sky}^4) + A_{top} h_{c,top} (T_{top} - T_a) \quad (3-16)$$

Finally, the last energy balance considers the control volume that includes only the parabolic concentrator.

$$A_{PVT}\epsilon_{PVT}(T_{PVT}^4 - T_{conc}^4) + GA_{conc}\alpha_{conc} = A_{conc}\epsilon_{conc,back}(T_{conc}^4 - T_{sky}^4) + A_{conc}h_{c,conc,front}(T_{conc} - T_a) + A_{conc}h_{c,conc,back}(T_{conc} - T_a) \quad (3-17)$$

Eqs. (3-12), (3-14), (3-15), (3-16), (3-17) represent a system of five equations in the above mentioned five unknowns. This system of equations is highly nonlinear as a consequence of the radiative terms included in the energy balances and also of the correlations for the calculations of heat transfer coefficients. This system must be solved by conventional numerical iterative techniques.

The overall performance of the CPVT is often evaluated using the well-known thermal and electrical efficiencies, which are conventionally related to the incident beam radiation and to the collector aperture area:

$$\eta_{CPVT,th} = \dot{m}_f (h_{out} - h_{in}) / A_{ap} I_b \quad (3-18)$$

$$\eta_{CPVT,el} = C_{PVT} A_{PVT} I_b \eta_{opt} \eta_{PV} IAM_{el} / A_{ap} I_b \quad (3-19)$$

CPVT design parameters are reported in Table 3.2 [77,78,84,87,88]. For the design parameters assumed in this table, the concentration ratio is 10.

Table 3.2: CPVT design parameters

Parameter	Symbol	Value	Unit
CPVT aperture area	A_{ap}	12	m ²
Top absorber area	A_{top}	0.60	m ²
PV layer area	A_{PVT}	1.2	m ²
Fluid channel diameter	d	0.03	M
Fluid specific heat	$c_{p,f}$	4.19	kJ/(kgK)
Rated fluid flow rate	\dot{m}_f	0.15	kg/s
Top surface absorptance	α_{top}	0.90	-
Concentrator absorptance	α_{conc}	0.03	-
Back surface concentrator emissivity	ϵ_{conc}	0.30	-
Top surface emissivity	ϵ_{top}	0.20	-
PV reflectance	ρ_{PVT}	0.03	-
PV emissivity	ϵ_{PVT}	0.20	-
IAM electrical coefficient	b_{0el}	0.28	-
IAM thermal coefficient	b_{0th}	0.14	-

3.5 Simulation and results

As stated above, the air conditioning system is switched on only during the summer (June 1st – September 15th) and in the winter (November 15th – March 31st). It is off on weekend days and during intermediate period (April 1st – May 30th and September 16th – November 14th). The simulations have been carried out using a time step of 1.5 min. The design parameters of the components have been set according to the values obtained from the experimental tests, when they are available. In all the other cases the design parameters were set on the basis of the rated values of the components. As CS in the summer period, a standard AHU in which the process air is mechanically dehumidified and then post-heated, was simulated. A vapor compression chiller with a cooling capacity of 16 kW fed the cooling coil whereas the 24 kW boiler ($\eta_B = 90.2\%$) fed the post-heating heat exchanger. In winter the CS and the AS are the same except for the source of heat that consists solely of the boiler in the CS. All electricity in the building-plant system is taken from the grid and DHW is produced with the boiler.

The classroom has no DHW demands, therefore it is assumed that such DHW is provided to a nearby building (i.e. a gym or a hotel) that has a constant daily DHW demand.

The simulation tool developed in this paper allows one to analyze the results on any time basis desired. In fact, simulations return both dynamic temperature and powers plots and such results may be integrated on whatever time-basis (hours, weeks, months, year, etc.). As a consequence, each simulation returns a huge amount of data useful for the designer of the system. For the sake of brevity in this analysis, dynamic plots will be shown only for two representative summer and winter days. Conversely, monthly-integrated results will be presented in order to show the variations of the main parameters during the year. Finally, the overall performance of the system under investigation is analyzed presenting the yearly values of the selected parameters. Results of simulations on a daily (with reference to a typical summer day and one winter), monthly and annual basis will be reported and analyzed below.

Figure 3.3 shows the thermal (a) and electrical powers (b) of a typical summer day (July 27th). Here, it is clearly shown that the load dramatically depends on the presence of people in the classroom. In particular, the latent load (Figure 3.3 a, gray line, Q_{lat}) shows a trend similar that of the occupancy (Figure 2.1).

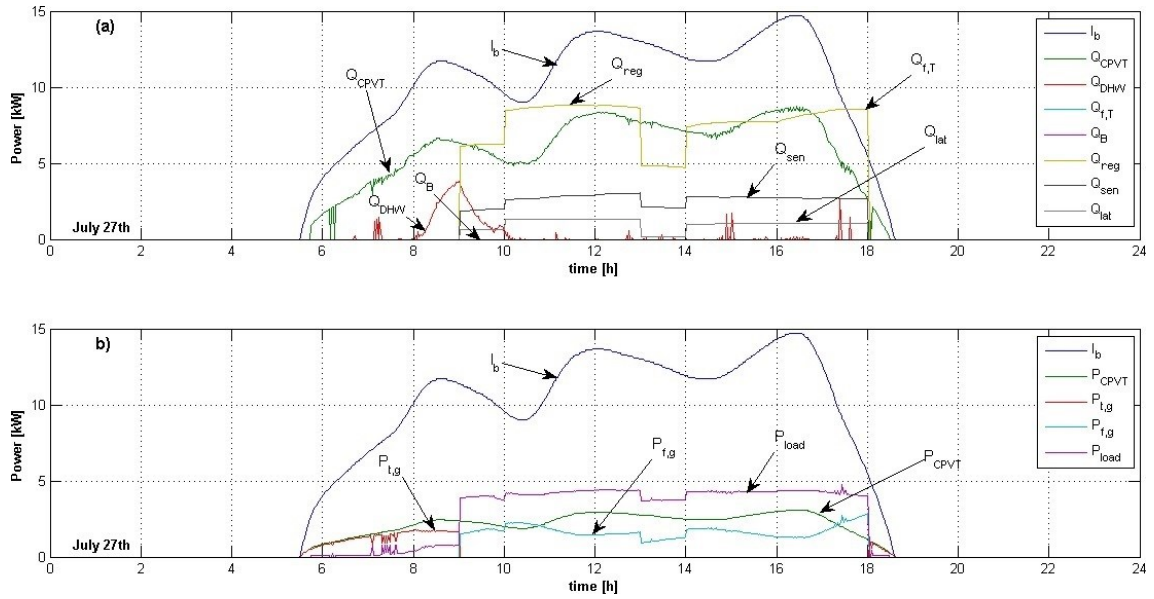


Figure 3.3: Typical summer weekday powers (27/07).

Concerning the combined production of electric energy and heat, as was reasonable to expect, the solar collector has higher efficiency in the thermal conversion than in the electric one. As expected, CPVT thermal and electrical powers (Q_{CPVT} , P_{CPVT}) dramatically depend on the availability of beam radiation (I_b). The figure also shows that the thermal flow produced by the CPVT is significantly higher than the electrical one. This is due to the fact that the thermal efficiency of the CPVT under investigation fluctuates around 50%, whereas the electrical efficiency is typically close to 20%. Such values, calculated with respect to the incident beam radiation, show excellent performance of the proposed CPVT from both thermal and electrical points of view. For the selected summer day, the thermal energy stored is adequate to regenerate the DW. In fact, the auxiliary power demanded to the boiler is negligible (Q_B , magenta line) and the curve representing the energy taken from the tank ($Q_{f,T}$) covers perfectly that of the regeneration (Q_{reg}). The CPVT thermal energy production (Q_{CPVT}) starts in the early morning when there is no heat demand from DW regeneration (Q_{reg}). During this period, CPVT heat is stored in the tank and a significant production of DHW (Q_{DHW}) takes place in the last part of this period (8:00-10:00). Further on, when the AHU is activated, CPVT thermal production (Q_{CPVT}) is sometimes higher than regeneration demand (Q_{reg}). As a consequence and in this circumstance, the tank is charged. Conversely, when CPVT thermal power is lower than DW regeneration demand, some heat is taken from the tank, which is discharged. For the selected summer day, a certain amount of thermal energy remains stored in the tank (3.31 kWh).

Figure 3.3 (b) also shown that CPVT electric energy in the early morning is almost entirely fed into the grid ($P_{CPVT} \approx P_{t,g}$). This happens until the air-conditioning system stays off, whereas in the central part of the day same power is taken from the grid ($P_{f,g}$), since CPVT electrical production is lower than system demand ($P_{CPVT} < P_{load}$).

As regards the winter day (February 14th), (Figure 3.4 (a)) one observes that the solar subsystem provides the majority of the thermal energy to the pre- and post-heating of the process air; the contribution of the boiler (Q_B) is limited to the initial and final part of the day. In particular, the pre and post-heating thermal energy (79 kWh) is balanced for about 83% by the tank energy and for the remaining 17% by the boiler energy. Here, CPVT thermal energy produced in the early morning (7:00-9:00) is stored in the tank and then is used in the afternoon. Figure 3.4 (a) also shows that after 3:00 in the afternoon and up to about 5:00 pm solar thermal production is lower than the load of pre- and post-heating ($Q_{CPVT} < Q_{pre} + Q_{post}$) and then becomes null. In this case, the tank is discharged, reducing its temperature, and provides a part of the demanded thermal power ($Q_{pre} + Q_{post}$). The additional amount of heat is produced by the boiler (Q_B , magenta curve).

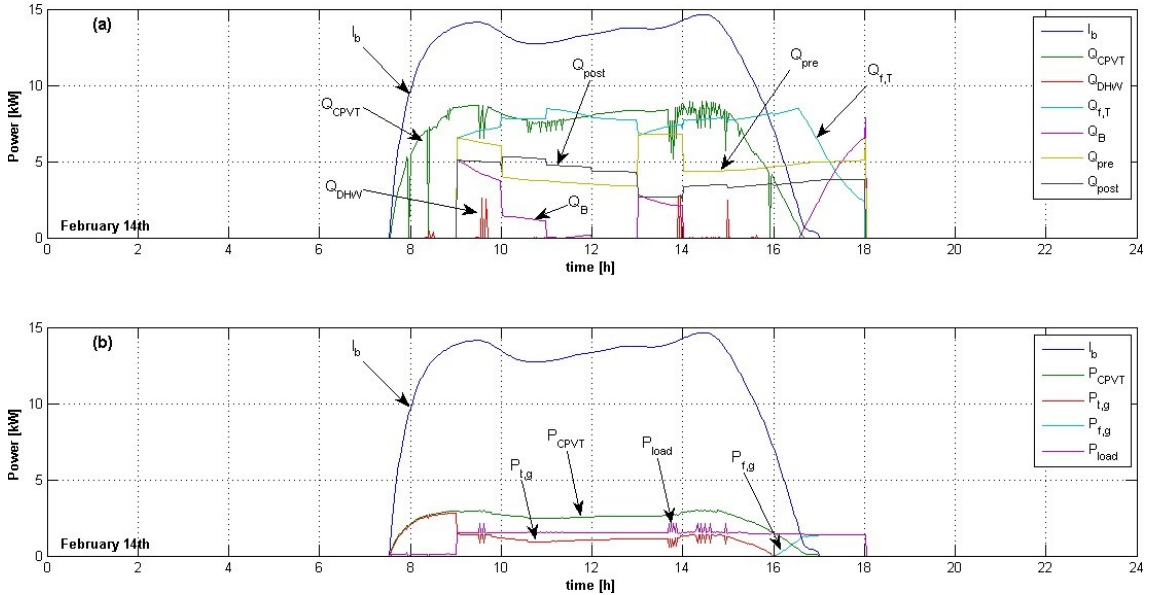


Figure 3.4: Typical winter weekday powers (14/02).

For the selected winter day, CPVT solar thermal energy production (64.0 kWh) is slightly lower than the energy taken from the tank (65.4 kWh). The DHW production is not significant (Q_{DHW}).

The electrical load of users is lower than CPVT generation ($P_{load} < P_{CPVT}$) because the electric chiller is off, however between 16:00 and 18:00, some power is taken from the

grid ($P_{f,g}$), and in the remaining part of the day there is always an amount of power ($P_{t,g}$) fed into the grid (10.7 kWh), (Figure 3.4 (b)).

Note that the thermal and electrical performance of the CPVT dramatically varies between the selected summer (Figure 3.3) and winter (Figure 3.4) day. This is due to the fact that the selected CPVT collector is particularly sensitive to the availability of beam radiation. As a consequence, during the winter both CPVT thermal and electrical performance dramatically decrease.

The monthly-integrated results in terms of thermal energy are shown in Figure 3.5, in Figure 3.6 electrical energy is reported.

As expected, CPVT thermal energy ($E_{th,CPVT}$) is very low in the months of January, February, November and December, significantly lower than half of the heating requirements of pre-and post-heating ($E_{pre+post}$) and DHW ($E_{th,DHW}$). Particularly in January and December, CPVT thermal energy is scarce and the majority of the demanded heat is provided by the boiler ($E_{th,B}^{AS}$). This is due to dramatic decrease of CPVT thermal performance during the winter, previously discussed. In the other three months, the availability of the solar source increases and the AHU thermal energy demand ($E_{pre+post}$) decreases simultaneously. As a consequence, a higher amount of DHW is also produced ($E_{th,DHW}$).

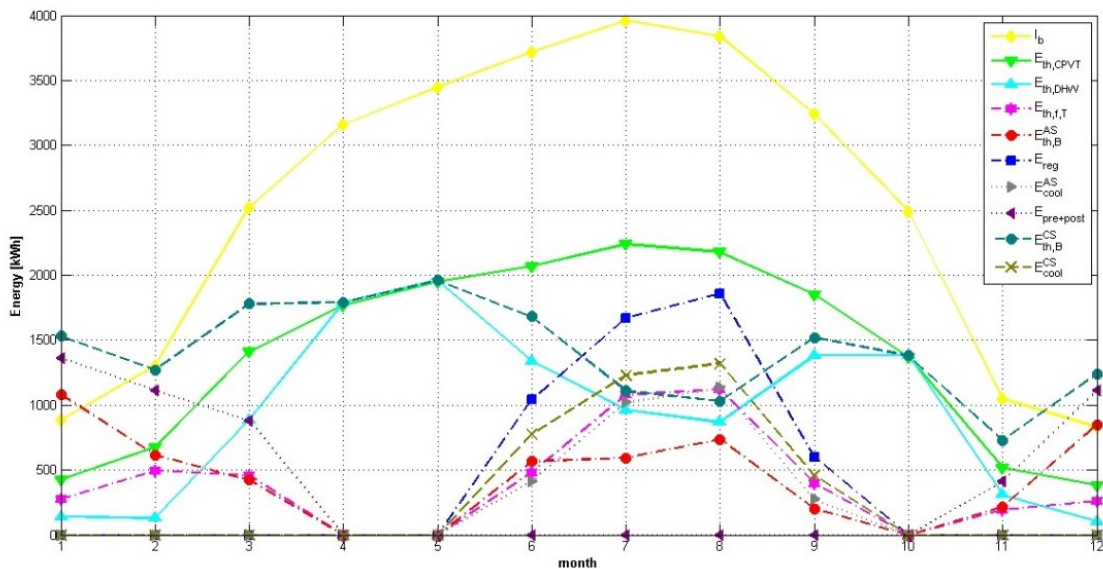


Figure 3.5: Monthly thermal energies of the conventional and alternative system.

Moving on to the intermediate period, Figure 3.5 shows that there is a high availability of solar thermal energy ($E_{th,CPVT}$), which is converted mainly in DHW ($E_{th,DHW}$) since no thermal demand comes from DW regeneration (E_{reg}).

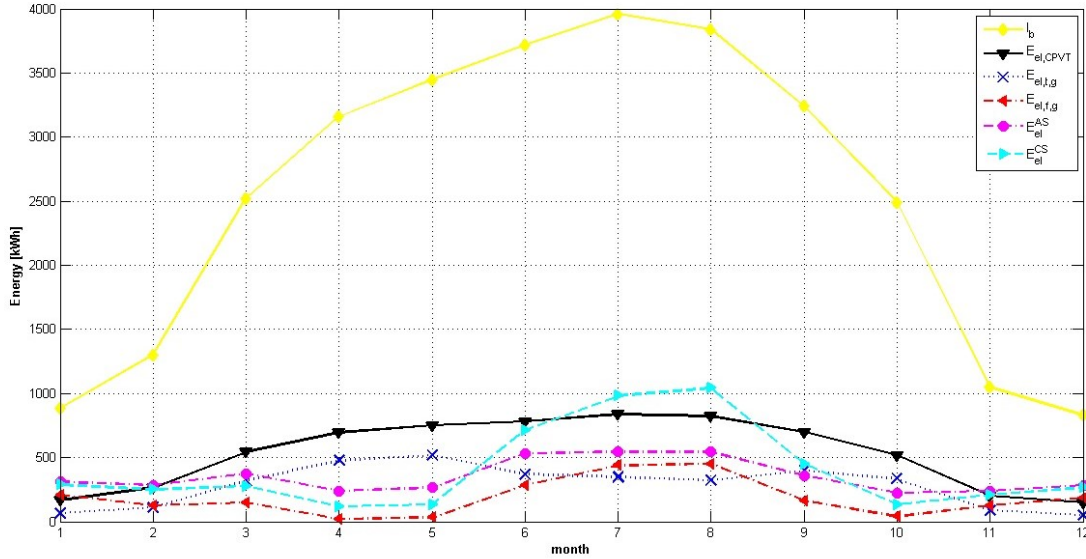


Figure 3.6: Monthly electric energies of the conventional and alternative system.

The production of DHW decreases in the summer period (June – September) since the load of regeneration (E_{reg}) grows and the thermal energy of CPVT ($E_{th,CPVT}$) is primarily used in the AHU. Approximately 2/3 of regenerative energy is drawn from the solar storage tank (pink curve, $E_{th,f,T}$) during the hottest months of July and August. Comparing, the reference system and the one presented in this paper, it is noted that the cooling energy supplied from the chiller in the reference system (dashed dark green line, E_{cool}^{CS}) is higher than that of the novel one (dotted grey line, E_{cool}^{AS}), while the thermal energy used in the reference AHU for the post heating is much lower than that of regeneration (E_{reg}). In fact, the contribution of the boiler in the reference system ($E_{th,B}^{CS} > E_{th,DHW}$) is slightly higher than that due to the DHW.

The electric load (including the user) of the proposed system (E_{el}^{AS}) proves to be always higher than the one of the reference system (E_{el}^{CS}) except in the summer months when the use of the electric chiller becomes predominant when compared to the surplus of electrical energy required to operate the solar subsystem. Taking into account that CPVT collectors also provide electric energy, the total energy taken from the grid ($E_{el,f,g}$) for the proposed novel system is always lower than that of the reference one (

E_{el}^{CS}). The peak of electricity fed into the grid ($E_{el,t,g}$) occurs in the intermediate season and not in the summer period when electricity demand of the auxiliary components of the system increases and consequently the on-site consumption grows.

The results concerning the electricity are shown in Figure 3.7 and in Figure 3.8. The electricity fed into the grid ($E_{el,t,g}$) exceeds the one taken from it ($E_{el,f,g}$). In particular, during weekend days the majority of the electrical energy (except for the consumption of the solar circuit pump) is fed into the grid. In addition, the energy fed into the grid decreases from the intermediate season, through the summer and to the winter period. However, during the cooling period the energy taken from the grid is at its maximum.

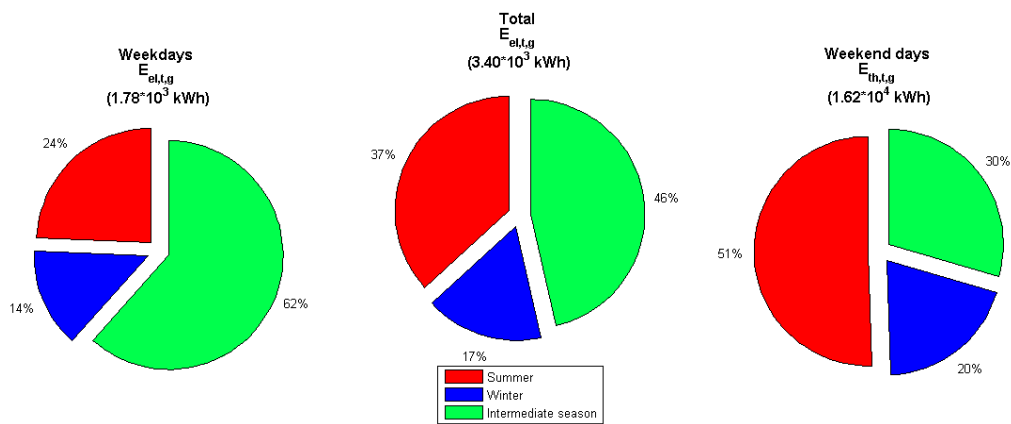


Figure 3.7: Electric energy fed into the grid.

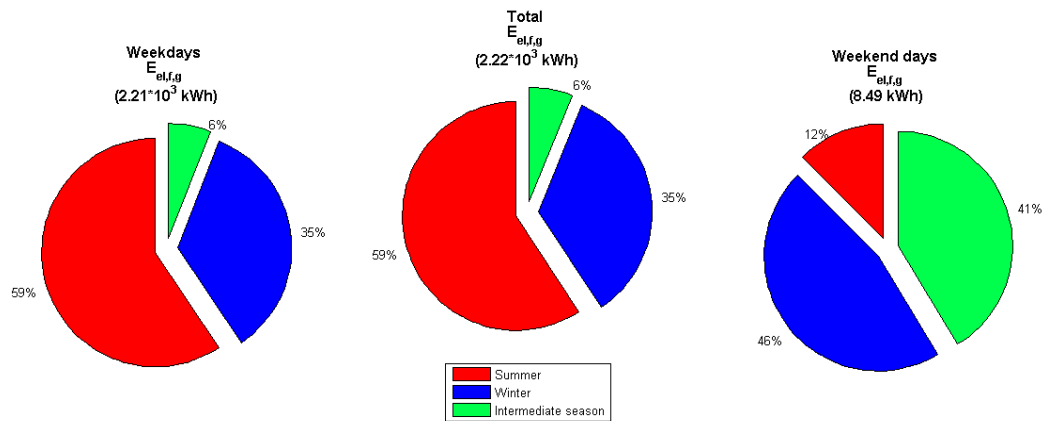


Figure 3.8: Electric energy taken from the grid.

The majority of the DHW thermal production ($E_{th,DHW}$) occurs during the weekdays and the intermediate seasons since there is no thermal energy demand by the plant, while the summer season provides the greatest contribution in the weekend days (Figure 3.9).

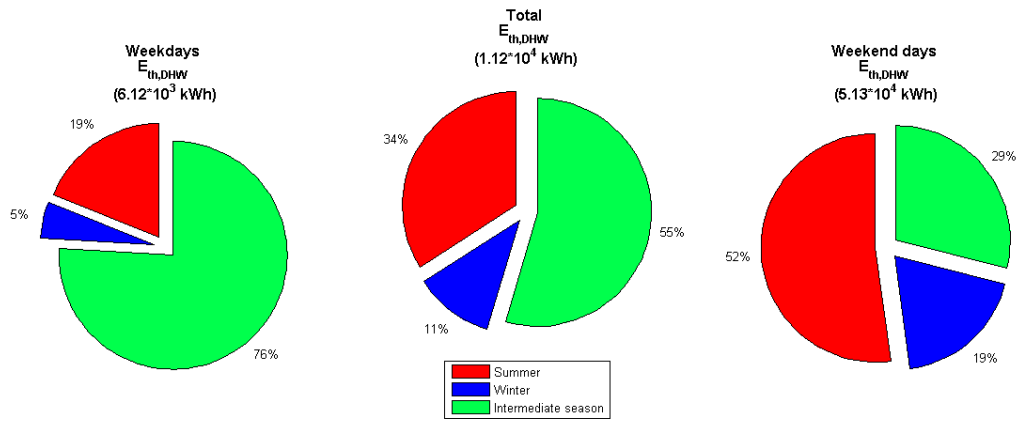


Figure 3.9: DHW energy production.

Considering the operation of the system in heating mode (Figure 3.10), it is clear that most of the electrical energy produced by the CPVT is consumed on-site ($E_{el,on-site}$) and this amount can balance about 40% of the total demand of the building-plant system (E_{el}^{AS}). As regards the thermal energy produced by the solar collector ($E_{th,CPVT}$), less than 15% is used for DHW ($E_{th,DHW}$), while the remaining part is stored ($E_{th,t,T}$). Regarding the heat required by the AHU ($E_{pre+post} = 5.86 \cdot 10^3$ kWh), the contribution of the boiler ($E_{th,B}^{AS}$) is slightly higher than the other contributions ($E_{th,f,T}$, $E_{th,Rec}$).

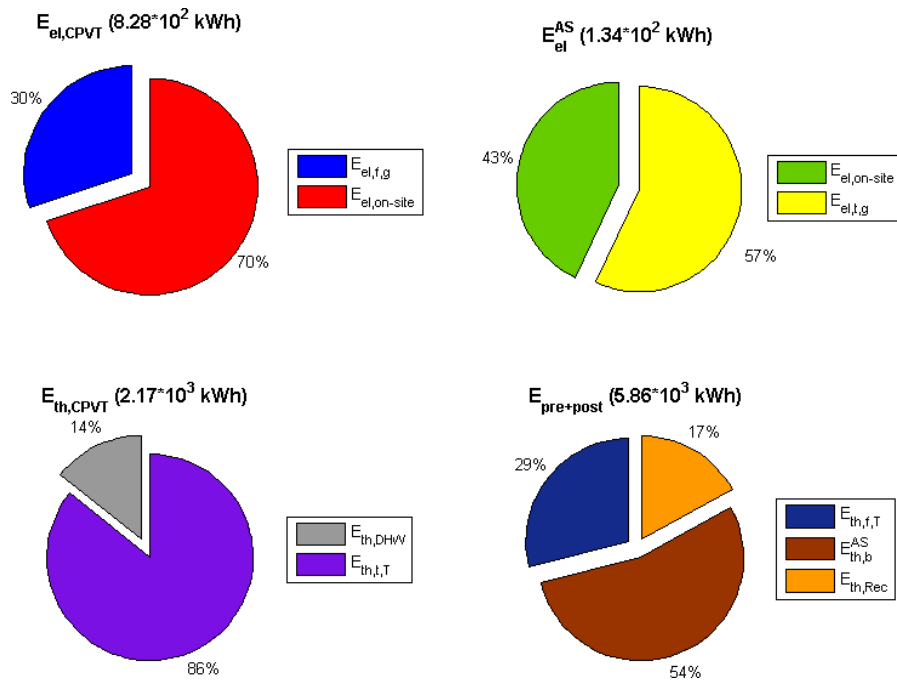


Figure 3.10: Seasonal results in heating mode operation.

Considering the operation of the system in cooling mode, Figure 3.11 shows that the majority of the electrical energy produced by the CPVT ($E_{el,CPVT}$) is consumed on-site ($E_{el,on-site}$) and this amount can balance over 50% of the total demand of the building-plant system (E_{el}^{AS}). Regarding the thermal energy produced by the solar collector ($E_{th,CPVT}$) a greater percentage compared to winter is used for the production of DHW ($E_{th,DHW}$). Regarding the thermal energy required for the DW regeneration (E_{reg}) the contribution of the boiler ($E_{th,B}^{AS}$) is slightly higher than 40%, this means that the solar fraction (the contribution taken from the storage tank, $E_{th,f,T}$) is about 60%.

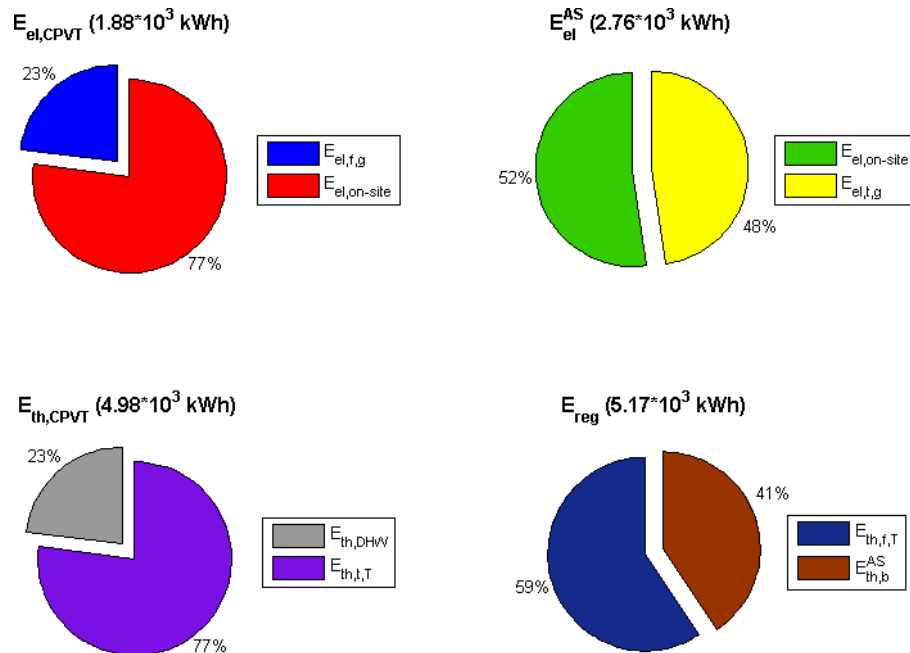


Figure 3.11: Summer energy distribution.

The annual results also show that the CPVT electrical and thermal efficiencies are respectively 21.15% and 55.32%. Note that such values are calculated with respect to the incident beam radiation and the thermal efficiency is similar to the one reported for other CPVT systems. Conversely a very high value of the electrical efficiency is achieved. Such good result is basically due to the use of III-V PV cells, showing ultra-high electrical efficiency.

Finally, PES and ΔCO_2 were evaluated considering different percentages of DHW usage (Figure 3.12). It is observed that a primary energy savings higher than 81% and emissions avoided for about 85% are an excellent result for the innovative plant,

although the DHW is not considered. This additional quantity further increases the energy and the environmental benefits achievable. The exploitation of solar collectors all year long (intermediate period, Saturday and Sunday) enhances these benefits though arguably the improvement is more impressive if the primary energies are considered. As a matter of fact, the primary energy of the traditional system passes from $1.80 \cdot 10^4$ kWh to $3.04 \cdot 10^4$ kWh, whether the DHW produced with the solar system is considered or not, instead that of the AS remains at $3.34 \cdot 10^3$ kWh.

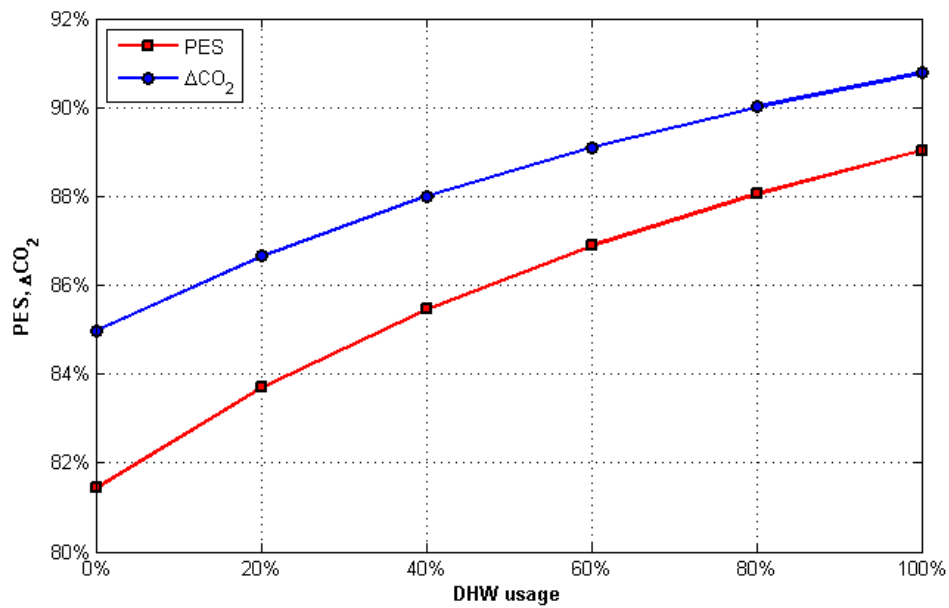


Figure 3.12: PES and ΔCO_2 as a function of DHW usage.

Chapter 4 Solar-assisted Desiccant-based Air Handling
Unit: Alternative Scenarios

4.1 Introduction

In the last few years the Desiccant and Evaporative Cooling (DEC) devices have been widely studied as a suitable alternative to conventional electrical-driven HVAC systems. They allow several benefits in terms of humidity control, indoor air quality, CO₂ emissions reduction, primary energy and electricity savings [89]. The last three advantages are further improved considering solar energy as the main source of energy for the plant.

The Solar-driven Desiccant and Evaporative Cooling systems (SDEC), as stated above, are composed of two main parts: a solar field and an air handling unit (AHU). Solar thermal energy collected by solar collectors is used to regenerate the hygroscopic material which ensures the dehumidification of process air. Storage and back-up systems are often used in these innovative plants to compensate for the temporary lack or reduction of the solar source. In order to improve the performance of SDEC plants, researchers have evaluated alternative solutions for both the solar subsystem and the AHU configurations.

In the two preceding Chapters the coupling of different collector types and solar field configurations with the desiccant-based AHU, modelled on the basis of the experimental one, have been described. Through TRNSYS dynamic simulations, the performances of these innovative systems have been evaluated considering also that the excesses of solar thermal energy can be dissipated, partially or completely exploited. Hereinafter, instead, three alternative AHU layouts are investigated to assess the energy, environmental and economics indices introduced before. However the analyses are developed considering flat plate and evacuated tube solar collector, three collecting surfaces, a range of value for the tilt angles and three percentages of the solar thermal energy surpluses usage. For an easier and more immediate identification of the alternative configurations, below, they will be denominated Scenarios. In order to have an immediate comparison of the results deriving from the standard and modified plants also the performance curves of the standard configuration, Scenario A, (Chapter 2) are shown.

The first analyzed alternative scenario (Scenario B) provides the use of the heat rejected by the condenser of the chiller to pre-heat the regeneration air flow. In the second alternative scenario (Scenario B), pre-heating of the regeneration air is realized with the warmer regeneration air exiting the desiccant wheel. In the third alternative scenario (Scenario D), pre-cooling of the process air before entering the desiccant wheel is

considered. These three modifications lead to a reduction of the required thermal energy for regeneration with respect to a reference system. Modifications involving regeneration air pre-heating determine very similar performance increases, while with the third solution (process air pre-cooling) the benefits, in terms of energy, emissions and economic analysis, are greater.

4.2 Loads characterization

As sensible and latent loads the energy demands of the university classroom located in Benevento are considered in the following analyses. Detailed information of the building features and occupancy are described in Section 2.2. Moreover, also in this case, further low temperature use of the solar thermal energy surpluses are taken into account.

4.3 Alternative layouts for the innovative system

Starting from the standard configuration of the innovative system (Figure 2.2), three alternative solutions for the cooling operation are proposed and described below. Instead, the heating layout remains the same in all scenarios (Figure 2.4). These modifications of the innovative AHU aim to improve system performance. The first alternative scenario (Scenario B) consists in the recovery of the heat rejected by the condenser of the chiller, to pre-heat the regeneration air flow. The second scenario (Scenario C) consists in the pre-heating of regeneration air with the warmer regeneration air exiting the desiccant wheel. The last scenario (Scenario D) involves the pre-cooling of the process air before entering the desiccant wheel.

These alternative AHU layouts allow to always maintain comfort conditions in the conditioned space.

With regard to the solar subsystem, as done in Chapter 2 several arrangements, differentiated by collector type (flat-plate and evacuated tubes), collecting surface (approximately 20, 27 and 34 m²) and tilt angle (20-55°) are considered. These arrangements are then combined with the three alternative previously introduced scenarios.

The AHU technical and operational details will be illustrated for the different scenarios in the following subsections.

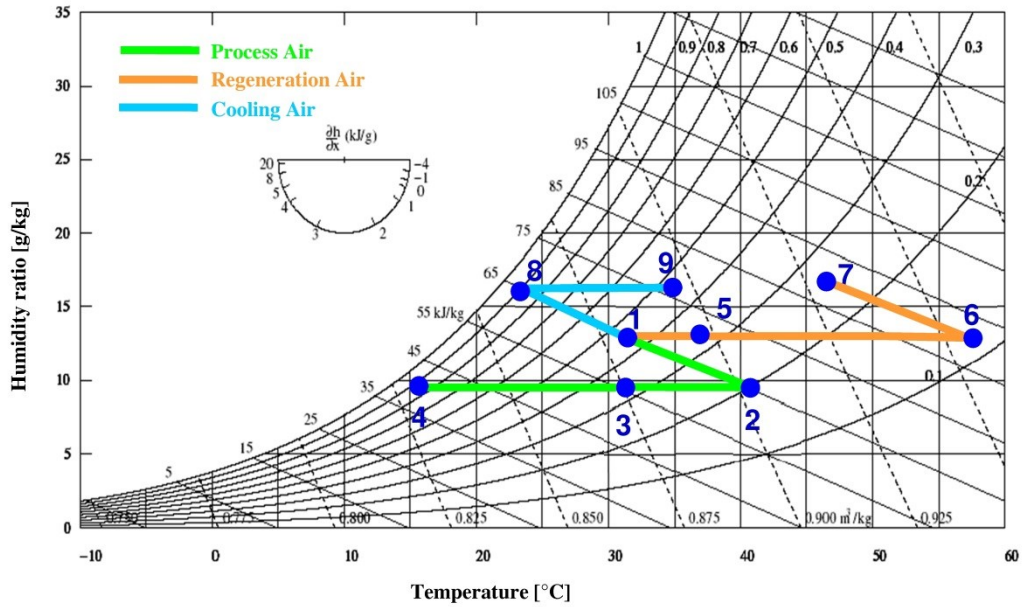


Figure 4.2: Psychrometric diagram with air transformation of the AHU with heat recovery from chiller condenser (cooling operation, Scenario B).

4.3.2 Desiccant-based AHU with cross-flow heat recovery unit (Scenario C)

In the hybrid AHU, the highest temperature level is reached by the regeneration air before passing through the desiccant wheel; at the outlet of this component, the air still has a temperature greater than the outside one, therefore it can be advantageously used to pre-heat the regeneration air flow, drawn from the outside.

Several devices exist for heat recovery [90]. In this case an other cross-flow heat exchanger, CF2 (Figure 4.3), is used, and simulated using experimental results for the cross flow heat exchanger of the test facility (CF) to calibrate and validate the model. Therefore, the regeneration air is pre-heated (1-5) in CF2, further heated in HC (5-6) with the thermal energy supplied by solar subsystem, then it proceeds to regenerate the DW (6-7) and passes through the recuperative heat exchanger CF2 (7-8), Figure 4.4. The HC has the task of ensuring the desired regeneration temperature.

Due to the presence of this new component a higher power requirement for the regeneration fan is assumed (350 W). Also in this scenario, the cooling and process air ducts remain identical to those of the standard plant.

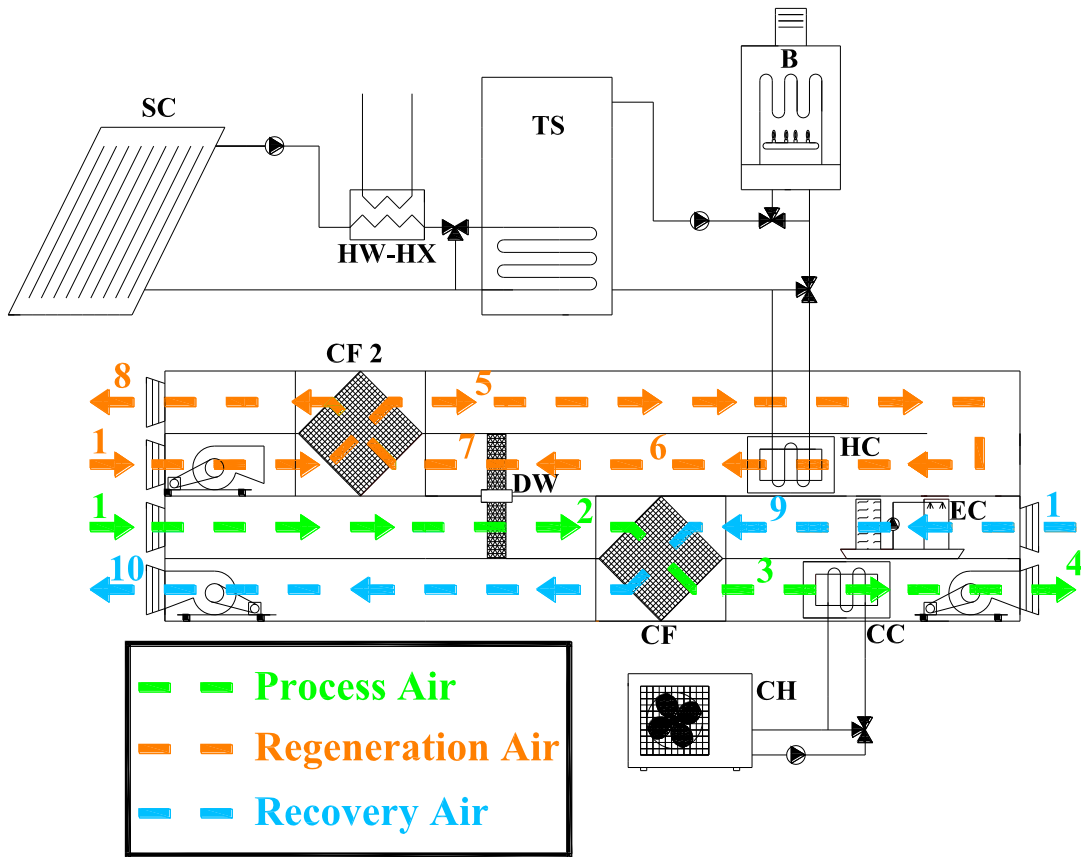


Figure 4.3: Scheme of the simulated Desiccant-based AHU with cross-flow heat recovery unit (cooling operation, Scenario C).

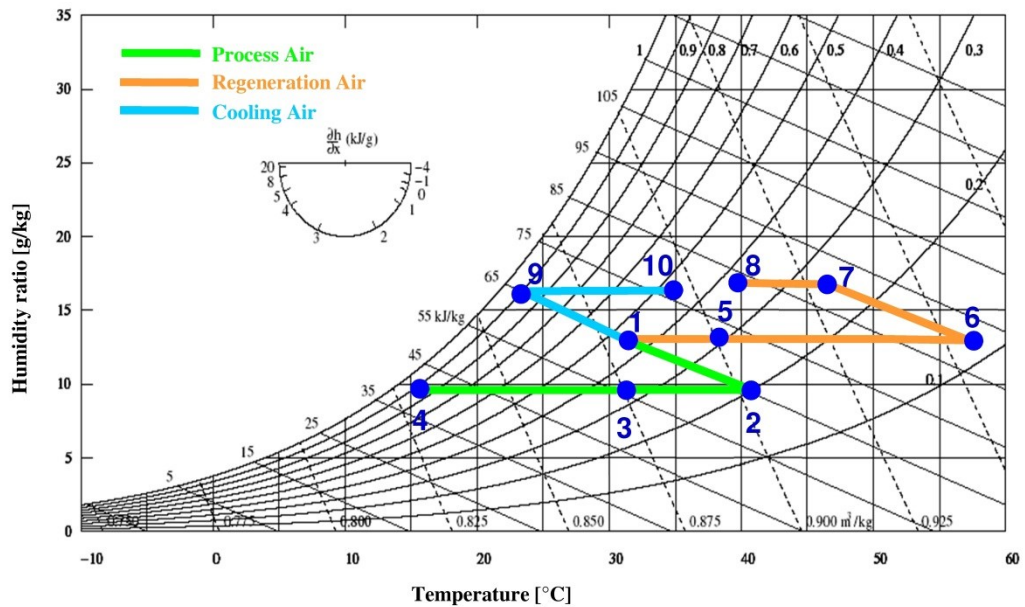


Figure 4.4: Psychrometric diagram with air transformation of the AHU with cross-flow heat recovery unit (cooling operation, Scenario C).

4.3.3 Desiccant-based AHU with pre-cooling of process air (Scenario D)

Pre-cooling/dehumidification of the process air before dehumidification with desiccant wheel has two advantages:

- 1) allows the operation even in places characterized by very humid climates [6];
- 2) reduces the regeneration temperature for a given value of the desired humidity ratio reduction [53].

Analyzing the simulated and experimental results of the standard configuration, one notes that the chilled water temperature after the heat exchange in the CC is still lower than that of the outside air, so the possibility of employing a pre-cooling coil (CC2) (Figure 4.5) can be evaluated. In some climatic conditions (high relative humidity), a slight pre-dehumidification process can also occur in this pre-cooling coil.

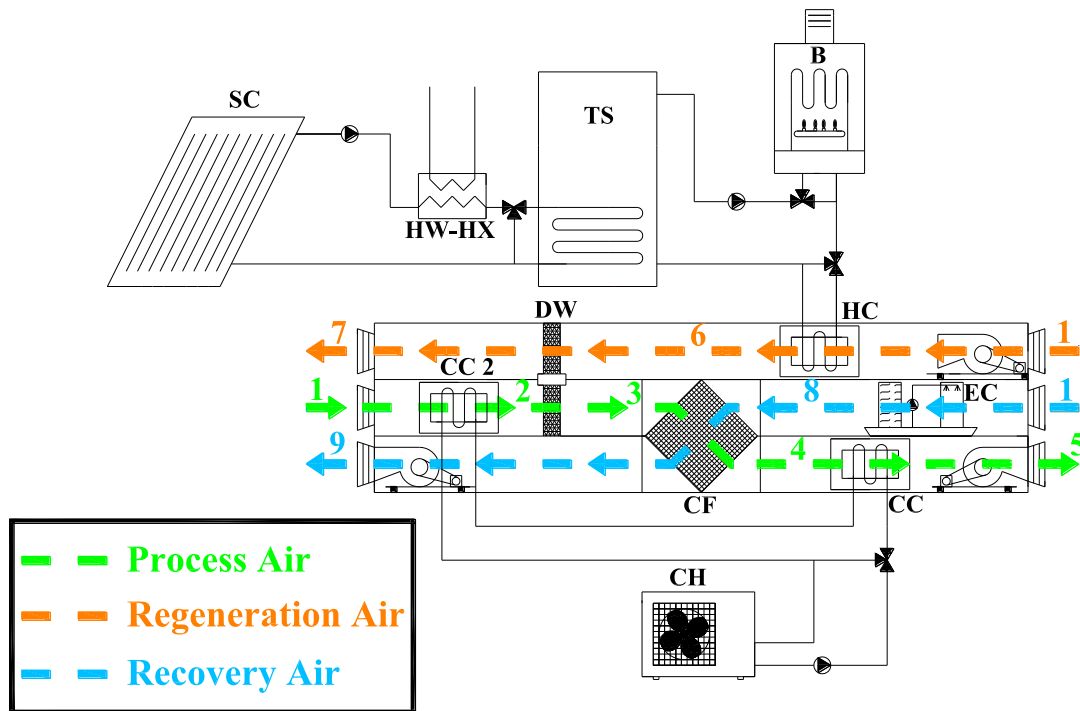


Figure 4.5: Scheme of the simulated Desiccant-based AHU with pre-cooling coil (cooling operation, Scenario D).

In this scenario, the transformations of the regeneration and cooling air remain unchanged with respect to standard configuration, instead the process air is firstly pre-cooled (1-2), then dehumidified by adsorption (2-3), cooled in CF (3-4), and finally cooled in CC (4-5), .

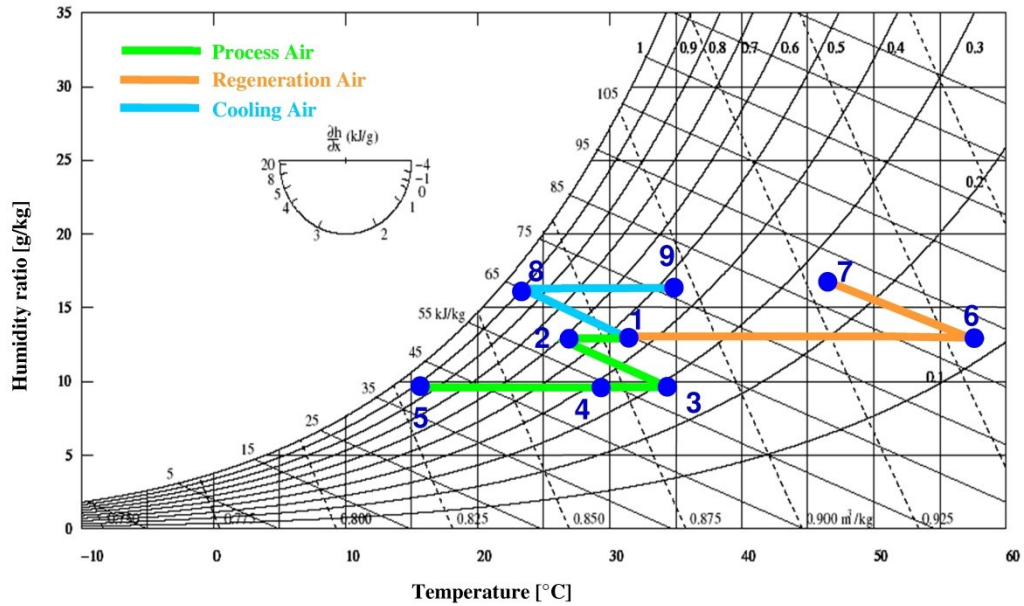


Figure 4.6: Psychrometric diagram with air transformation of the AHU with pre-cooling coil (cooling operation, Scenario D).

4.4 Models and performance assessment methodology

Dynamic simulations with a time step of 1.5 min have been carried out using the software “TRNSYS 17” [58] integrated with the “TESS” libraries [59]. The models of the main plant components are described and characterized in detail in the works of Angrisani et al. [52], [71] and reported in Chapter 2. Energy, environmental and economic performances are assessed by evaluating the Primary Energy Saving (PES, eq. 2-7), the equivalent CO_2 avoided emission (ΔCO_2 , eq. 2-9) and the Simple Pay Back period (SPB, eq. 2-11).

The components parameters have been chosen on the basis of experimental values, when available, or according to the rated values otherwise (see Chapter 2). The new components included in the modified configurations are chosen with the same characteristic of those already used in the experimental plant. Therefore the mathematical models are not described again.

4.5 Simulation and results

The operation of the alternative and conventional systems is simulated considering Space cooling energy demands during weekdays of summer season (June 1st – September 15th); space heating energy demands during weekdays of winter period

(November 15th – March 31st); hot water production for further thermal energy demands (with solar thermal energy surplus) all year long.

The electrical devices of the classroom are turned on during its opening hours.

Three further sub-scenarios are considered: 0%, 50% and 100% of the hot water produced from solar surplus is effectively used for further thermal energy demands.

In order to have an immediate view of the advantages deriving from the plant modification also the performance curves of the standard configuration, Scenario A, (Chapter 2) are shown below. Regarding the energy analysis, the PES index, as a function of the solar collector slope and area, is reported in Figure 4.7, Figure 4.9 and Figure 4.11 for the hybrid AHU with flat collectors and in Figure 4.8, Figure 4.10 and Figure 4.12 for the same AHU with evacuated tube collectors. The results reveal that:

- 1) the PES is always positive, therefore ASs are always energetically convenient with respect to CS;
- 2) the energy performance, as expected, improves with increasing collector area except for Scenario D when 0% of solar thermal energy surplus used is considered (Figure 4.7d);

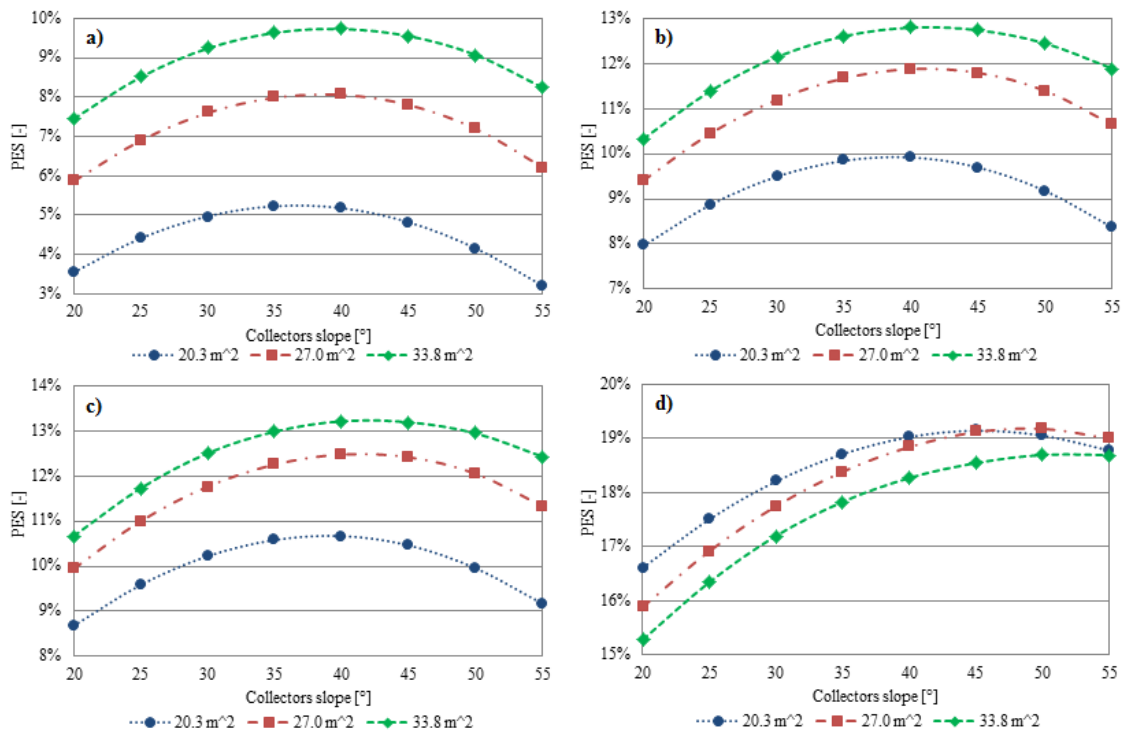


Figure 4.7: Primary Energy Saving of the Alternative Systems with 0% of solar thermal energy surplus used and flat plate collectors in the four alternative configurations: a) Scenario A, b) Scenario B, c) Scenario C, d) Scenario D.

- 3) the systems with evacuated tube collectors are generally more efficient than those with flat-plate collectors: there is a difference of about ten percentage points in the standard configuration (Scenario A, Figures 4.7a and 4.8a) and in those with the pre-heating process (Scenarios B and C, Figures 4.7b, c and 4.8 b, c); six percentage points in the system with the pre-cooling coil (scenario D, Figures 4.7d and 4.8d);
- 4) modifications to the AHU when it is coupled to evacuated tube collectors provide lower improvements in the annual operation (Figure 4.8 b, c), in fact there is an increase of only 2-3 percentage points in the scenarios that involve pre-heating of the regeneration air (Scenarios B and C) compared to the standard system (Scenario A). With flat plate collectors, the increase is slightly higher, 3-5 percentage points (Figure 4.7 b, c);
- 5) although the trends of Scenario D and A are not similar, the Scenario D associated with evacuated collectors provides an average smaller percentage improvements to the Scenario A with respect to the same configuration coupled with flat plate collectors (Figures 4.7 and 4.11 d);

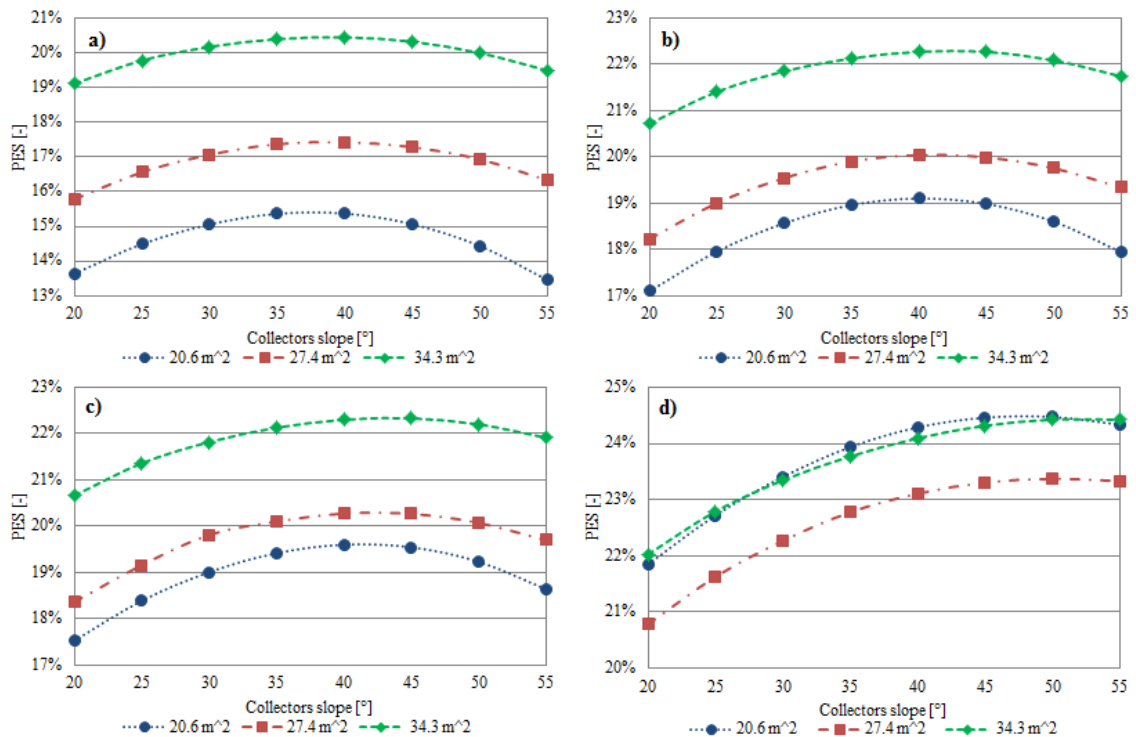


Figure 4.8: Primary Energy Saving of the Alternative Systems with 0% of solar thermal energy surplus used and evacuated tube collectors in the four alternative configurations: a) Scenario A, b) Scenario B, c) Scenario C, d) Scenario D.

- 6) Scenario D shows some anomalies when 0% of solar thermal energy surplus used is considered (Figures 4.7 and 4.8d). It allows to get the best performance but it is also the least affected by the increase of collectors area, confirming the fact that with the process air pre-cooling less energy is required to regenerate the desiccant wheel;
- 7) Scenario B and C with 0% of solar thermal energy surplus used show similar performance, the second one is slightly more effective (Figures 4.7 and 4.8 b, c);
- 8) With 0% of solar thermal energy surplus used and flat plate collectors, the maximum PES is obtained for a tilt angle of 40°, except than in Scenario D (Figure 4.7), while with evacuated tube collectors the optimum tilt angle is 40-45° (Figure 4.8);
- 9) for Scenario D with 0% of solar thermal energy surplus used (Figures 4.7d and 4.8d) the maximum PES occurs at tilt angles of 45-55° as the energy benefits are especially derived from the winter exploitation of solar energy when the sun is lower on the horizon, while the regeneration energy is significantly reduced;
- 10) if a certain amount of solar thermal energy surplus is used, a homogenization of PES curves appears and for all the analyzed solutions the optimal tilt angle is 35° (Figures 4.9-4.12). Because of the long periods (intermediate season and weekends) in which the AHU is off and the solar energy is not exploited for air conditioning, the amount of energy associated with the solar surplus becomes preponderant with respect to the other thermal energy flows;
- 11) even if only 50% of the solar thermal energy surplus is used, a huge performance improvement appears, the best solution (34 m² of collectors and pre-cooling coil, scenario D) ensures a PES of about 50% with flat plate collectors (Figure 4.9d), that grows over 61% with evacuated tube collectors (Figure 4.10d);

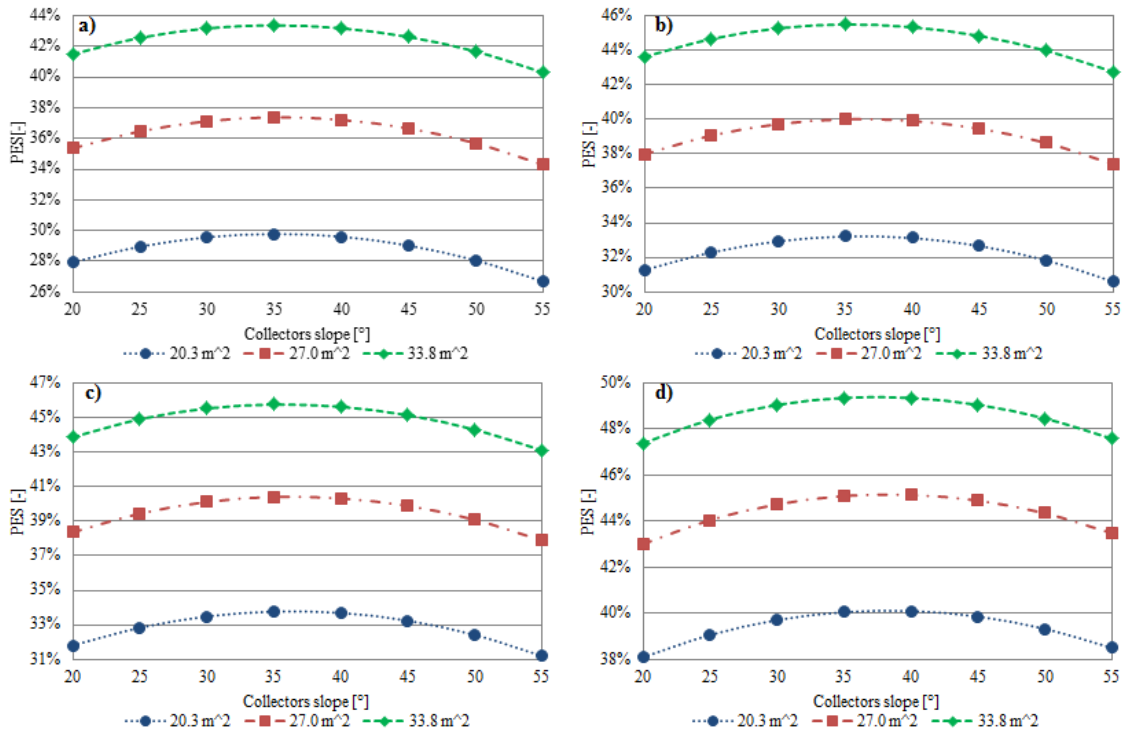


Figure 4.9: Primary Energy Saving of the Alternative Systems with 50% of solar thermal energy surplus used and flat plate collectors in the four alternative configurations a) Scenario A, b) Scenario B, c) Scenario C, d) Scenario D.

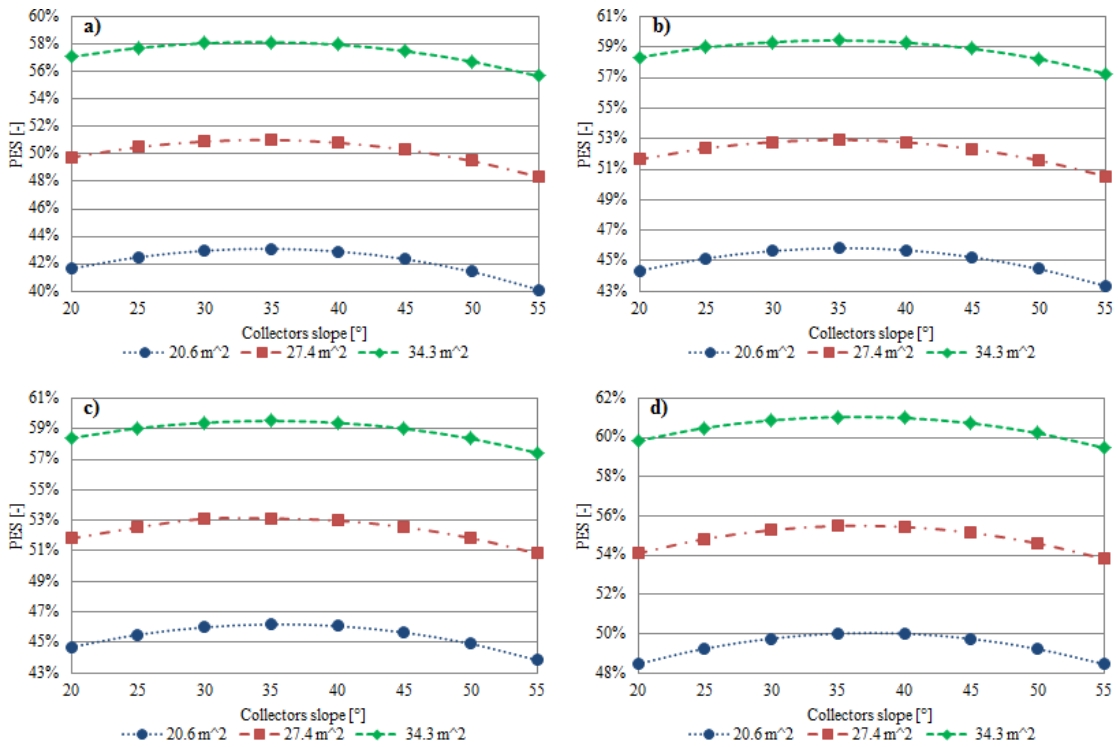


Figure 4.10: Primary Energy Saving of the Alternative Systems with 50% of solar thermal energy surplus used and evacuated collectors in the four alternative configurations: a) Scenario A, b) Scenario B, c) Scenario C, d) Scenario D.

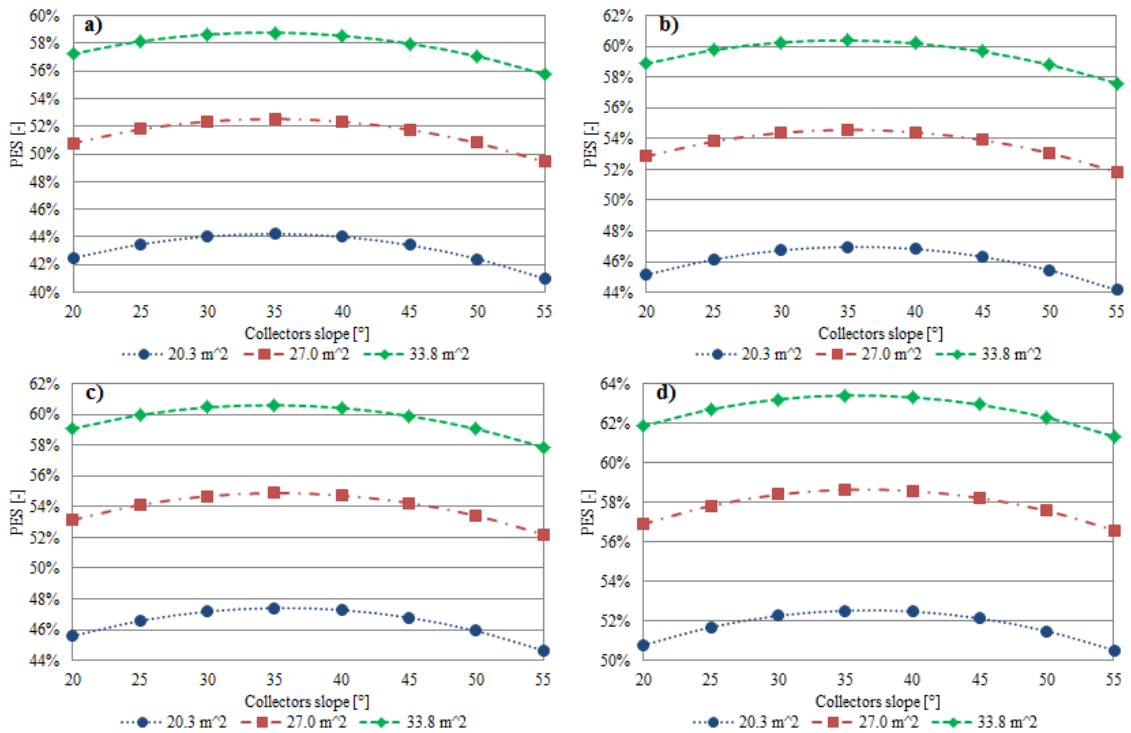


Figure 4.11: Primary Energy Saving of the Alternative Systems with 100% of solar thermal energy surplus used and flat plate collectors in the four alternative configurations: a) Scenario A, b) Scenario B, c) Scenario C, d) Scenario D.

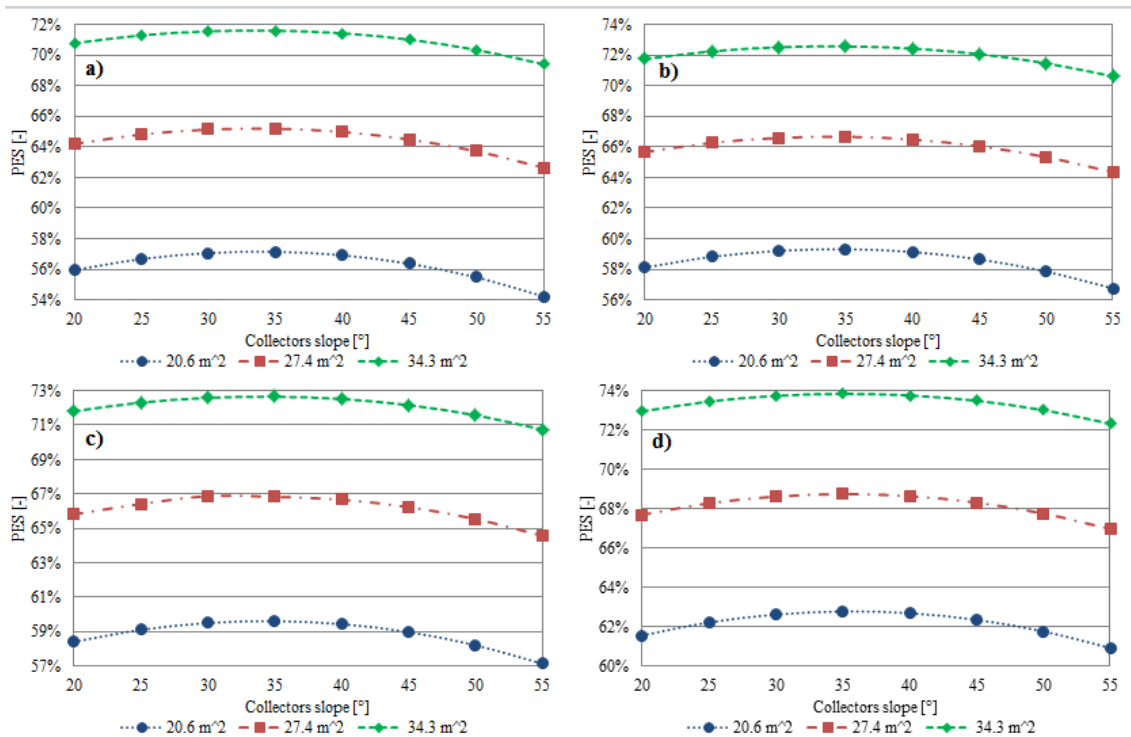


Figure 4.12: Primary Energy Saving of the Alternative Systems with 100% of solar thermal energy surplus used and evacuated tube collectors in the four alternative configurations: a) Scenario A, b) Scenario B, c) Scenario C, d) Scenario D.

- 12) taking into account 100% use of solar thermal energy surplus, the maximum PES always occurs in Scenario D and with a tilt angle of 35°. The performance grows up to a PES of over 63% (Figure 4.11d) and about 74% (Figure 4.12d) with the maximum surface of flat plate and evacuated tube collectors, respectively;
- 13) in scenario D, with flat plate collectors and tilt angles up to 45° (Figure 4.7d), the system is more efficient with lower absorbing surfaces. This situation arises from the fact that with 0% of solar thermal energy surplus used, the annual increase in electricity demand ($E_{p,el,WD,Su}$; $E_{p,el,WD,Wi}$; $E_{p,el,Int}$; $E_{p,el,WED}$ in terms of primary energy), due to the operation of the solar loop, is not accompanied by a sufficient reduction of the thermal energy ($E_{p,th,WD,Su}$ in terms of primary energy) required by the AHU in the summer (for example see Figure 4.13). In fact the summer solar fraction (the percentage of thermal energy for regeneration supplied by the solar subsystem) is very high, about 85%, even with 20 m² of collectors.

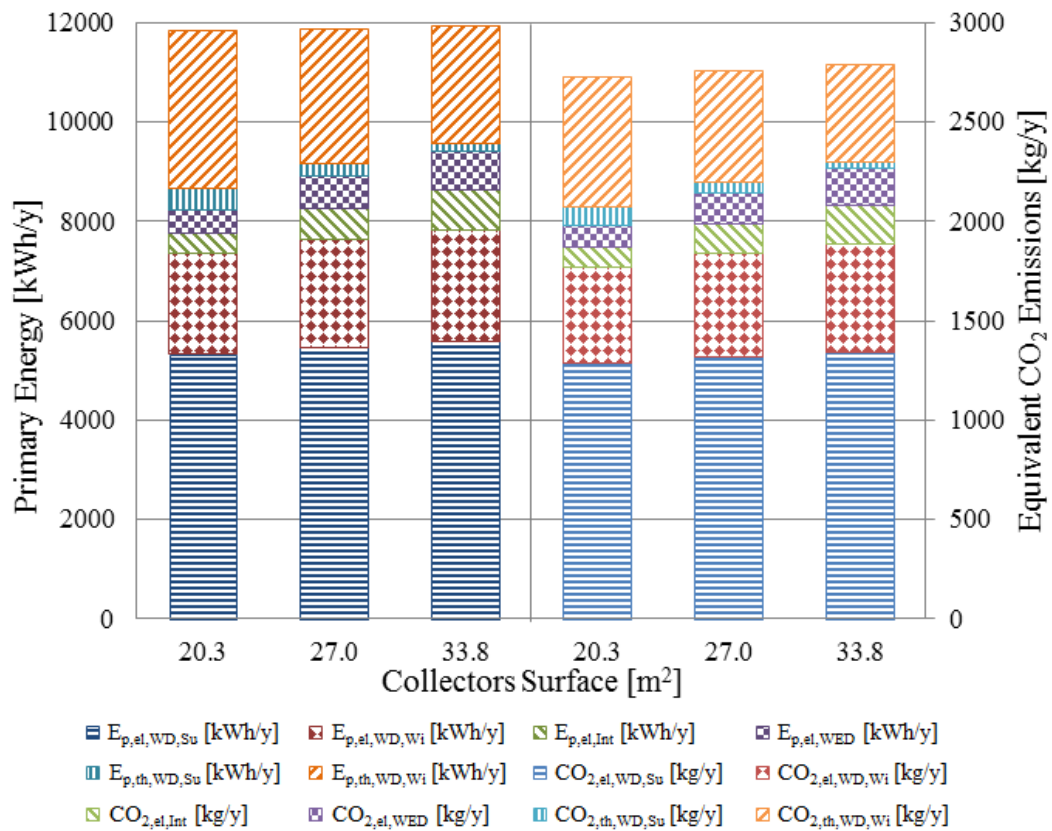


Figure 4.13: Annual primary energy and equivalent CO₂ emission associated with seasonal electric and thermal demands for the plant with pre-cooling coil (Scenario D), flat plate collectors, 40° tilt angle and 0% of solar thermal energy surplus used.

14) Scenario D with 27 m² of evacuated tube collectors shows the worst performance (Figures 4.8d and 4.14) among the investigated surfaces. The curves for 20 and 34 m² almost overlap, as, moving from the former to the latter, the increase in electricity demand of the solar subsystem balances the increased availability of thermal energy on an annual basis. The summer solar fraction is greater than 94% with 20 m² of collectors.

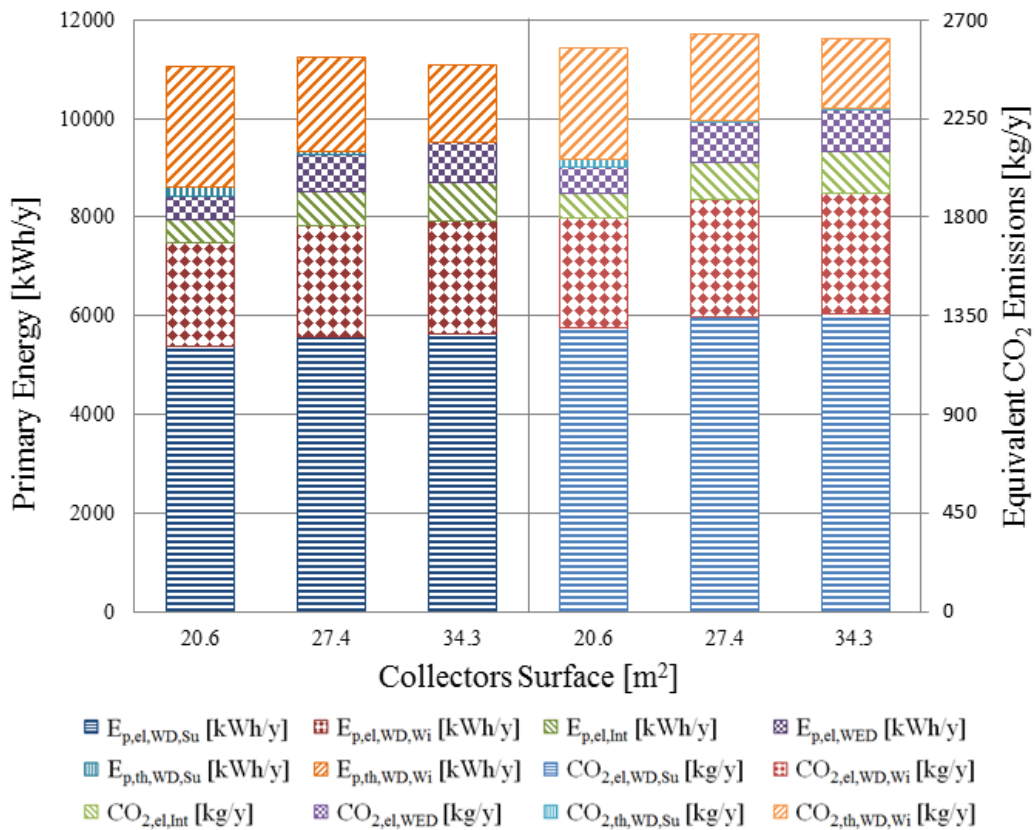


Figure 4.14: Annual primary energy and equivalent CO₂ emission associated with seasonal electric and thermal demands for the plant with pre-cooling coil (Scenario D), evacuated tube collector, 40° tilt angle and 0% of solar thermal energy surplus used.

With regard to the equivalent CO₂ emissions, the results are in part different from the energetic ones. In particular:

- 1) Scenario D with flat plate collectors operate always better with smaller collecting surfaces (Figure 4.15d),
- 2) Scenario D with evacuated tube collectors (Figure 4.16d) and a collecting surface of 27 m² has higher emissions, it is better with 34 m² and even better with 20 m²,

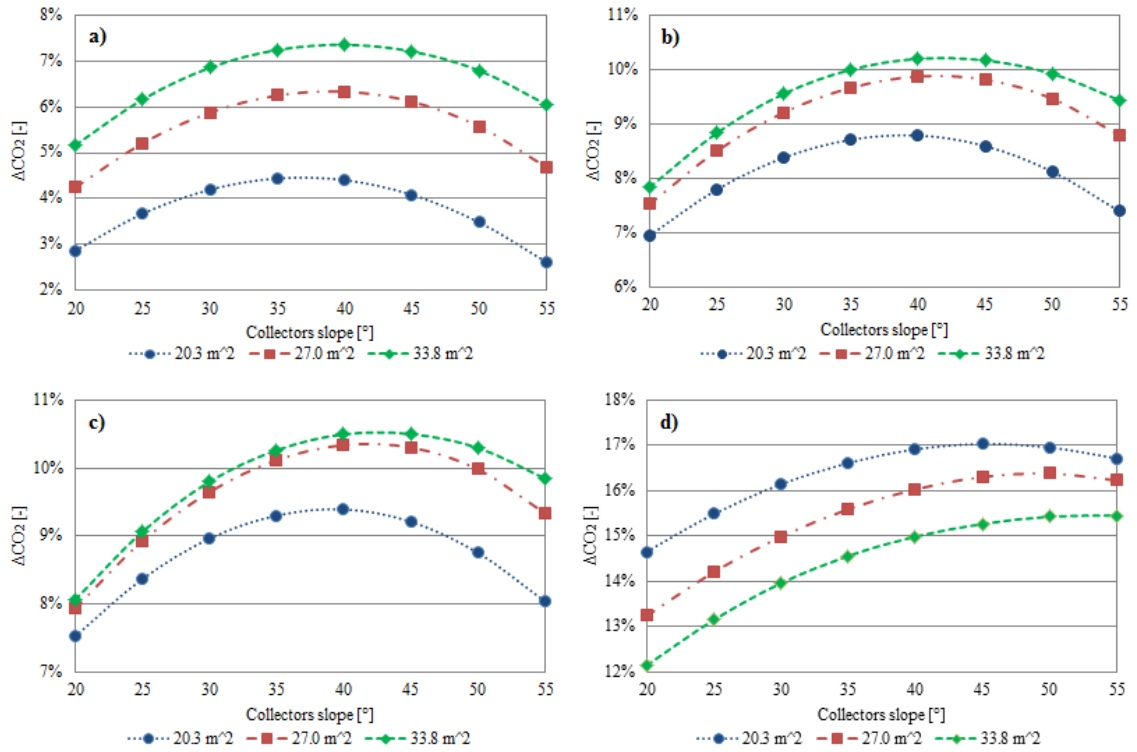


Figure 4.15: Equivalent CO₂ avoided emissions of the Alternative Systems with 0% of solar thermal energy surplus used and with flat plate collectors in the four alternative configurations: a) Scenario A, b) Scenario B, c) Scenario C, d) Scenario D.

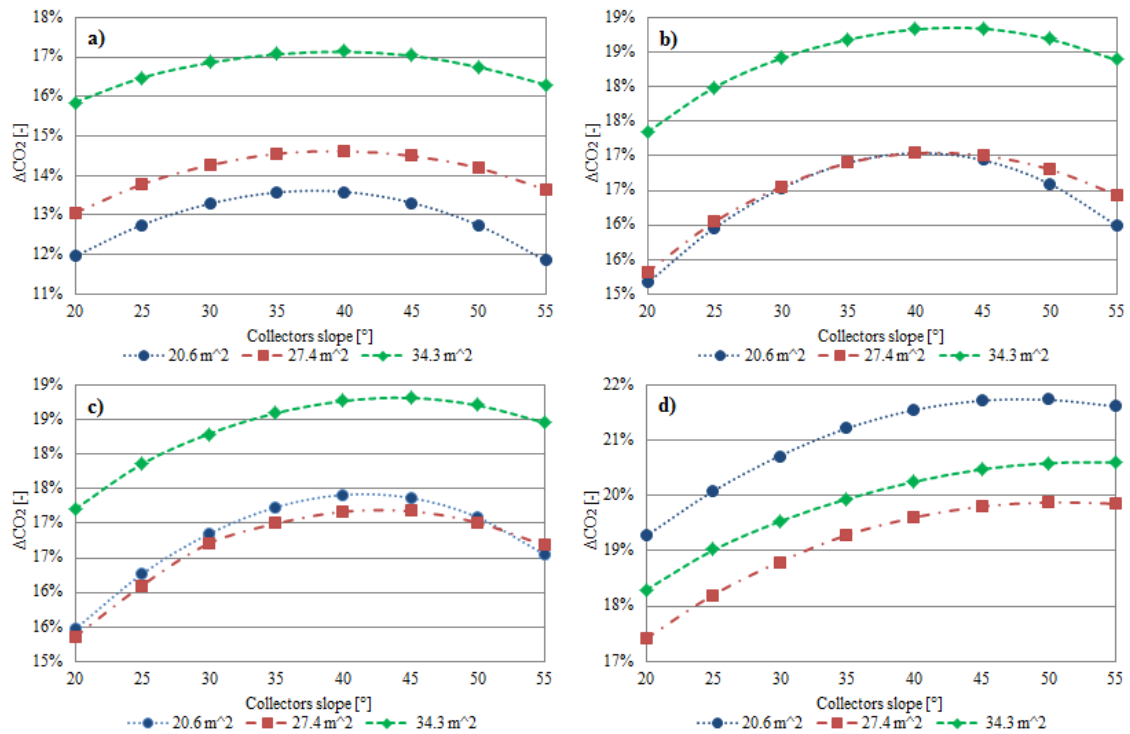


Figure 4.16: Equivalent CO₂ avoided emissions of the Alternative Systems with 0% of solar thermal energy surplus used and with evacuated tube collectors in the four alternative configurations a) Scenario A, b) Scenario B, c) Scenario C, d) Scenario D.

- 3) Scenarios B and C with flat plate collectors (Figure 4.16 b, c) show that, by increasing the absorbing surface from 27 to 34 m², emissions benefits decrease with respect to the increase from 20 to 27 m². On the contrary, the environmental performance of systems with 20 and 27 m² of evacuated tube collectors are very similar (Figure 4.16 b, c).

For the sake of brevity the curves of the avoided equivalent CO₂ emissions in the case of total and partial (50%) use of solar thermal energy surplus are not shown. Their trends, as a function of the tilt angle and of the collectors surface, are similar to those of PES.

In order to find the energy demands that mainly affect energy and environmental performance, in Figures 4.13, 4.14 and 4.17 the different shares of primary energy and CO₂ emissions are shown. The subscripts *el* and *th* indicate the primary energy associated respectively to the electrical and thermal demands of the plant. Assuming the emission factors as in Chapter 2, (0.207 kg of equivalent CO₂ are emitted into the atmosphere per kWh of primary energy due to natural gas consumption and 0.241 kg of equivalent CO₂ are emitted per kWh of primary energy due to electricity), it is observed that:

- 1) the primary energy and the equivalent CO₂ emission associated with the summer electrical requirements of the system ($E_{p,el,WD,Su}$ and $CO_{2,el,WD,Su}$) is always the largest amount and increases with the absorbing surface;
- 2) the primary energy and the equivalent CO₂ emission associated with the electrical requirements of the periods when the air conditioning is turned off ($E_{p,el,Int}$; $E_{p,el,WED}$ and $CO_{2,el,Int}$; $CO_{2,el,WED}$) increase with the collectors area, but represent a share less important than the other electrical loads;
- 3) the primary energy demand of the boiler in winter ($E_{p,th,WD,Wi}$) is higher than in summer ($E_{p,th,WD,Sum}$);
- 4) the primary energy and the equivalent CO₂ emission associated with the heat supplied by the boiler in the winter period ($E_{p,th,WD,Wi}$ and $CO_{2,th,WD,Wi}$) has a decreasing trend with the surface of the solar field;
- 5) the thermal energy provided by the boiler during summer ($E_{p,th,WD,Sum}$) insignificantly contributes to the total primary energy and equivalent CO₂ emissions when referring to systems with evacuated tube collectors (Figures 4.14 and 4.17).

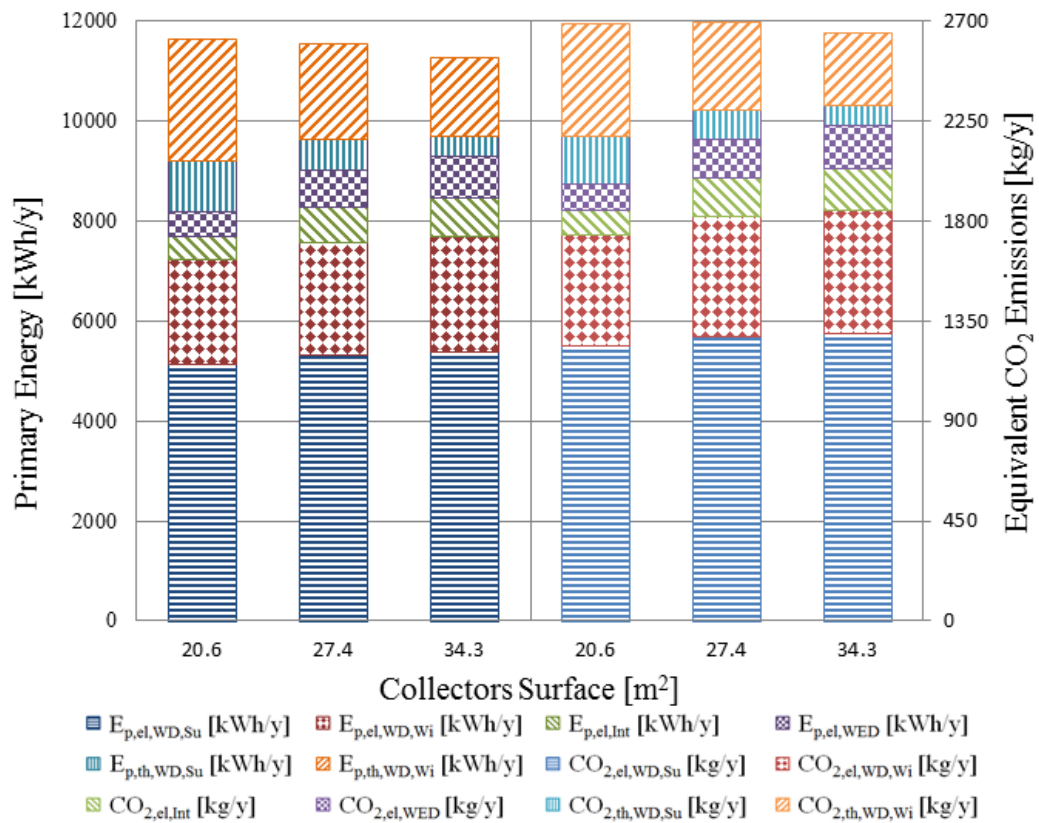


Figure 4.17: Annual primary energy and equivalent CO₂ emission associated with seasonal electric and thermal demands for the plant with cross-flow heat recovery unit (scenario C), evacuated tube collectors, tilt angle of 40° and 0% of solar thermal energy surplus used.

As regards economic analysis, the SDEC system are more expensive than conventional plants, mainly due to the presence of a DW, a solar field and a thermal storage tank.

The Italian financial support mechanism, currently applicable to this type of renewable energy based plant, establishes a contribution that depends on the surface and kind of solar collectors employed, but it does not take into account the typology of solar cooling system installed (with absorption or adsorption heat pumps, DEC etc.). For the specific applications considered in this paper, it occurs that economic subsidy is low to obtain an acceptable payback period if these systems are only used for the air-conditioning.

If 50% of surplus solar thermal energy is exploited, the SPB period ranges between 20 and 7 years, with the lowest value obtained when the maximum flat plate solar collectors surface (about 34 m²), optimal tilt angle and pre-cooling/dehumidification coil (Scenario D) are chosen. The largest value, instead, occurs for the standard system (Scenario A) worse tilt angle and a solar field of 20 m² of flat plat collectors.

When the total use of solar thermal energy surplus is assumed, the differences between the various scenarios reduce, and the most influential factor becomes the collectors

surface. SPB ranges between 9 years (Scenario A, 20 m² of flat collectors and optimal tilt angle) and 3 years (system with pre-cooling and 34 m² of flat plate collectors). The SPB period for plants with evacuated tube collectors remains 9 years in scenario A with 20 m² of collectors and optimal tilt angle, while a minimum value of 5 years is obtained in scenario D with 34 m² of collectors.

In order to summarize the best energy, environmental and economic results Tables 4.1 and 4.2 show PES, ΔCO_2 and SPB for the four analyzed scenarios with 0, 50 and 100% use of the solar thermal energy surplus, when the optimal configuration (surface and tilt angle) are chosen respectively for plants with flat plate and evacuated tube collectors. The SPB values for cases with 0% use of the solar thermal energy surplus are not reported because they exceed the useful life of the plant.

Table 4.1: Best energy, environmental and economic results with flat plate collectors.

Sub-scenario	Scenario A			Scenario B		
	PES [%]	ΔCO_2 [%]	SPB [y]	PES [%]	ΔCO_2 [%]	SPB [y]
0%	9.74	7.36	-	12.80	10.20	-
50%	43.38	40.13	8	45.50	42.17	7
100%	58.78	55.81	4	60.40	57.40	4
Sub-scenario	Scenario C			Scenario D		
	PES [%]	ΔCO_2 [%]	SPB [y]	PES [%]	ΔCO_2 [%]	SPB [y]
0%	13.22	10.50	-	19.18	17.03	-
50%	45.77	42.37	7	49.37	45.72	7
100%	60.61	57.56	4	63.41	60.23	3

Table 4.2: Best energy, environmental and economic results with evacuated tube collectors.

Sub-scenario	Scenario A			Scenario B		
	PES [%]	ΔCO_2 [%]	SPB [y]	PES [%]	ΔCO_2 [%]	SPB [y]
0%	20.45	17.14	-	22.27	18.84	-
50%	58.14	54.72	10	59.44	56.00	10
100%	71.60	68.86	5	72.58	69.84	5

Sub-scenario	Scenario C			Scenario D		
	PES [%]	ΔCO_2 [%]	SPB [y]	PES [%]	ΔCO_2 [%]	SPB [y]
0%	22.33	18.81	-	24.47	21.74	-
50%	59.52	56.04	9	61.05	57.47	9
100%	72.65	69.89	5	73.84	71.04	5

Chapter 5 Micro-trigeneration system with a desiccant-based air handling unit in Southern Italy climatic conditions

5.1 Introduction

The aim of this Chapter, starting from experimental tests carried out in a test facility located at “Università degli Studi del Sannio”, in Benevento, is to describe and investigate the technical feasibility of an Micro Combined Cooling, Heating and Power (MCCHP) system, mainly consisting of a hybrid AHU and a microcogenerator. The system provides the air-conditioning service to the well-known lecture room (see previous Chapters) during summer and winter periods. Furthermore, over the whole year, the cogeneration plant provides thermal energy for DHW production, to a nearby user (a multifamily house, MFH). The MCCHP system (alternative system, AS) is compared with a system based on a traditional AHU and on separate electric, thermal and cooling production (conventional or reference system, CS). Experimental and manufacturers’ data are used to calibrate and validate models of the main components and energy conversion devices. These models are used to simulate both systems by means of the TRNSYS software [58,59], in order to evaluate operational data and performance parameters. Simulation models taking into account the transient nature of building and loads, the part-load characteristics of devices and the system energy management and control are applied. Furthermore, a sensitivity analysis is performed, to analyze the effect of the share of cogenerated electricity consumed on-site on the overall techno-economic performance.

5.2 Loads characterization

The 30 seats lecture room is considered again as the building air-conditioned by the desiccant-based AHU (see Chapter 2). It is assumed that the lecture room has the same characteristics described in the previous chapters but an activation schedule of the air-conditioning service from Monday to Saturday, from 8:30 to 19:00 during summer and winter periods [57].

In addition the DHW demands of the MFH is simulated. Jordan and Vajen have developed a tool to generate realistic domestic hot water load profiles in the framework of IEA/SHC Task 26 [91,92]. Those load profiles can be used with TRNSYS. Each profile consists of a value of water flow rate for every time step; the values of the flow rate and the time of occurrence of every incidence were selected by statistical means. A requirement of 1200 l per day was set, corresponding to a MFH with 30 persons, with an average requirement of 40 l/(person·day). As an example, Figure 5.1 shows the domestic hot water demand profile in the time scale of 1 min during a day. Considering

the domestic hot water supply temperature of 45 °C and simulating the temperature of cold water from the mains, the annual energy requirement for DHW production is 18.2 MWh/year.

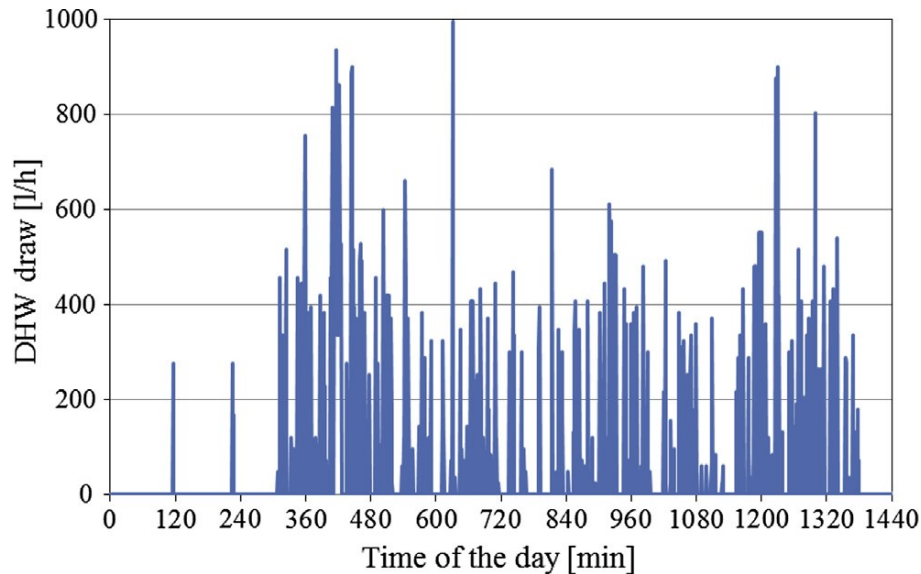


Figure 5.1: Profile of domestic hot water draw.

5.3 Plant configuration and operation

The simulated plant in this case is arranged in a manner more similar to the actual test facility. The main components are (Figure 5.2):

- the AHU equipped with a DW,
- the microgenerator ([51]) fuelled by natural gas (MCHP),
- the electric air-cooled water chiller (CH),
- the natural gas boiler (B),
- the thermal energy storage (TS).

The air handling unit is the hybrid system that operates in summer configuration with thermal energy for regeneration purposes provided by the MCHP and/or by the boiler and cooling energy provided by the electric chiller. A certain amount of electricity serves for the chiller and for the other auxiliary devices (pumps and fans). This energy is supplied by the cogenerator and/or by the electric grid. Thermal energy from the MCHP can be either transferred directly to the heating coil (HC) of the regeneration air duct or in the TS. The thermal recovery circuit of the MCHP is connected to the internal heat exchanger placed at the bottom of the TS.

In the situation depicted in Figure 5.2, the lower heat exchanger of the tank and the first heating coil of the AHU are connected to the MHCP. The second heating coil (HC3) in

the air handling unit directly interacts in open circuit with the fluid stored in the TS: hot water is drawn from the upper part of the tank, further heated-up by the boiler (if necessary to achieve the required regeneration temperature) and sent to the heating coil. Then the water returns to the TES in the lower part of the tank.

As regards the air handling unit, transformations of the process and cooling air remain the same, however, those of the regeneration air changes with respect to the solar-driven plants. In particular, the heating process is performed, if necessary, in two phases (see Figure 1.7): (1-5) in the heating coil (HC) and (5-6) in the coil HC3. The DW requires a certain regeneration temperature, mainly depending on the desired humidity ratio reduction of moist air. If thermal energy from the storage is not enough to heat the regeneration air up to the required temperature, the boiler provides further thermal energy at the required temperature level.

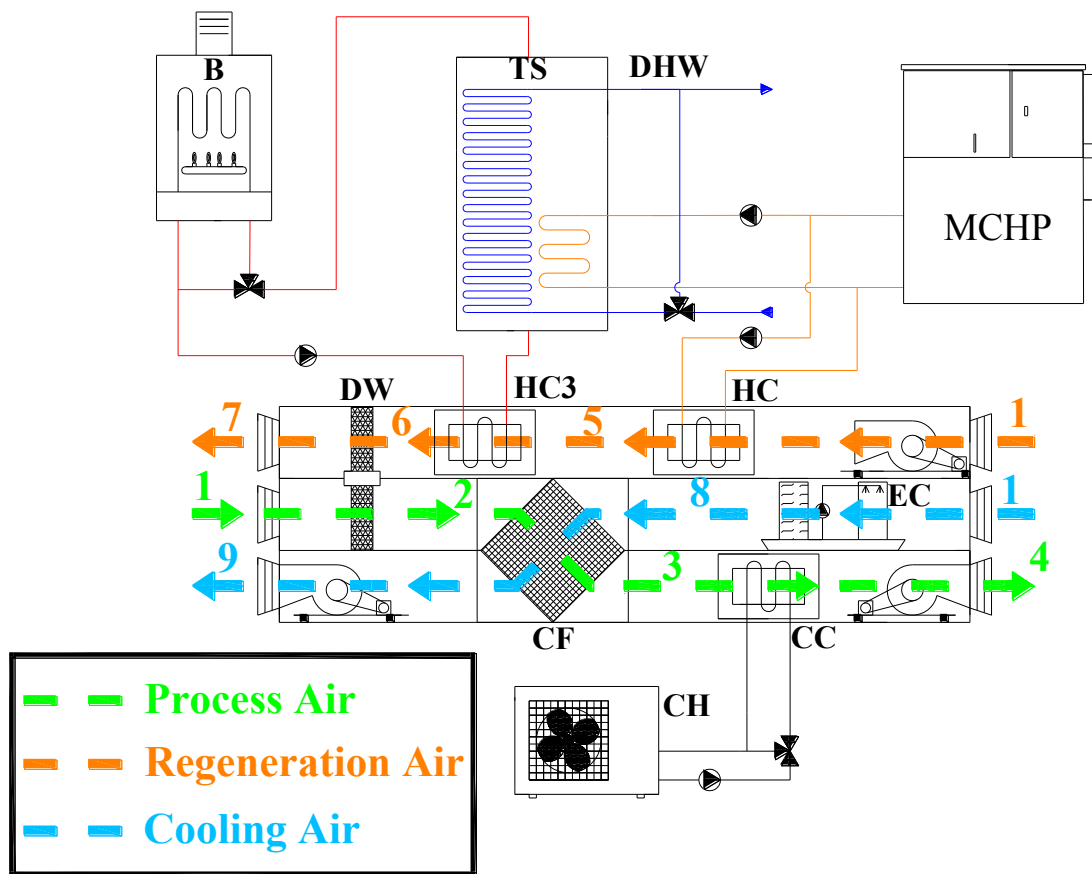


Figure 5.2: The layout of the desiccant-based AHU.

During the summer air conditioning service, 3 pumps and 3 fans are active, with a total electric requirements of auxiliaries equal to 1410 W. When the electric power from the MCHP is low compared to the amount required, further electric power is taken from the

electric grid; on the contrary, when the power from the microcogenerator exceeds use, the surplus is fed into the grid.

The main energy flows of the trigeneration system during summer operation are shown in Figure 5.3. Specific superscripts and subscripts, referring to energy conversion devices involved in an energy flow and to energy vectors, have been used.

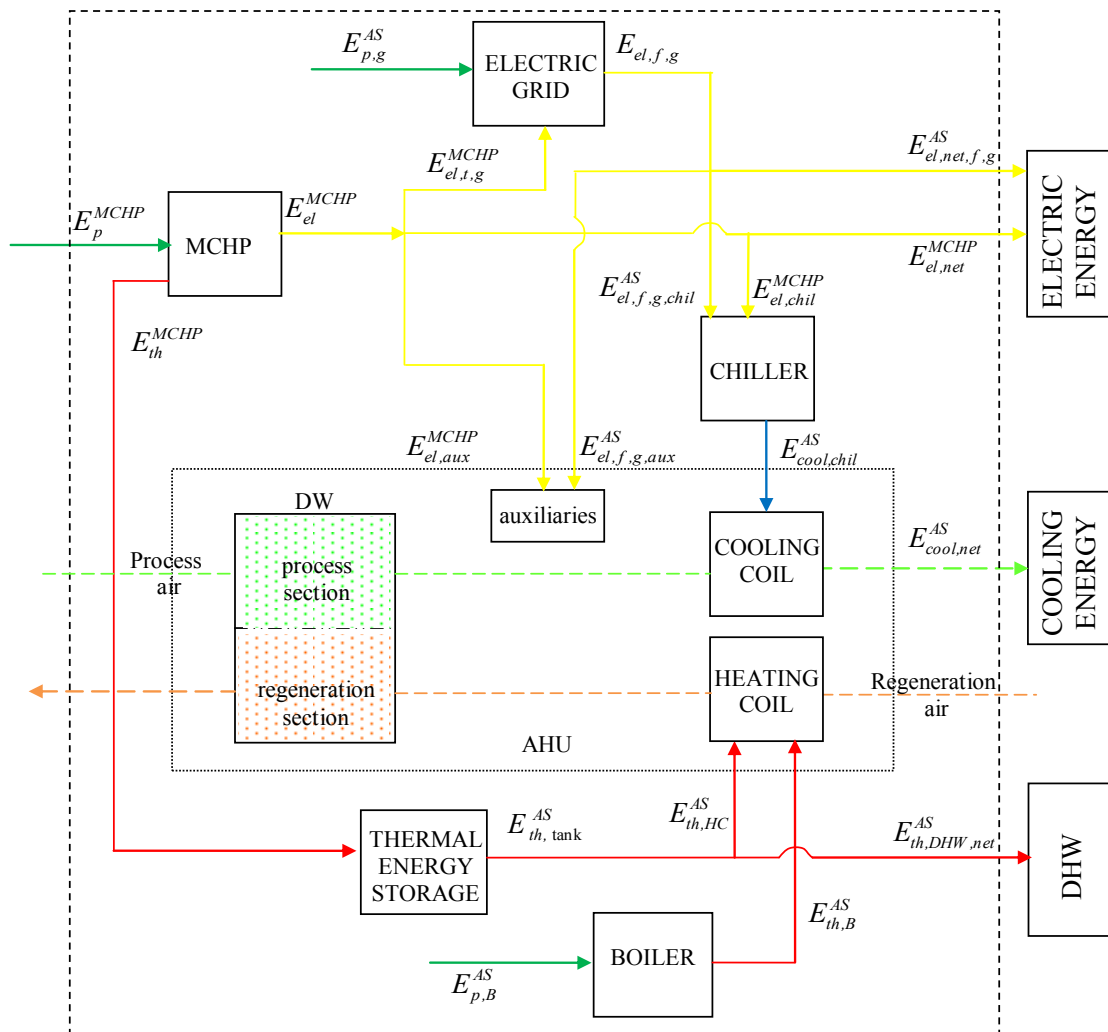


Figure 5.3: Main energy flows of the trigeneration system during summer operation.

During winter operation, to meet the sensible and latent loads of the lecture room, the simulated innovative AHU of Figure 5.2 is modified as described in Section 2.3.2. The two heating coil (HC1 and HC2) of the process air duct are fed with the water stored in the tank (Figure 5.4).

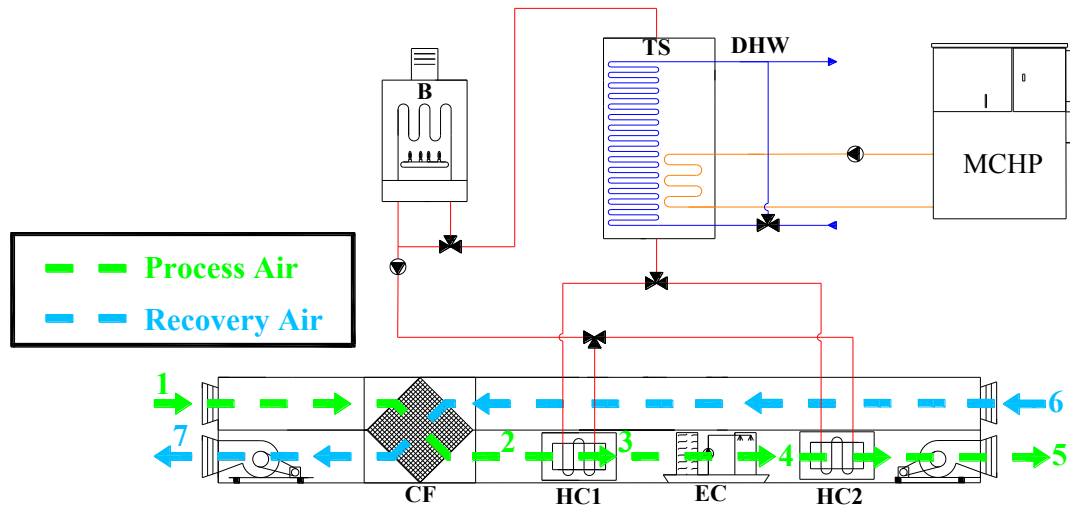


Figure 5.4: Layout of the AHU in the PS for winter operation.

The control system evaluates the temperature of the water coming out from the TES, when it is less than that required for the pre-and post-heating processes, it turns on the auxiliary boiler to heat-up the fluid to the correct temperature level.

In this layout, the wet pack humidifier operates on the process air that goes to the indoor conditioned ambient, therefore the quality of the sprayed water should be periodically controlled to avoid any problem related to the occurrence of Legionella bacteria; if necessary, the supplied water has to be filtered and disinfected, and the humidifier has to be periodically cleaned.

During the winter air conditioning service, 2 pumps and 2 fans are active, with a total electric requirements of auxiliaries equal to 940 W.

When the AHU is switched off, the thermal energy requirements are related to the DHW demand only. In this case, electricity is used to activate the MCHP pump (150 W) and the electric appliances of the lecture room.

Over the whole year, a certain amount of the stored thermal energy is used for DHW production for the MFH. Cold water coming from the mains is heated in the TS through the internal heat exchanger (in both Figure 5.2 and Figure 5.4) and supplied to the end-user at 45 °C. To meet the DHW demands, a three-way valve operates so that the right amount of mains water by-passes the TS and mixes with the hot fluid exiting the storage, to reach the desired temperature of 45 °C. If the temperature of DHW exiting the tank is lower than 45 °C, a heating system (boiler), installed in the premises of the MFH, is assumed to provide for the shortage.

The MCHP electric energy drives the pumps, the AHU auxiliaries, the electric chiller and satisfies the electric load of the lecture room.

The MCHP system is controlled with a thermal load-following operation; the unit operates according to a temperature signal coming from a thermostat placed on the TS near the inlet of the internal heat exchanger connected to the microcogenerator (in both Figure 5.2 and

Figure 5.4): when this temperature is lower than 58 °C, the unit is activated; when this temperature is higher than 60 °C, the unit is turned off. The electricity generation is a by-product and any unused excess of electricity is sent to the grid, that is also used to cover the peak load.

5.4 Mathematical models

The software and then the models used to simulate the components of this plant are the same described in the previous chapters. The approach followed to simulate the DHW demands of the MFH and to manage the lecture room electric load, the model of the MCHP, that have not been hitherto introduced are specifically described below. Furthermore a different mechanism of financial support is considered for microcogeneration with respect to those of the solar systems.

5.4.1 Loads and external factors

The building has an electricity requirement (for computers, lighting, appliances, etc.) of 139 kWh/m²/year (8.83MWh/year), that is a typical value of electric energy consumption in office applications [93]. Electricity hourly demand profiles of the user were not defined in here, but a sensitivity analysis was performed with respect to the parameter electric surplus factor, defined as [94]:

$$\psi_{el} = E_{el,t,g}^{MCHP} / E_{el}^{MCHP} \quad (5-1)$$

that represents the ratio between the share of electricity from the MCHP exported to the grid ($E_{el,t,g}^{MCHP}$) and the overall output (E_{el}^{MCHP}).

As regards the energy demands for DHW of the MFH they are evaluated in TRNSYS starting from the DHW profile that consists of a value of water flow rate for every time step (Section 5.2). The corresponding thermal power related to DHW draw is:

$$\dot{Q}_{DHW} = \dot{m}_{DHW} c_p (T_S - T_m) \quad (5-2)$$

where \dot{m}_{DHW} is the mass flow rate of DHW drawn, c_p is the specific heat capacity, T_m is the temperature of cold water from the mains, entering the TS. It has been evaluated considering the profile defined by the Type 15–6 (included in TRNSYS library). T_s is the temperature of the hot water supplied to the end-user (45 °C). The annual energy requirement for DHW production is 18.2 MWh/year.

5.4.2 Reciprocating internal combustion engine cogeneration model

To simulate the microgenerator operation, the TRNSYS RIC (reciprocating internal combustion) engine model has been used, by means of the type 907 of the TESS (Thermal Energy System Specialists) additional library. It employs a table of performance data to determine the outputs of the engine, given a set of input conditions. The model relies on an external data file which contains efficiency (both mechanical and electrical) and heat transfer data (fraction of total thermal power recovered and the fraction dissipated to the environment) as a function of the intake temperature and the part load ratio (PLR, actual power over rated power). It is not possible to measure the mechanical power transferred from the engine to the electric generator in the test facility; therefore, a constant value of 0.95 has been assumed for the electrical efficiency of the generator.

The performance of the engine are reported in Table 5.1 [95,96]. The MHCP is modelled by three components, that are the RIC engine, a plate heat exchanger (type 5), used to transfer the recovered thermal power to a secondary fluid (i.e. water), and a threeway valve (type 11), that mixes the part of solution flow rate that passes through the plate heat exchanger and the one that is bypassed toward the engine. A control system that manages the thermal recovery circuit of the microgenerator is also modelled.

The desired electric output is converted to a PLR value and then used to refer to the performance map which contains information on efficiency, exhaust flow and heat distribution. From this performance map, the fuel use and thermal output can be derived.

To validate the MCHP model, a comparison between measured and experimental values of water temperature at the outlet of the heat exchanger (secondary circuit – cold side) was performed in [54].

No values are outside the $\pm 5\%$ error band; furthermore, a RMSE (Root Mean Standard Error) of 0.714 °C was obtained.

Table 5.1: Performance data for the internal combustion engine.

PLR (-)	0.170	0.342	0.512	0.676	0.840	1.000
Electrical rate (kW)	1.02	2.05	3.07	4.06	5.04	6.00
Primary energy rate (kW)	10.3	12.7	15.1	17.4	19.6	21.7
Total waste heat rate (kW)	9.30	10.7	12.0	13.4	14.5	15.7
Waste heat recovered rate (kW)	6.60	7.80	8.90	9.90	10.8	11.7
Electrical efficiency (-)	0.100	0.161	0.203	0.233	0.257	0.276
Mechanical efficiency (-)	0.102	0.170	0.214	0.246	0.271	0.291
Fraction of waste heat recovered (-)	0.710	0.729	0.742	0.739	0.745	0.745
Fraction of the waste heat to environment (-)	0.290	0.271	0.258	0.261	0.255	0.255

The validation was also based on an energy balance approach and to this aim a specific test was carried out. It had a duration of 75 min, during which the electrical power output of the microgenerator was increased from 2 to 6 kW with steps of 1 kW. Simultaneously, the temperature of water entering the plate heat exchanger was linearly increased from 40 to 56 °C.

The same forcing functions were also applied in a TRNSYS simulation of the MCHP; the error between measured and simulated values are 4.71% and 3.98%, in terms of overall thermal energy produced and overall primary energy required, respectively. Results are considered satisfactory, taking into account that the analyzed model does not evaluate transient effects.

5.4.3 Assessment of economic performance

The assessment of the SPB period is performed considering: a subsidy on gas price, a CHP generation bonus and an investment subsidy. In this section are also considered:

- an unitary price of electricity from grid, that is reference system for electricity supply (ratio of electric energy cost to delivered electric energy), $c_{el} = 0.211$ €/kWh_{el} [97]; an average value for the three time slots currently adopted in Italy is assumed;
- an unitary price of natural gas (ratio of natural gas cost to its volume) in Italy, $c_{NG} = 0.941$ €/Nm³ [97];
- feed-in tariff for electricity exported to the Italian grid, $FIT = 0.0879$ €/kWh_{el}. It was evaluated considering the average of the three time slots of the economic

value of electricity exported to the grid, according to the net metering scheme, introduced by Italian Authority for Electricity and Gas (AEEG) for cogeneration plants with electric power up to 200 kW [98].

As regards the subsidy on gas price for CHP, the support mechanism ([99] and related subsequent additions) states that 0.22 m³ of gas per kWh of generated electricity can access a reduced excise tax (0.0004493 €/m³, reduced to 0.00013479 €/m³ if more than 70% of cogenerated electricity is consumed on site); the remaining amount of consumed natural gas can access, in the case of trigeneration systems, the excise tax for industrial uses (0.012498 €/m³), that is much lower than the one for civil uses (from 0.12 to 0.15 €/m³, depending on the range of annual consumption). Therefore, the resulting reduced unitary price of natural gas for both the MCHP and the boiler in the AS is $c_{NG}^s = 0.771$ €/Nm³ [97], [100].

As regards the CHP generation bonus, it was evaluated by calculating the revenues related to the white certificates achieved by the MCHP, according with the Ministerial Decree of 5 September 2011[101].

As regards the investment subsidy, the same Decree foresees that, for high-efficiency cogenerators, the white certificates mechanism can be combined with guarantee or revolving funds, as well as with other public grants not exceeding 40% of the investment cost for plants with electric power up to 200 kW. Therefore, a reduction of 40% of the investment cost was assumed for the MCHP unit.

As regards maintenance costs, the following values were assumed:

- MC^{MCHP} , maintenance cost for the MCHP (0.0896 €/h [102])
- MC_B^{AS} , maintenance cost of the gas boiler in the AS (80 €/y);
- MC_{chil}^{AS} , maintenance cost of the chiller in the AS (150 €/y);
- MC_B^{CS} , maintenance cost of the gas boiler in the reference system (120 €/y); it is higher than the MC_B^{AS} , as the B in the CS has a higher size than the one in the AS;
- MC_{chil}^{CS} , maintenance cost of the chiller in the CS (288 €/y); it is higher than the MC_{chil}^{AS} , as the chiller in the CS has a higher size than the one in the AS.

Finally, the following investment costs of the equipment were assumed:

- MCHP: 18,000 €, with an investment subsidy of 7,200 €, that reduces the investment cost to 10,800 €;
- storage tank: 3,000 €;

- gas boiler: 1,500 € for the PS, 3,000 € for the CS;
- major cost of the desiccant-based AHU (AS) with respect to the conventional one (CS): 10,000 €;
- chiller: 3,000 € for the AS, 6000 € for the CS.

The resulting extra cost (EC) is 19,300 €.

5.5 Simulation and Results

The microtrigeneration system is installed in Benevento (Southern Italy, mean annual temperature 13.8 °C), for which the corresponding “Meteonorm” climatic file was used in the simulation. Benevento belongs to Italian climatic zone C, with 1316 HDD and a heating period from November 15th to March 31st, as defined by Italian legislation. The length of the cooling period is not specified in Italy, but the activation period of the air conditioning service for the lecture room was assumed from June 1st to September 15th. A time step of 1 min was used in the simulations.

The CS, both in summer and winter periods, has to ensure the same air-conditioning service and electricity demand to the lecture room and the same DHW production to the MFH provided by the proposed one. For summer air conditioning purposes, the CS is equipped with a standard configuration of the AHU (see Section 1.1.1). A conventional boiler is used in summer to provide thermal energy to the system (both for post-heating and DHW), while electrical energy to activate the appliances of the lecture room, the chiller and the auxiliaries of the AHU is taken from the grid.

The AHU of the reference system in the winter season has the same configuration of the one in the proposed system, with the difference that the heating coils for pre-and post-heating are fed by

the boiler only, that provides thermal energy for DHW too. Finally, also for the CS, when the AHU is switched off, the only thermal energy requirements are related to the DHW demand.

First of all, the energy production on a yearly basis of the energy conversion devices of the AS (MCHP and boiler), as well as electric (chiller, auxiliaries and electric appliances) and thermal energy requirements (DW regeneration, winter space heating and DHW) are reported in Table 5.2.

Thermal energy consumption is lower than production, the difference (2.50MWh/y, about 7.8% of the production) is the energy losses of the TS. Thermal energy for DHW

production (16.0MWh, about 88% of the overall requirement) is provided by the MCHP only.

Table 5.2: Annual energy balance for the equipment of the AS.

Components	Primary energy consumption [MWh/y]	Thermal energy production [MWh/y]	Thermal energy consumption [MWh/y]	Net electricity production [MWh/y]	Electricity consumption [MWh/y]
MCHP	54.0	30.0	-	14.3	-
Boiler	2.17	1.96	-	-	-
Chiller	-	-	-	-	1.40
Auxiliaries	-	-	-	-	2.58
Electric Appliance	-	-	-	-	8.83
DW regeneration	-	-	6.95	-	-
Space heating	-	-	6.51	-	-
DHW	-	-	16.0	-	-
Total	56.2	32.0	29.5	14.3	12.8

The data related to the microcogenerator allow to calculate a thermal efficiency of 55.6%, a net electric efficiency of 26.5% and an overall efficiency (PER, primary energy ratio) of 82.1%. These efficiency values allow to calculate the electric allocation factor [94] as:

$$\xi_{el} = \eta_{el}^{MCHP} / (\eta_{el}^{MCHP} + \eta_{th}^{MCHP}) = 0.323 \quad (5-3)$$

The allocation factors are used to partition the input of a process (i.e. primary energy) to one or more outputs (i.e. electric and thermal energy). If an energy vector leaves the boundary system (e.g. it is fed into the electrical or thermal grid), the corresponding primary energy demand has to be evaluated, in order to obtain the primary energy demand related to the products which remain within the system. In the analyzed case, as the MCHP is heat-led, a share of the electric energy output can exit the system; therefore, only the electric allocation factor is calculated, while the thermal one is zero. Taking into account the allocation and surplus factors, the effective primary energy consumption to ascribe to the MCHP is [94]:

$$E_p^{*MCHP} = E_p^{MCHP} (1 - \xi_{el} \psi_{el}) \quad (5-4)$$

where $E_p^{MCHP} = 54.0$ MWh (Table 5.2), $\xi_{el} = 0.323$ and ψ_{el} has been varied in the range 10–80%, according to a sensitivity analysis, described later.

The overall primary energy consumption of AS is therefore:

$$E_p^{AS} = E_p^{*MCHP} + E_{p,B}^{AS} + E_{el,f,g}^{AS} / \eta_{el,ref} \quad (5-5)$$

where $E_{p,B}^{AS} = 2.17$ MWh (Table 5.2), while the electricity drawn from the grid, that is the sum of the amounts required by the chiller, the auxiliaries and the net energy provided to the final user ($E_{el,f,g}^{AS} = E_{el,f,g,chil}^{AS} + E_{el,f,g,aux}^{AS} + E_{el,net,f,g}^{AS}$ Figure 5.3), depends on the value of ψ_{el} . For example, if $\psi_{el} = 0.8$, it means that 80% of the overall electricity production ($E_{el}^{MCHP} = 14.3$ MWh, Table 5.2) is sold to the grid ($E_{el,t,g}^{MCHP} = 11.4$ MWh) and 20% is consumed on-site (2.86 MWh). As the overall electricity consumption in the AS is 12.8 MWh (Table 5.2), therefore $E_{el,f,g}^{AS} = 12.8 - 2.86$ MWh = 9.94 MWh and $E_p^{AS} = 65.9$ MWh.

The equivalent CO₂ emissions of the AS are evaluated as:

$$CO_2^{AS} = (E_p^{*MCHP} + E_{p,B}^{AS}) \beta + E_{el,f,g}^{AS} \gamma \quad (5-6)$$

Finally, the operating costs of the AS are evaluated as:

$$OC^{AS} = (E_p^{*MCHP} + E_{p,B}^{AS}) c_{NG}^s + E_{el,f,g}^{AS} c_{el} - E_{el}^{MCHP} \cdot CHP_Bonus - E_{el,t,g}^{MCHP} \cdot FIT + MC^{MCHP} \cdot h^{MCHP} + MC_B^{AS} + MC_{chil}^{AS} \quad (5-7)$$

where h^{MCHP} is the number of operating hours of the MCHP (2552) and CHP_Bonus is the bonus related to white certificates achieved by the CHP.

The necessary condition to obtain white certificates (*WC*), the subsidy on gas price, investment subsidies and the access to the net metering scheme, is that the MCHP is recognized as high efficiency, as defined by [103]. For a microgenerator with electric power lower than 50 kW_{el}, the criterion for high efficiency certification is that primary energy saving (PES_{HEC}) > 0. This index is evaluated as:

$$PES_{HEC} = 1 - E_p^{MCHP} / (E_{el}^{MCHP} / \eta_{el,ref} + E_{th}^{MCHP} / \eta_{th,ref}) \quad (5-8)$$

where E_{el}^{MCHP} coincides with the overall electricity produced only if the PER of the MCHP is higher than a certain value (75% for internal combustion engine-based units). This effectively occurs in this case, as PER is 82.1%. $\eta_{el,ref}$ and $\eta_{th,ref}$ are the reference electric and thermal efficiency, respectively [104]. In particular, the value of the reference electric efficiency depends on some factors, such as installation year of the cogeneration unit, fuel, climatic conditions, electricity used on-site and avoided grid losses due to decentralized production. Reference thermal efficiency, instead, depends on the type of fuel and the way the available thermal energy is exploited (direct use of exhaust gases or ‘‘production’’ of steam/hot water). With respect to the MCHP units considered, the evaluation of PES_{HEC} has been carried out considering that:

- thermal energy recovered by MCHP is used to produce hot water;
- it is fuelled with natural gas ($\eta_{th,ref} = 90\%$);
- it is installed during 2013 (baseline value of $\eta_{el,ref}$ is 52.5%);
- the average Italian ambient temperature is 16.0 °C (0.1%-point reduction of $\eta_{el,ref}$ with respect to a reference temperature of 15 °C);
- it is connected to the low voltage grid (<400 V).

The correction factor of $\eta_{el,ref}$ for avoided grid losses, besides the voltage level, depends on the shares of electricity exported to the grid and consumed on-site. It is 0.925 if all electricity is exported, 0.860 if all electricity is consumed on-site.

To evaluate CHP_Bonus , first of all the methodology defined by the Ministerial Decree of 5 September 2011 [101] to calculate the white certificates that an MCHP unit can obtain has been applied:

$$NS = E_{el}^{MCHP} / \eta_{el,ref} + E_{th}^{MCHP} / \eta_{th,ref} - E_p^{MCHP} \quad (5-9)$$

where NS is the net saving in toe. The number of WC to which the system is entitled is then evaluated by

$$WC = NS \cdot f_T \cdot K \quad (5-10)$$

where K is a correction factor depending on the size of the MCHP, equal to 1.4 for MCHPs, and $f_T = 0.086$ toe/MWh is the conversion factor from MWh to toe. The related revenues can be evaluated considering a specific value for the WC of 106.03 €/toe, [105], while CHP_Bonus is simply the ratio between these revenues and the electricity production.

PES , NS and CHP_Bonus are shown as a function of the electric surplus factor in Figure 5.5. The primary energy saving is higher than 0 in all cases, therefore the investigated cogenerator is a high efficiency unit and it can access the support mechanisms. All the indices achieve the maximum value for the lowest electric surplus factor, as in this case the correction factor of $\eta_{el,ref}$ for avoided grid losses is the minimum.

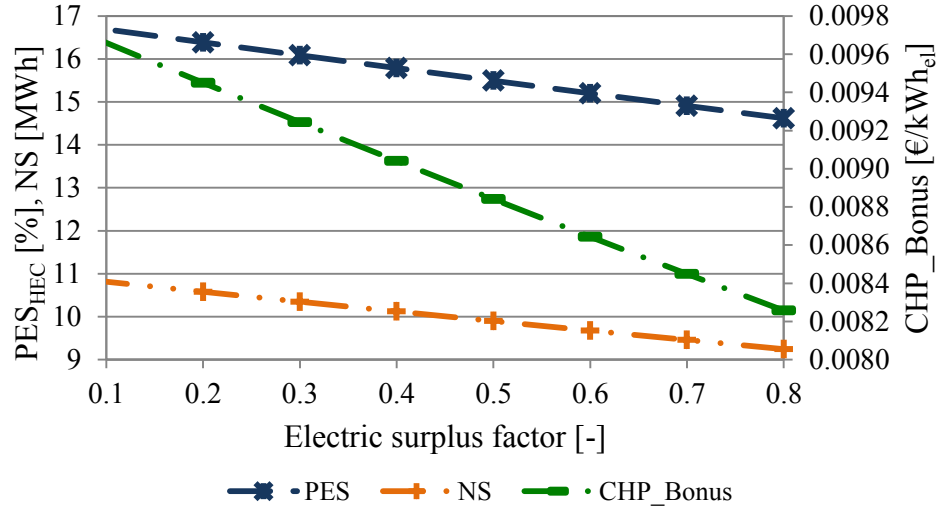


Figure 5.5: Primary energy saving, net saving and CHP generation bonus as a function of the electric surplus factor.

The energy production on a yearly basis of the boiler in the AS, as well as electric (chiller, auxiliaries and electric appliances) and thermal energy requirements (summer air post-heating, winter space heating and DHW) are reported in Table 5.3. In this case, thermal energy production coincides with consumption, as no storage losses are present. DHW production is the same of the MCHP in the proposed system (16.0 MWh).

The overall primary energy consumption of CS is:

$$E_p^{CS} = E_{p,B}^{CS} + E_{el,f,g}^{CS} / \eta_{el,ref} = 26.6 MWh + 13.5 MWh = 58.7 MWh \quad (5-11)$$

The equivalent CO₂ emissions of the CS are evaluated as:

$$CO_2^{CS} = E_{p,B}^{CS} \beta + E_{el,f,g}^{CS} \gamma = 13.2 t / y \quad (5-12)$$

Finally, the operating costs of the CS are evaluated as:

$$OC^{CS} = E_{p,B}^{CS} c_{NG} + E_{el,f,g}^{CS} c_{el} + MC_B^{CS} + MC_{chil}^{CS} \quad (5-13)$$

The SPB is therefore:

$$SPB = EC / (OC^{CS} - OC^{AS}) \quad (5-14)$$

Table 5.3: Annual energy balance for the equipment of the CS.

Components	Primary energy consumption MWh/y	Thermal energy production MWh/y	Thermal energy consumption MWh/y	Electricity consumption MWh/y
Boiler	26.6	23.9	-	-
Chiller	-	-	-	3.1
Auxiliaries	-	-	-	1.55
Electric Appliance	-	-	-	8.83
Air post-heating	-	-	1.41	-
Space heating	-	-	6.51	-
DHW	-	-	16.0	-
Total	26.6	23.9	23.9	13.5

The performance of the AS strongly depend on several operating conditions, first of all the matching between the electric demand and production profiles, that influences the electric surplus factor.

The results of the sensitivity analysis, with the surplus factor varying in the range 0.1–0.8, are shown in Figure 5.6.

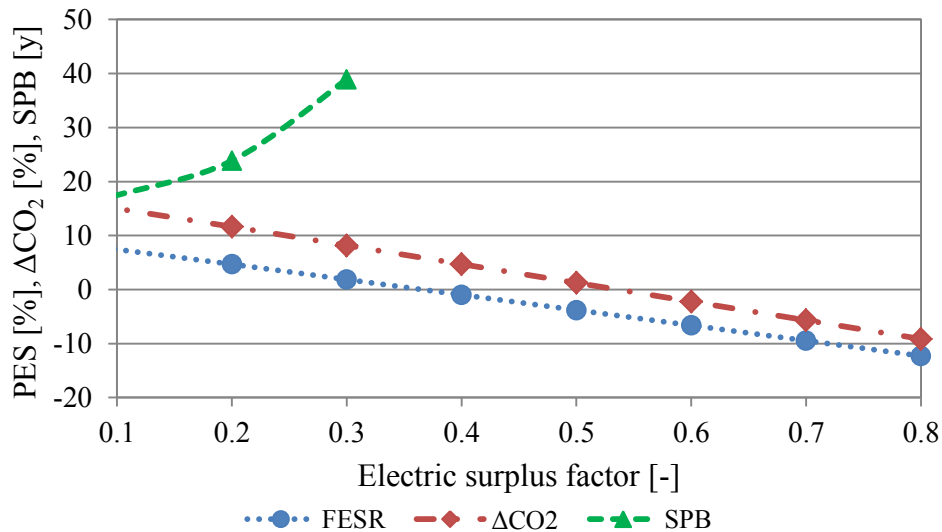


Figure 5.6: The results of the thermo-economic analysis as a function of the electric surplus factor.

The best case is achieved with the minimum value of ψ_{el} , that corresponds to the maximum share of cogenerated electricity used on-site; when $\psi_{el} = 0.1$, 10% of the cogenerated electricity is exported to the grid and no electricity is drawn from the grid for electric appliances, chiller and auxiliaries; in this case, $PES = 7.70\%$, $\Delta CO_2 = 15.3\%$ and $SPB = 16.9$ years.

The performance of the AS then reduces when ψ_{el} increases; in particular, to obtain both primary energy and emissions savings from the investigated trigeneration system, a surplus factor lower than about 40% has to be considered, i.e. about 60% of cogenerated electricity has to be consumed on-site.

As regards the economic analysis, the SPB parameter is the most sensitive to the variation of ψ_{el} , as it drastically increases with the electric surplus factor, becoming negative for values of ψ greater than 0.3 (not shown in Figure 5.6). At the current energy prices and installation costs of the devices, the economic feasibility of the investigated micro-trigeneration system cannot be achieved, even if it can access all the support mechanisms introduced by Italian legislation for small scale gas fuelled trigeneration systems: a lower taxation on gas price, the white certificates mechanism, an investment subsidy (up to 40% of the investment cost) and the net metering scheme. In fact, the SPB is considerably long for this type of installations, even in the best case (minimum electricity export).

Conclusions

The innovative desiccant-based air handling units (AHU) are a very interesting solution for air conditioning of buildings in the residential and tertiary sector as they operate with low temperature thermal energy. These HVAC systems can use a “free” thermal energy source, such as waste heat recovered from a microcogenerator or especially solar energy.

In recent years there has been a rapid growth in demands for air conditioning and indoor air quality both in industrialized and in emerging Countries, the so-called solar cooling systems are an excellent choice to limit energy and environmental issues deriving from the massive spread of electrically-driven air conditioners.

Solar radiation is widely available in summer and simultaneously there are the greatest demands for cooling, but solar energy can be used advantageously also to balance the winter thermal load. Therefore, typically, solar heating and cooling systems are realized. In the most common configuration, desiccant cooling system are equipped with a desiccant wheel, in which moist air is dehumidified by the adsorbent material and then cooled down by the evaporation of water and/or through an electric chiller (hybrid plants).

These alternative plants allow a more accurate humidity control, a better indoor air quality, a significant reduction in CO₂ emissions, primary energy and electricity savings.

A hybrid air conditioning device with silica-gel desiccant wheel is installed in the laboratories of the Università degli Studi del Sannio, and currently operate coupled with a microcogenerator and a natural gas boiler. The system in its actual configuration can operate only in cooling mode.

In this thesis the operation of the experimental air handling unit coupled with different types of solar collectors and three AHU modified layouts have been evaluated through dynamic simulations performed with the commercial software TRNSYS 17. In addition, in order to allow the system operation even in winter mode, suitable modifications have been identified and implemented in the model.

Experimental data acquired in the test facility, as well as, data provided by manufacturer, were used to calibrate and validate models of the main components and energy conversion devices. These models were used to simulate the operation of the innovative system and that of a conventional system in order to evaluate operational data and performance parameters.

With the results of the simulations the comparison of proposed and conventional systems is performed on an energy environmental and economic basis. Primary energy saving (*PES*), equivalent CO₂ avoided emission (ΔCO_2) and simple pay back period (*SPB*) were evaluated.

These air conditioning systems were used to balance the sensible and latent load of a 63.5 m² university classroom. Moreover, during the intermediate period, in the weekends and whenever there is a surplus of thermal energy the possibility of exploiting this energy in excess for further heating purpose is considered.

First of all the coupling of the experimental desiccant based air handling unit, and a solar field consisting of flat plate and evacuated tube collectors, was investigated. Simulations were performed for two different cities: Benevento (Southern Italy) and Milan (Northern Italy) in order to assess the influence of the collectors type (flat plate, evacuated tube), collecting surface (20, 27, 34 m²) and tilt angle (20-55°) on the energy, environment and economic performance of the plants. A further analysis is performed, considering different percent use (0, 50 and 100%) of the solar thermal energy surplus, that is the solar energy not used for air conditioning purposes and that can be used for other heating purposes, for example domestic hot water and/or low temperature heating of a gym, a university campus, a swimming pool, etc. The exploitation of this surplus becomes fundamental for the achievement of acceptable *SPB* periods, even in presence of economic incentives.

Considering the air conditioning operation only, with the best configuration and flat plate solar collectors, a primary energy savings of about 10% in Benevento and over 11% in Milan is obtained. Evacuated tube collectors give greater improvements in installations with colder climates although this is not evident when considering a relative index, such as the Primary Energy Saving. A primary energy saving of approximately 20% is reached. The exploitation of solar thermal energy that is not used for the regeneration of the desiccant wheel in summer and for the heating in winter increases very significantly the energy performance index. For an exploitation of 50%, optimum solar collectors inclination and widest surface of the solar field, *PES* becomes equal to a maximum of about 44 and 58%, respectively, with flat plate and evacuated tube collectors in Benevento and of about 31 and 45% in Milano. The full exploitation of solar thermal energy surplus brings those values to about 59, 72, 43 and 58%.

The economic analysis is not encouraging if further thermal energy demands are not considered. Systems with evacuated tube collectors are preferable from an economic

point of view when there is little space available for the solar field (20 m²), while with larger collecting surfaces (27 and 34 m²) flat plate collectors are advantageous. The shortest SPB periods are 4 and 6 years for Benevento and Milano, respectively.

Another type of solar collector considered for the coupling with the innovative air handling unit is a novel CPVT collector, consisting of a parabolic trough concentrator and a linear triangular receiver. This kind of collector is equipped with triple junction PV cells, capable to achieve ultra-high electrical efficiencies.

The solar field in this case provides thermal energy and electricity. Electrical energy is used to power the auxiliaries of the AHU, the chiller and further electric loads, while thermal energy is employed to heat the regeneration air flow during the summer period and the process air in the winter. Electricity in excess is sold to the grid, whereas the thermal energy surplus is exploited for domestic hot water (DHW). Integrations of electricity and thermal energy are provided by the electric grid and by a gas-fired boiler, respectively.

Annual energy and environmental performance of the overall system are evaluated in terms of Primary Energy Saving and emission reduction with respect to a reference case. The heat provided by the CPVT is about 60% of the regeneration energy and 30% of the energy needed for pre- and post-heating of the process air. The electricity, instead, is consumed on site for more than 70%. On an annual basis the analyzed system obtains a Primary Energy Savings between 81% and 89% depending on the DHW used. Suitable modifications to the standard layout of the desiccant-based air handling unit can deliver significant performance improvements and cost reductions.

The hybrid AHU was modelled in TRNSYS, both in the standard configuration and applying some modifications to reduce the thermal energy required for regeneration of the desiccant wheel. The introduced modifications concern:

- the pre-heating of the regeneration air with heat recovery from chiller condenser;
- the pre-heating of the regeneration air with heat recovery from the exhaust regeneration air in a cross-flow heat exchanger;
- the pre-cooling/dehumidification of the process air.

Moreover for each configuration, different collector types (flat plate, evacuated tube), surface (~20, 27, 34 m²) and tilt angle (20-55°) were considered.

Simulations of the innovative AHU, coupled to a solar field, were carried out in order to develop a thermo-economic assessment.

The obtained results show that the evacuated tube collectors improve the energy and environmental performance of the hybrid desiccant systems compared to conventional ones (up to 24% of primary energy saving with optimal tilt angle and surface) but they are more expensive than flat-plate collectors, that can provide primary energy savings up to 19%, with optimal tilt angle and surface. With regard to the equivalent CO₂ avoided emissions, they range between 2.5% and 17% in the scenarios with flat plate collectors and between 12% and 22% with evacuated tube collectors.

For both collector types, the best plant modification is the pre-cooling of the process air. Also the analysis, considering three sub-scenarios: 0, 50 and 100% of the solar thermal energy surplus use was performed. If 50% of solar thermal energy surplus is used, the SPB period ranges between 20 and 7 years (for the standard configuration with 20 m² of flat plate collectors and the pre-cooling modification with 34 m² of flat plate collectors, respectively, the optimal tilt angle is assumed in the best case).

The best energy, environmental and economic results reached in the innovative plants (in particular in Scenario D) with flat plate and evacuated tube collectors when 100% of solar thermal energy surplus is used are: $PES=63%$, $\Delta CO_2=60%$, $SPB=3$ years and $PES=74%$, $\Delta CO_2=71%$, $SPB=5$ years respectively.

Finally, a system similar to the test facility was considered. It constitutes a small scale trigeneration system, in which the heat-led microcogenerator interacts with the desiccant-based air handling unit. The system provides, once again the air-conditioning service to a lecture room during summer and winter periods, as well as the domestic hot water service to a Multi Family House through all the year.

During the summer season, the AHU operates as a desiccant cooling system, the silica-gel rotor balances the latent load of the process air, while an electric chiller manages the sensible load. The MCHP provides thermal energy to regenerate the desiccant wheel, by means of a thermal energy storage; a peak load boiler, fuelled with natural gas, provides thermal energy integration. Electricity from the cogenerator is used to drive the electric chiller, the auxiliaries of the AHU and of the MCHP itself (fans and pumps) as well as further electric appliances of the lecture room.

During the winter season, the MCHP and the boiler provide thermal energy for space heating purposes. Electricity is supplied to auxiliaries and electric appliances. When the AHU is inactive, cogenerated electricity is only supplied to electric appliances of the lecture room and thermal energy is only used for domestic hot water purposes.

This trigeneration system is compared with the reference system.

In particular, a sensitivity analysis has been performed, considering different values of the electric surplus factor, that represents the share of electricity from the MCHP that is exported to the grid.

From this performance assessment study, the following main conclusions can be derived:

- desiccant cooling is a very interesting technology, as it can achieve a reduction of both energy consumption and greenhouse gas emissions;
- in regions characterized by quite low thermal energy needs for space heating of buildings, it is crucial to utilize thermal energy available from the MCHP also for DHW requirements and to supply thermally-activated cooling systems, in order to increase the operating hours of the system;
- a sensitivity analysis showed that the energy, environmental and economic performance of the system strongly depend on the share of cogenerated electricity used on-site, in particular in terms of economic feasibility with respect to a reference system; the best values are: $PES = 7.70\%$, $\Delta CO_2 = 15.3\%$ and $SPB = 16.9$ years;
- the thermal and electric load profiles of the users should match so that the minimum amount of electricity is exported to the grid by the heat-led MCHP;
- the investment costs for this equipment (mainly MCHP and desiccant cooling system) are still quite high at the moment, and it cannot achieve economic feasibility even if all the support mechanisms introduced by Italian legislation for small scale gas fuelled trigeneration systems are exploited. A reduction of the installation cost is therefore desirable, to benefit from the energy and environmental advantages of micro-trigeneration systems based on desiccant cooling.

At the conclusion of this work one can say that a desiccant-based air handling unit fed with a renewable energy source such as solar energy can advantageously replace a conventional air conditioning systems with electrically-driven vapor compression cooling units if only energy and environmental performance are taken into account. However economic feasibility is still hard to obtain. For the considered application economic benefits do not occur together with the advantages mentioned above, although one considers incentives for the production of thermal energy from a renewable source. Only if the use of solar thermal is maximized considering other low temperature heating

purposes (for example domestic hot water or swimming pools heating) in addition to the air conditioning economic advantages can take place.

Nomenclature

A	Area [m^2]
a_1	Efficiency slope [$\text{W}/(\text{m}^2 \text{K})$]
a_2	Efficiency curvature [$\text{W}/(\text{m}^2 \text{K}^2)$]
b_0	IAM curve coefficient [-]
c	Unitary cost [$\text{€}/\text{Nm}^3$] or [$\text{€}/\text{kWh}$]
c_p	Specific Heat [$\text{J}/(\text{kg K})$]
C	Valorization coefficient [$\text{€}/\text{m}^2$]
C_{PVT}	Concentration ratio [-]
CHP_Bonus	Bonus related to energy savings of CHP [$\text{€}/\text{kWh}_{el}$]
CO_2	Equivalent CO_2 emission [kg/y]
d	Fluid channel diameter [m]
E	Energy [kWh/y]
EC	Extra cost [€]
E_p	Primary Energy [kWh/y]
F_1	F_1 Potential [-]
F_2	F_2 Potential [-]
F	Cash flow per year [$\text{€}/\text{y}$]
FIT	Feed-in tariff [$\text{€}/\text{kWh}_{el}$]
f_T	Conversion factor from MWh to tep [tep/MWh]
G	Total Incident Radiation [W/m^2]
G_{PVT}	Incident radiative flow [W/m^2]
g	Total solar energy transmittance [-]
h	Number of operating hours [-]
h_c	Convective heat transfer coefficient [$\text{W}/(\text{m}^2 \text{K})$]
h_f	Convective heat transfer coefficient of the fluid [$\text{W}/(\text{m}^2 \text{K})$]
$I_{a,tot}$	Annual incentive [$\text{€}/\text{y}$]
I_b	Beam radiation [W/m^2]
IAM	Incident Angle Modifier [-]
k	Tank fluid thermal conductivity [$\text{W}/(\text{m K})$]
K	Correction factor for white certificates calculation [-]
LHV	Lower Heating Value [kWh/Nm^3]
m	Mass of node [kg]

MC	Maintenance cost [€/h] or [€/y]
\dot{m}_f	Fluid mass flow rate [kg/s]
\dot{m}_{down}	Bulk fluid flowrate down the tank [kg/s]
\dot{m}_{up}	Bulk fluid flowrate up the tank [kg/s]
\dot{m}_{1in}	Mass flowrate entering at inlet 1 [kg/s]
\dot{m}_{1out}	Mass flowrate leaving at outlet 1 [kg/s]
\dot{m}_{2in}	Mass flowrate entering at inlet 2 [kg/s]
\dot{m}_{2out}	Mass flowrate leaving at outlet 2 [kg/s]
N	Number of years [-]
OC	Operating costs [€/y]
P	Electric power [W]
PER	Primary Energy Ratio[-]
PES	Primary Energy Saving [-]
Q	Thermal power [W]
r	Area specific thermal resistance [m^2K/W]
S	Gross solar collector area [m^2]
t	Temperature [$^{\circ}C$]
T	Temperature [K]
T_{1in}	Temperature of the fluid entering at inlet 1 [K]
T_{2in}	Temperature of the fluid entering at inlet 2 [K]
U	Total loss coefficient [$W/(m^2 K)$]
V	Volume [Nm^3/y]
WC	White Certificate [-]

Acronyms

AHU	Air Handling Unit
AS	Alternative System
B	Boiler
BN	Benevento
CC	Cooling Coil
CF	Cross-Flow heat exchanger
CH	Chiller
CHP	Combined heat and power

<i>COP</i>	Coefficient of performance
<i>CPVT</i>	Concentrating Photovoltaic/Thermal
<i>CS</i>	Conventional System
<i>DEC</i>	Desiccant and Evaporative Cooling
<i>DHW</i>	Domestic Hot Water
<i>DW</i>	Desiccant Wheel
<i>EC</i>	Evaporative Cooler
<i>HC</i>	Heating Coil
<i>HC2</i>	Post-Heating Coil
<i>HDD</i>	Heating Degree Day
<i>HVAC</i>	Heating, Ventilation and Air Conditioning systems
<i>HW</i>	Hot Water
<i>HW-HX</i>	Hot Water Heat Exchanger
<i>IAM</i>	incidence angle modifier
<i>IHE</i>	internal heat exchanger
<i>LHV</i>	Lower Heating Value
<i>MCCHP</i>	Micro combined cooling, heat and power
<i>MCHP</i>	Micro combined heat and power
<i>MFH</i>	Multifamily house
<i>MI</i>	Milano
<i>PLR</i>	Partial load ratio
<i>PV</i>	PhotoVoltaic cell
<i>PVT</i>	PhotoVoltaic-thermal collector
<i>R-HX</i>	Rotary heat exchanger
<i>RMSE</i>	Root mean standard error
<i>SC</i>	Solar Thermal Collectors
<i>SDEC</i>	Solar-driven Desiccant and Evaporative Cooling system
<i>SPB</i>	Simple Pay Back
<i>TS</i>	Tank Storage

Greek symbols

α	Absorptance
β	specific emission factor for primary related to natural gas combustion [kgCO ₂ /kWh _{Ep}]

γ	specific emission factor of electricity supplied by the grid [kgCO ₂ /kWh _{el}]
ΔCO_2	Equivalent CO ₂ avoided emission [-]
Δk	De-stratification conductivity [W/(m·K)]
ΔT	Temperature difference [K]
ΔT_{ln}	Logarithmic mean temperature difference [K]
$\Delta x_{i+1 \rightarrow i}$	Distance between node i and the node below it (i+1) [m]
$\Delta x_{i-1 \rightarrow i}$	Distance between node i and the node above it (i-1) [m]
ΔU	Additional loss coefficient [W/(m ² ·K)]
ε	Emittance [-]
η	Efficiency [-]
η_B	Boiler efficiency [-]
η_{col}	Collector efficiency [-]
η_{EG}	Italian national electric system efficiency [-]
η_{inv}	Inverter efficiency [-]
η_{mod}	Module efficiency [-]
η_{opt}	Optical efficiency [-]
η_{PV}	PV efficiency [-]
η_0	Intercept efficiency [-]
ξ	Allocation factor [-]
ρ_{PVT}	PVT reflectance [-]
σ	Stefan-Boltzmann constant [W/(m ² K ⁴)]
τ	time [s] or [h]
ψ	Surplus factor[-]
ω	Air humidity ratio [g/kg]

Subscripts

<i>a</i>	Ambient
<i>ap</i>	Aperture
<i>aux</i>	Auxiliaries
<i>B</i>	Boiler
<i>back</i>	Back surface
<i>c</i>	Cross section area of the node
<i>chil</i>	Chiller
<i>conc</i>	Concentrator

<i>conv</i>	Convective
<i>cool</i>	Cooling
<i>CPVT</i>	Concentrating Photovoltaic/Thermal
<i>DHW</i>	Domestic Hot Water
<i>el</i>	Electrical
<i>f</i>	Fluid
<i>front</i>	Front
<i>F₁</i>	F ₁ Potential
<i>F₂</i>	F ₂ Potential
<i>f,g</i>	From the grid
<i>f,T</i>	From the tank
<i>g</i>	Grid
<i>gross</i>	Gross
<i>HC</i>	Heating coil
<i>HEC</i>	High efficiency cogeneration
<i>hx</i>	Heat exchanger
<i>i</i>	Generic node
<i>in</i>	Inlet
<i>Int</i>	Intermediate season
<i>j</i>	Generic air state
<i>k</i>	Generic year
<i>lat</i>	latent
<i>load</i>	Load
<i>m</i>	Cold water from the mains
<i>on-site</i>	On-site consumption
<i>net</i>	Net
<i>NG</i>	Natural gas
<i>out</i>	Outlet
<i>pre</i>	Pre-heating
<i>post</i>	Post-heating
<i>PVT</i>	Photovoltaic/Thermal
<i>r</i>	Generic bracket
<i>Rec</i>	Recovery
<i>ref</i>	Reference value

<i>reg</i>	Regeneration
<i>S</i>	Hot water supplied to the end-user
<i>s</i>	Surface of the node
<i>sen</i>	sensible
<i>sky</i>	Sky
<i>Su</i>	Summer period
<i>sub</i>	Metallic substrate
<i>tank</i>	Storage tank
<i>th</i>	Thermal
<i>top</i>	Top surface
<i>tot</i>	Total
<i>t,g</i>	To the grid
<i>.0</i>	To the tank
<i>WD</i>	Week days
<i>WED</i>	Weekend days
<i>Wi</i>	Winter period

Superscripts

*	Related to effective primary energy consumption of MCHP
<i>AS</i>	Alternative System
<i>CS</i>	Conventional System
<i>MCHP</i>	Micro combined heat and power
<i>s</i>	With subsidy

References

- [1] L. Bellia, P. Mazzei, F. Minichiello D. Palma, *Aria Umida - Climatizzazione ed involucro edilizio*, Liguori Editore, 2006. [in Italian]
- [2] G. Angrisani, A. Capozzoli, F. Minichiello, C. Roselli, M. Sasso, Desiccant wheel regenerated by thermal energy from a microcogenerator: experimental assessment of the performances. *Applied Energy* 88 (2011), 1354–1365.
- [3] G. Angrisani, C. Roselli, M. Sasso, Distributed microtrigeneration systems. *Progress in Energy and Combustion Science* 38 (4) (2012), 502– 521.
- [4] J. Jeong, S. Yamaguchi, K. Saito, S. Kawai, Performance analysis of desiccant dehumidification systems driven by low-grade heat source. *International Journal of Refrigeration* 34 (2011) 928-945.
- [5] G. Angrisani, F. Minichiello, C. Roselli, M. Sasso, Experimental investigation to optimise a desiccant HVAC system coupled to a small size cogenerator. *Applied Thermal Engineering* 31 (2011), 506–512.
- [6] H.M. Henning, T. Pagano, S. Mola, E. Wiemken, Micro tri-generation system for indoor air conditioning in the Mediterranean climate. *Applied Thermal Engineering* 27 (2007), 2188–2194.
- [7] S. Misha, S. Mat, M.H. Ruslan, K. Sopian, Review of solid/liquid desiccant in the drying applications and its regeneration methods. *Renewable and Sustainable Energy Reviews* 16 (2012), 4686–4707.
- [8] A. Myat, K. Thu, N.K. Choon, The experimental investigation on the performance of a low temperature wasteheat-driven multi-bed desiccant dehumidifier (MBDD) and minimization of entropy generation. *Applied Thermal Engineering* 39 (2012), 70-77.
- [9] F. Calise, M. Dentice d'Accadia, C. Roselli, M. Sasso, F. Tariello, Desiccant-based AHU interacting with a CPVT collector: Simulation of energy and environmental performance. *Solar Energy* 103 (2014), 574–594.
- [10] G. Angrisani, C. Roselli, M. Sasso, F. Tariello, Assessment of Energy, Environmental and Economic Performance of a Solar Desiccant Cooling System with Different Collector Types. *Energies* 7 (2014), 6741-6764.
- [11] Pennington, N.A., 1955. Humidity Changer for Air Conditioning, USA Patent No. 2700537.

- [12] D. La, Y.J. Dai, Y. Li, R.Z. Wang, T.S. Ge, Technical development of rotary desiccant dehumidification and air conditioning: a review. *Renewable and Sustainable Energy Reviews* 14 (2010), 130–147.
- [13] R. Collier, F. Arnold, R. Barlow, An overview of open-circle desiccant cooling systems and materials. *Journal of Solar Energy Engineering* 104 (1) (1982), 28–34.
- [14] A.A. Pesaran, T.R. Penney, A.W. Czanderna,. *Desiccant Cooling: State-of-the-Art Assessment*. National Renewable Energy Laboratory, Golden, Colorado, 1992.
- [15] Y. Li, K. Sumathy, Y.J. Dai, J.H. Zhong, R.Z. Wang, Experimental study on a hybrid desiccant dehumidification and air conditioning system. *Journal of Solar Energy Engineering* 128 (1) (2006), 77– 82.
- [16] D. La, Y. Dai, Y. Li, T. Ge, R. Wang, Case study and theoretical analysis of a solar driven two-stage rotary desiccant cooling system assisted by vapor compression air-conditioning. *Solar Energy* 85 (2011), 2997–3009.
- [17] D. La, Y.J. Dai, Y. Li, R.Z. Wang, T.S. Ge, Technical development of rotary desiccant dehumidification and air conditioning: a review. *Renewable and Sustainable Energy Reviews* 14 (2010), 130–147.
- [18] D. La, Y.J. Dai, Y. Li, T.S. Ge, R.Z. Wang, Use of regenerative evaporative cooling to improve the performance of a novel one-rotor two-stage solar desiccant dehumidification unit. *Applied Thermal Engineering* 42 (2012), 11–17.
- [19] T.S. Ge, Y.J. Dai, R.Z. Wang, Y. Li, Experimental investigation on a one-rotor two-stage rotary desiccant cooling system. *Energy* 33 (2008), 1807–1815.
- [20] D. La, Y. Li, Y.J. Dai, T.S. Ge, R.Z. Wang, Development of a novel rotary desiccant cooling cycle with isothermal dehumidification and regenerative evaporative cooling using thermodynamic analysis method. *Energy* 44 (2012), 778–791.
- [21] T.S. Ge, F. Ziegler, R.Z. Wang, H. Wang, Performance comparison between a solar driven rotary desiccant cooling system and conventional vapor compression system (performance study of desiccant cooling). *Applied Thermal Engineering* 30 (2010), 724–731.
- [22] H. Li, Y.J. Dai, Y. Li, D. La, R.Z. Wang, Case study of a two-stage rotary desiccant cooling/heating system driven by evacuated glass tube solar air collectors. *Energy and Buildings* 47 (2012), 107–112.
- [23] N. Enteria, H. Yoshino, A. Mochida, R. Takaki, A. Satake, R. Yoshie, T. Mitamura, S. Baba,. Construction and initial operation of the combined solar

- thermal and electric desiccant cooling system. *Solar Energy* 83 (2009), 1300–1311.
- [24] N. Enteria, H. Yoshino, A. Mochida, R. Takaki, A. Satake, R. Yoshie, T. Mitamura, S. Baba, Development and construction of the novel solar thermal desiccant cooling system incorporating hot water production. *Applied Energy* 87 (2010), 478–486.
- [25] N. Enteria, H. Yoshino, A. Mochida, A. Satake, R. Yoshie, R. Takaki, H. Yonekura, T. Mitamura, Y. Tanaka, Performance of solar-desiccant cooling system with silica-gel (SiO₂) and titanium dioxide (TiO₂) desiccant wheel applied in East Asian climates. *Solar Energy* 86 (2012), 1261–1279.
- [26] S.D. White, P. Kohlenbach, C. Bongs, Indoor temperature variations resulting from solar desiccant cooling in a building without thermal backup. *International Journal of Refrigeration* 32 (2009), 695–704.
- [27] M. Beccali, P. Finocchiaro, B. Nocke, Energy performance evaluation of a demo solar desiccant cooling system with heat recovery for the regeneration of the adsorption material. *Renewable Energy* 44 (2012), 40–52.
- [28] U. Eicker, U. Schürger, M. Köhler, T. Ge, Y. Dai, H. Li, R. Wang, Experimental investigations on desiccant wheels. *Applied Thermal Engineering* 42 (2012), 71–80.
- [29] P. Bourdoukan, E. Wurtz, P. Joubert, M. Spérandio, Potential of solar heat pipe vacuum collectors in the desiccant cooling process: Modelling and experimental results. *Solar Energy* 82 (2008), 1209–1219.
- [30] H. Li, Y.J. Dai, M. Köhler, R.Z. Wang, Simulation and parameter analysis of a two-stage desiccant cooling/heating system driven by solar air collectors. *Energy Conversion and Management* 67 (2013), 309–317.
- [31] A. Khalid, M. Mahmood, M. Asif, T. Muneer, Solar assisted, pre-cooled hybrid desiccant cooling system for Pakistan, *Renewable Energy* 34 (2009), 151–157.
- [32] Z. Hatami, M.H. Saidi, M. Mohammadian, C. Aghanajafi, Optimization of solar collector surface in solar desiccant wheel cycle. *Energy and Buildings* 45 (2012), 549–568.
- [33] K.F. Fong, T.T. Chow, C.K. Lee, Z. Lin, L.S. Chan, Advancement of solar desiccant cooling system for building use in subtropical Hong Kong. *Energy and Buildings* 42 (2010), 2386–2399.

- [34] M. Beccali, P. Finocchiaro, B. Nocke, Energy and economic assessment of desiccant cooling systems coupled with single glazed air and hybrid PV/thermal solar collectors for applications in hot and humid climate. *Solar Energy* 83 (2009), 1828–1846.
- [35] L. Mei, D. Infield, U. Eicker, D. Loveday, V. Fux, 2006. Cooling potential of ventilated PV façade and solar air heaters combined with a desiccant cooling machine. *Renewable Energy* 31, 1265–1278.
- [36] Y. Sukamongkol, S. Chungpaibulpatana, B. Limmeechokchai, P. Sripadungtham, Condenser heat recovery with a PV/T air heating collector to regenerate desiccant for reducing energy use of an air conditioning room. *Energy and Buildings* 42 (2010), 315–325.
- [37] A. Al-Alili, Y. Hwang, R. Radermacher, I. Kubo, A high efficiency solar air conditioner using concentrating photovoltaic/thermal collectors. *Applied Energy* 93 (2012), 138–147.
- [38] A. Al-Alili, Y. Hwang, R. Radermacher A hybrid solar air conditioner: Experimental investigation. *International Journal of Refrigeration* 39 (2014), 117-124.
- [39] K. Ghali, Energy savings potential of a hybrid desiccant dehumidification air conditioning system in Beirut. *Energy Conversion and Management* 49 (2008), 3387-3390.
- [40] Y. Sheng, Y. Zhang, Y. Sun, L. Fang, J. Nie, L. Ma, Experimental analysis and regression prediction of desiccant wheel behavior in high temperature heat pump and desiccant wheel air-conditioning system. *Energy and Buildings* 80 (2014), 358–365.
- [41] I. Uçkan, T. Yılmaz, E. Hürdoğan, O. Büyükalaca, Exergy analysis of a novel configuration of desiccant based evaporative air conditioning system. *Energy Conversion and Management* 84 (2014), 524-532.
- [42] A.M. Elzahzby, A.E. Kabeel, M.M. Bassuoni, M. Abdelgaied, A mathematical model for predicting the performance of the solar energy assisted hybrid air conditioning system, with one-rotor six-stage rotary desiccant cooling system. *Energy Conversion and Management* 77 (2014), 129-142.
- [43] J. Zhu, W. Chen, Energy and exergy performance analysis of a marine rotary desiccant air-conditioning system based on orthogonal experiment. *Energy* 77 (2014), 953-962.

- [44] D. La, Y.J. Dai, Y. Li, Z.Y. Tang, T.S. Ge, R.Z. Wang, An experimental investigation on the integration of two-stage dehumidification and regenerative evaporative cooling. *Applied Energy* 102 (2013), 1218–1228.
- [45] T. Rang, L. Xiao-Hua, J. Yi, Performance analysis of a new kind of heat pump-driven outdoor air processor using solid desiccant. *Renewable Energy* 57 (2013), 101-110.
- [46] C. Bongs, A. Morgenstern, Y. Lukitob, H.M. Henning, Advanced performance of an open desiccant cycle with internal evaporative cooling, *Solar Energy* 104 (2014), 103–114.
- [47] M.J. Goldsworthy, S. White, Design and performance of an internal heat exchange desiccant wheel. *International Journal of Refrigeration* 39 (2014), 152-159.
- [48] R. Narayanan, W.Y. Saman, S.D. White, A non-adiabatic desiccant wheel: Modeling and experimental validation. *Applied Thermal Engineering* 61 (2013), 178-185.
- [49] P. Finocchiaro, M. Beccali, B. Nocke, Advanced solar assisted desiccant and evaporative cooling system equipped with wet heat exchangers. *Solar Energy* 86 (2012), 608–618.
- [50] J. Wrobel, P.S. Walter, G. Schmitz, Performance of a solar assisted air conditioning system at different locations. *Solar Energy* 92 (2013), 69–83.
- [51] R. Possidente, C. Roselli, M. Sasso, S. Sibilio, Experimental analysis of microgeneration units based on reciprocating internal combustion engine. *Energy and Buildings* 38 (2006), 1417–1422.
- [52] G. Angrisani, C. Roselli, M. Sasso, Experimental validation of constant efficiency models for the subsystems of an unconventional desiccant-based Air Handling Unit and investigation of its performance. *Applied Thermal Engineering* 33–34 (2012), 100–108.
- [53] G. Angrisani, F. Minichiello, C. Roselli, M. Sasso, Experimental analysis on the dehumidification and thermal performances of a desiccant wheel. *Applied Energy* 92 (2012), 563–572.
- [54] G. Angrisani, Experimental and simulative analysis of a microtrigeneration system based on an air handling unit with desiccant wheel, Ph.D. Thesis, University of Naples Federico II (2011).

- [55] Decree of the president of the Italian Republic 26 August 1993, n. 412, <<http://www.gazzettaufficiale.it/eli/id/1993/10/14/093G0451/sg>> [in Italian].
- [56] Angrisani G, Minichiello F, Roselli C, Sasso M. Desiccant HVAC system driven by a micro-CHP: Experimental analysis. *Energy and Buildings* 2010;42:2028–2035.
- [57] G. Angrisani, C. Roselli, M. Sasso, F. Tariello, Dynamic performance assessment of a micro-trigeneration system with a desiccant-based air handling unit in Southern Italy climatic conditions. *Energy Conversion and Management* 80 (2014), 188-201.
- [58] Solar Energy Laboratory . TRNSYS 17, a TRaNsient System Simulation program. University of Wisconsin, Madison, 2010.
- [59] T.E.S.S. Component Libraries v.17.01 for TRNSYS v.17.0 and the TRNSYS Simulation Studio, Parameter/Input/Output Reference Manual, Thermal Energy System Specialists,LLC, 2004.
- [60] A. Buonomano, F. Calise, G. Ferruzzi, Thermo-economic analysis of storage systems for solar heating and cooling systems: A comparison between variable-volume and fixed-volume tanks. *Energy* 59 (2013), 600-616.
- [61] M. Noro, R.M. Lazzarin, F. Busato, Solar cooling and heating plants: an energy and economic analysis of liquid sensible vs phase change material (PCM) heat storage. *International Journal of Refrigeration, International Journal of Refrigeration* 39 (2014), 104-116.
- [62] H. Yin, D. Lili, M. Qu, P. Srinivas, Multi-objective optimization of integrated solar absorption cooling and heating systems for medium-sized office buildings. *Renewable Energy* 52 (2013), 67-78.
- [63] N. Enteria, H. Yoshino, R. Takaki, A. Mochida, A. Satake, S. Baba, H. Ishihara, R. Yoshie Case analysis of utilizing alternative energy sources and technologies for the single family detached house. *Solar Energy* 105 (2014), 243–263.
- [64] J.A. Duffie, W.A. Beckmann, *Solar Engineering of Thermal Processes*. Third ed. New York: John Wiley & Sons; 2006.
- [65] Thermital, solar collectors model TSOL 35, <http://www.thermital.it/prodotti/solare-termico/collettori/tsol-35-sottovuoto> [in Italian].
- [66] Kloben, solar collectors model KF25A, <http://www.kloben.it/products/view/4> [in Italian].

- [67] I.L. Maclaine-Cross, P.J. Banks, Coupled heat and mass transfer in regenerators— predictions using an analogy with heat transfer. *International Journal of Heat and Mass Transfer* 15 (6) (1972), 1225–1242.
- [68] R.R. Howe, Model and Performance Characteristics of a Conditioning System Which Utilizes a Rotary Desiccant Dehumidifier, MS thesis, University of Wisconsin, Madison, USA (1983).
- [69] J.J. Jurinak, Open cycle solid desiccant cooling: component models and system Simulations, Ph.D. thesis, University of Wisconsin, Madison, USA (1982).
- [70] P.J. Banks. Prediction of Heat and Mass Regenerator performance using nonlinear analogy method: part 1– basis, *ASME Journal of Heat Transfer* 107 (1985), 222-229.
- [71] G. Angrisani, M. Canelli, C. Roselli, M. Sasso, Calibration and validation of a thermal energy storage model: Influence on simulation results. *Applied Thermal Engineering* 67 (2014), 190-200.
- [72] TERNA, Statistiche e previsioni, Dati statistici, Produzione, 2011, (in Italian) <<http://www.terna.it/LinkClick.aspx?fileticket=axZsbhFJBW8%3d&tabid=418&mid=2501>>.
- [73] TERNA, Nota di sintesi, Dati statistici sull’energia elettrica in Italia, 2011, (in Italian) <<http://www.terna.it/LinkClick.aspx?fileticket=b%2B6DNrXsUBA%3D&tabid=649>>.
- [74] AEEG (Autorità per l’Energia Elettrica e il Gas Direzione Mercati), Revisione dei fattori di perdita di energia elettrica, applicati all’energia elettrica immessa nelle reti di media e bassa tensione (in Italian), 2012, <<http://www.autorita.energia.it/allegati/docs/12/013-12.pdf>>.
- [75] Ministerial Decree of 28 December 2012, “Incentivazione della produzione di energia termica da impianti a fonti rinnovabili ed interventi di efficienza energetica di piccolo dimensioni” (in Italian) <http://www.gazzettaufficiale.it/atto/serie_generale/caricaDettaglioAtto/originario?atto.dataPubblicazioneGazzetta=2013-01-02&atto.codiceRedazionale=12A13722>.

- [76] F. Calise, L. Vanoli, Parabolic trough photovoltaic/thermal collectors: design and simulation model. *Energies* 5 (10) (2012), 4186–4208.
- [77] R. Bernardo, Retrofitted Solar Thermal System for Domestic Hot Water for Single Family Electrically Heated Houses, Development and Testing. Faculty of Engineering. Lund University 2010.
- [78] L.R. Bernardo, B. Perers, H. Håkansson, B. Karlsson, Performance evaluation of low concentrating photovoltaic/thermal systems: A case study from Sweden. *Solar Energy* 85 (2011), 1499–1510.
- [79] X. Zhang, X. Zhao, S. Smith, J. Xu, X. Yu, Review of R&D progress and practical application of the solar photovoltaic/thermal (PV/T) technologies. *Renewable and Sustainable Energy Reviews* 16 (2012), 599–617.
- [80] F. Calise, a. Design of a hybrid polygeneration system with solar collectors and a solid oxide fuel cell: dynamic simulation and economic assessment. *International Journal of Hydrogen Energy* 36 (2011), 6128–6150.
- [81] F. Calise, , b. High temperature solar heating and cooling systems for different mediterranean climates: dynamic simulation and economic assessment. *Applied Thermal Engineering* 32 (2011), 108–124.
- [82] F. Calise, M. Dentice D'Accadia, A. Palombo, L. Vanoli, Dynamic Simulation of High Temperature Solar Heating And Cooling Systems. In: *Proceeding of Eurosun 2010 – International Conference on Solar Heating, Cooling and Buildings*, Graz (AU), 2010.
- [83] K. Nishioka, T. Takamoto, T. Agui, M. Kaneiwa, Y. Uraoka, T. Fuyuki,. Annual output estimation of concentrator photovoltaic systems using high-efficiency InGaP/InGaAs/Ge triple-junction solar cells based on experimental solar cell's characteristics and field-test meteorological data. *Solar Energy Materials and Solar Cells* 90 (2006), 57–67.
- [84] G. Mittelman, A. Kribus, A. Dayan, Solar cooling with concentrating photovoltaic/thermal (CPVT) systems. *Energy Conversion and Management* 48 (2007), 2481–2490.
- [85] F.P. Incropera, D.P. DeWitt, *Fundamentals of Heat and Mass Transfer*, fifth ed. Wiley & Son Inc; 2001.
- [86] S. Kakac, H. Liu, *Heat Exchanger Selection, Rating and Thermal Design*. CRC Press, Boca Raton, Fla., c1998.

- [87] A. Kribus, D. Kaftori, G. Mittelman, A. Hirshfeld, Y. Flitsanov, A. Dayan, A miniature concentrating photovoltaic and thermal system. *Energy Conversion and Management* 47 (2006), 3582–3590.
- [88] G. Mittelman, A. Kribus, O. Mouchtar, A. Dayan, Water desalination with concentrating photovoltaic/thermal (CPVT) systems. *Solar Energy* 83 (2007), 1322–1334.
- [89] G. Angrisani, C. Roselli, M. Sasso, Effect of rotational speed on the performances of a desiccant wheel. *Applied Energy* 104 (2013), 268–275.
- [90] A. Mardiana, S.B. Riffat, Review on physical and performance parameters of heat recovery systems for building applications. *Renewable and Sustainable Energy Reviews* 28 (2013), 174–190.
- [91] U. Jordan, K. Vajen, Realistic domestic hot-water profiles in different time scales. <<http://sel.me.wisc.edu/trnsys/trnlib/iea-shc-task26/iea-shc-task26-load-profiles-description-jordan.pdf>>; 2001.
- [92] International Energy Agency – solar heating and cooling – task 26. <<http://archive.iea-shc.org/task26/publications/index.html>>.
- [93] E. Santini, S. Elia, G. Fasano, Caratterizzazione dei consumi energetici nazionali delle strutture ad uso ufficio. Report RSE/2009/121. <http://www.enea.it/it/Ricerca_sviluppo/documenti/ricerca-di-sistema_elettrico/governance/rse121.pdf> [in Italian].
- [94] E. Pohl, D. Diarra, Assessment method for primary energy savings of CHP systems in domestic energy supply, MicrogenIII. In: Proceedings the 3rd edition of the international conference on microgeneration and related technologies. Naples, Italy, April 15–17; 2013.
- [95] P. Gonçalves, G. Angrisani, C. Roselli, A.R. Gaspar, M. Gameiro da Silva, Comparative energy and exergy performance assessments of a microgenerator unit in different electricity mix scenarios. *Energy Conversion and Management* 73 (2013), 195–206.
- [96] P. Gonçalves, G. Angrisani, C. Roselli, A.R. Gaspar, M.G. Silva, Energy and exergy-based modeling and evaluation of a micro-combined heat and power unit for residential applications. In: MicrogenIII: proceedings of the 3rd edition of the international conference on microgeneration and related technologies. Naples, Italy, April 15–17; 2013 [ISBN 9788890848902].

- [97] Statistical data on energy prices, Autorità per l'Energia Elettrica e il Gas. <http://www.autorita.energia.it/it/dati/elenco_dati.htm> [last accessed 19.06.13, AEEG, in Italian].
- [98] Resolution June 3, 2008-ARG/elt 74/08, Autorità per l'Energia Elettrica e il Gas. <<http://www.autorita.energia.it/allegati/docs/08/074-08arg.pdf>> [AEEG, in Italian].
- [99] Legislative Decree 26 October 1995, n. 504. <<http://www.normattiva.it/urires/N2Ls?urn:nir:stato:decreto.legislativo:1995:504>> [in Italian].
- [100] D. Di Santo, Incentivi e fiscalità per la cogenerazione ad alto rendimento, convegno Polygen-SolarExpo, 10 May 2012, Verona. <<http://www.fire-italia.it/convegni/polygen2012/di%20santo.pdf>> [in Italian].
- [101] Ministerial Decree of 5 September 2011 – support scheme for high-efficiency cogeneration. <<http://www.sviluppoeconomico.gov.it/images/stories/normativa/DM-5-SETTEMBRE2011.pdf>>.
- [102] Technical documentation of AISIN SEIKI microcogenerator. <<http://www.tecno-casa.com/Public/file/MCHP.pdf>>.
- [103] Directive 2004/8/EC of the European Parliament and of the Council of the 11 February 2004 on the promotion of cogeneration based on the useful heat demand in the internal energy market and amending Directive 92/42/EEC. Official Journal of the European Union; 2004.
- [104] European Commission Decision of 21st December 2006. Official Journal of the European Union, 06.02.2007 [in Italian].
- [105] <http://www.mercatoelettrico.org/It/Esiti/TEE/TEE.aspx> [in Italian].

List of tables

Table 2.1: Building characteristics [9].	35
Table 2.2: Building Gains and Loads for Benevento (BN) and Milano (MI).	35
Table 2.3: Main climatic variables of Benevento (BN) and Milano (MI).	36
Table 2.4: Solar collectors configurations.	38
Table 2.5: Evacuated tube collectors IAM factors	46
Table 2.6: Flat plate collectors parameters.	47
Table 2.7: Evacuated tube collectors parameters.	47
Table 2.8: Desiccant Wheel parameters.	49
Table 2.9: Tank parameters	50
Table 2.10: Main models used for the simulation and their main parameters.	52
Table 2.11: Unitary costs.	55
Table 2.12: Net solar thermal energy in the plants with 34 m ² of solar collectors 40° tilt angle.	59
Table 3.1: Building loads.	66
Table 3.2: CPVT design parameters	74
Table 4.1: Best energy, environmental and economic results with flat plate collectors.	102
Table 4.2: Best energy, environmental and economic results with evacuated tube collectors.	102
Table 5.1: Performance data for the internal combustion engine.	112
Table 5.2: Annual energy balance for the equipment of the AS.	115
Table 5.3: Annual energy balance for the equipment of the CS.	119

List of figures

Figure 1.1: Layout of the AHU in the CS for summer operation.....	15
Figure 1.2: Psychrometric diagram with standard AHU transformations.	15
Figure 1.3: Example of hybrid DEC AHU layout.	16
Figure 1.4: Psychrometric diagram with hybrid DEC AHU transformations.	17
Figure 1.5: Layout of the experimental plant.	27
Figure 1.6: The desiccant-based AHU.....	28
Figure 1.7: Psychrometric diagram with experimental desiccant-based AHU transformations.	28
Figure 1.8: The desiccant wheel and the rotor matrix.	29
Figure 1.9: The microcogenerator.	30
Figure 1.10: The boiler.	30
Figure 1.11: The chiller.	31
Figure 1.12: The storage tank.	31
Figure 2.1: Classroom attendance.....	34
Figure 2.2: Scheme of the simulated innovative plant (cooling mode).....	38
Figure 2.3: Psychrometric diagram with standard AHU transformation in cooling mode.	40
Figure 2.4: Scheme of the simulated innovative plant (heating mode).	41
Figure 2.5: Psychrometric diagram with AHU transformation in winter operation.	42
Figure 2.6: Psychrometric diagram with AHU transformation in winter operation control 1.	43
Figure 2.7: Psychrometric diagram with AHU transformation in winter operation control 2.	43
Figure 2.8: Scheme of the simulated conventional plant (heating mode).	44
Figure 2.9: Generic node of a detailed stratified tank storage.	50
Figure 2.10: Primary Energy Saving of the Alternative Systems without further energy thermal demands and with flat plate collectors in Benevento (BN) and Milano (MI).	57
Figure 2.11: Primary Energy Saving of the Alternative Systems without further thermal energy demands and with evacuated tube collectors in Benevento (BN) and Milano (MI).	58

Figure 2.12: Primary Energy Saving of the Alternative Systems with 50% of solar thermal energy surplus exploited and with flat plate collectors in Benevento (BN) and Milano (MI).	59
Figure 2.13: Primary Energy Saving of the Alternative Systems with 50% of solar thermal energy surplus exploited and with evacuated tube collectors in Benevento (BN) and Milano (MI).	60
Figure 2.14: Primary Energy Saving of the Alternative Systems with 100% of solar thermal energy surplus exploited and with flat plate collectors in Benevento (BN) and Milano (MI).	61
Figure 2.15: Primary Energy Saving of the Alternative Systems with 100% of solar thermal energy surplus exploited and with evacuated tube collectors in Benevento (BN) and Milano (MI).	62
Figure 2.16: The best Simple Pay Back periods of the Alternative System with flat plate collectors in Benevento (BN) and Milano (MI).	63
Figure 2.17: The best Simple Pay Back periods of the Alternative System with evacuated tube collectors in Benevento (BN) and Milano (MI).	64
Figure 3.1: Scheme of the simulated plant in summer period.	67
Figure 3.2: CPVT layout [76].	69
Figure 3.3: Typical summer weekday powers (27/07).	76
Figure 3.4: Typical winter weekday powers (14/02).	77
Figure 3.5: Monthly thermal energies of the conventional and alternative system.	78
Figure 3.6: Monthly electric energies of the conventional and alternative system.	79
Figure 3.7: Electric energy fed into the grid.	80
Figure 3.8: Electric energy taken from the grid.	80
Figure 3.9: DHW energy production.	81
Figure 3.10: Seasonal results in heating mode operation.	81
Figure 3.11: Summer energy distribution.	82
Figure 3.12: PES and ΔCO_2 as a function of DHW usage.	83
Figure 4.1: Scheme of the simulated Desiccant-based AHU with heat recovery from chiller condenser (cooling operation, Scenario B).	87
Figure 4.2: Psychrometric diagram with air transformation of the AHU with heat recovery from chiller condenser (cooling operation, Scenario B).	88
Figure 4.3: Scheme of the simulated Desiccant-based AHU with cross-flow heat recovery unit (cooling operation, Scenario C).	89

Figure 4.4: Psychrometric diagram with air transformation of the AHU with cross-flow heat recovery unit (cooling operation, Scenario C).	89
Figure 4.5: Scheme of the simulated Desiccant-based AHU with pre-cooling coil (cooling operation, Scenario D).	90
Figure 4.6: Psychrometric diagram with air transformation of the AHU with pre-cooling coil (cooling operation, Scenario D).	91
Figure 4.7: Primary Energy Saving of the Alternative Systems with 0% of solar thermal energy surplus used and flat plate collectors in the four alternative configurations: a) Scenario A, b) Scenario B, c) Scenario C, d) Scenario D.	92
Figure 4.8: Primary Energy Saving of the Alternative Systems with 0% of solar thermal energy surplus used and evacuated tube collectors in the four alternative configurations: a) Scenario A, b) Scenario B, c) Scenario C, d) Scenario D.	93
Figure 4.9: Primary Energy Saving of the Alternative Systems with 50% of solar thermal energy surplus used and flat plate collectors in the four alternative configurations a) Scenario A, b) Scenario B, c) Scenario C, d) Scenario D.	95
Figure 4.10: Primary Energy Saving of the Alternative Systems with 50% of solar thermal energy surplus used and evacuated collectors in the four alternative configurations: a) Scenario A, b) Scenario B, c) Scenario C, d) Scenario D.	95
Figure 4.11: Primary Energy Saving of the Alternative Systems with 100% of solar thermal energy surplus used and flat plate collectors in the four alternative configurations: a) Scenario A, b) Scenario B, c) Scenario C, d) Scenario D.	96
Figure 4.12: Primary Energy Saving of the Alternative Systems with 100% of solar thermal energy surplus used and evacuated tube collectors in the four alternative configurations: a) Scenario A, b) Scenario B, c) Scenario C, d) Scenario D.	96
Figure 4.13: Annual primary energy and equivalent CO ₂ emission associated with seasonal electric and thermal demands for the plant with pre-cooling coil (Scenario D), flat plate collectors, 40° tilt angle and 0% of solar thermal energy surplus used.	97

Figure 4.14: Annual primary energy and equivalent CO ₂ emission associated with seasonal electric and thermal demands for the plant with pre-cooling coil (Scenario D), evacuated tube collector, 40° tilt angle and 0% of solar thermal energy surplus used.....	98
Figure 4.15: Equivalent CO ₂ avoided emissions of the Alternative Systems with 0% of solar thermal energy surplus used and with flat plate collectors in the four alternative configurations: a) Scenario A, b) Scenario B, c) Scenario C, d) Scenario D.....	99
Figure 4.16: Equivalent CO ₂ avoided emissions of the Alternative Systems with 0% of solar thermal energy surplus used and with evacuated tube collectors in the four alternative configurations a) Scenario A, b) Scenario B, c) Scenario C, d) Scenario D.	99
Figure 4.17: Annual primary energy and equivalent CO ₂ emission associated with seasonal electric and thermal demands for the plant with cross-flow heat recovery unit (scenario C), evacuated tube collectors, tilt angle of 40° and 0% of solar thermal energy surplus used.	101
Figure 5.1: Profile of domestic hot water draw.	106
Figure 5.2: The layout of the desiccant-based AHU.	107
Figure 5.3: Main energy flows of the trigeneration system during summer operation.	108
Figure 5.4: Layout of the AHU in the PS for winter operation.	109
Figure 5.5: Primary energy saving, net saving and CHP generation bonus as a function of the electric surplus factor.....	118
Figure 5.6: The results of the thermo-economic analysis as a function of the electric surplus factor.....	119